December 2021

Design methodology for input shapers using genetic algorithms in flexible nonlinear systems

Mohab Adel Hakim Meshreki
The American University in Cairo AUC

THE AMERICAN UNIVERSITY IN CAIRO
SCHOOL OF SCIENCE AND ENGINEERING
INTERDISCIPLINARY ENGINEERING PROGRAMS

Design Methodology for Input Shapers Using Genetic Algorithms in Flexible Nonlinear Systems

by

Mohab Adel Hakim Meshreki

A thesis submitted in partial fulfillment of the requirements for the degree of:

Master of Science in Engineering

With specialization in:

Design

Under the supervision of:

Dr. Keith Hekman
Associate Professor, Mechanical Engineering Department
and
Dr. Ashraf Nassef
Associate Professor, Mechanical Engineering Department

The American University in Cairo
School of Sciences and Engineering

2004/32

Design Methodology for Input Shapers Using Genetic Algorithms in Flexible Nonlinear Systems

A Thesis Submitted by

Mohab Adel Hakim Meshreki

to the Interdisciplinary Engineering Programs

June 9, 2004

in partial fulfillment of the requirements for the degree of

Master of Science in Engineering with Specialization in Design

has been approved by

Dr. Keith Hekman, (Advisor)
Associate Professor, Mechanical Engineering Department, AUC

[redacted]

Dr. Ashraf Nassef, (Advisor)
Associate Professor, Mechanical Engineering Department, AUC

[redacted]

Dr. Sayed M. Metwalli
Professor, Faculty of Engineering, Cairo University

[redacted]

Dr. Maher Y.A. Younan
Professor, Mechanical Engineering Department, AUC

[redacted]

Dr. Emad Imam
Professor, Construction Engineering Department, AUC

[redacted]

[redacted] JUNE 13, 2004

[redacted] June 14, 2004
Date

ACKNOWLEDGEMENT

The author wishes to express his deep gratitude to Dr. Keith Hekman for his thorough supervision, frequent advice and invaluable assistance in the theoretical and experimental work. Moreover, the author wishes to acknowledge Dr. Ashraf Nassef for his constant guidance and help in the all optimization codes, and his continuous encouragement throughout the research work. The author appreciates the constant support of the administrative staff of the mechanical engineering department of the American University in Cairo.

To my family who supported me throughout this research and gave me confidence and care, thank you.

ABSTRACT

This thesis covers the topic of command input shaping for flexible systems. Input shaping is a set of commands designed in order to cancel the residual vibration of a system. Traditional input shaping commands do not take into consideration the effect of nonlinearities such as Coulomb friction and saturation of the system because of the difficulty of obtaining a closed form solution for such problems. In this research, a methodology for generating input commands is introduced. Examples are given for a one degree of freedom system under a proportional-integral (PI) controller and a two degree of freedom cart-pendulum system. For the one degree of freedom under PI control, nonlinearities of Coulomb friction and saturation are included in the shaper development. A model is developed and the time solution of the motion is solved numerically. Global and local optimization methods are used to determine the optimum command set for the system. The two degree of freedom systems considered had a proportional-derivative (PD) controller, and nonlinearities including the effect of Coulomb friction and saturation. For both models, a comparison with linear input commands is done, and genetic algorithm is used to determine a near optimum command. Experimental results for the models are tested and compared to simulated commands. It is shown in the results that the newly developed commands offer better response than the linear ones with respect to residual oscillations.

TABLE OF CONTENT

LIST OF FIGURES

LIST OF TABLES

NOMENCLATURE

A_i	: ith Impulse or step amplitude (incremental values)
EI	: Extra insensitive input shaping commands
F	: Total force on the system
F_{cont}	: Controller force
I_m	: Current to the motor
J_o	:The moment of inertia of the pendulum around the pin
J_r	:The moment of inertia of the pendulum around its centroid
K_g	:Gear box ratio
K_m	:Motor torque constant
L	:Half the length of the pendulum
N	:Normal reaction (y-direction)
Objfun	: Objective function definition
Objfun1	: First objective function used in the one degree for a three step command
Objfun2	: Second objective function used in the one degree for a three step command
PD	: Proportional-derivative controller
PI	: Proportional-integral controller
PID	: Proportional-integral-derivative controller
R_m	:Motor armature resistance
Trad.Obj	: Traditional objective function
V_{in}	:The input voltage to the cart
V	: Residual vibration of a system
V_1	: Residual vibration of the first mode
V_2	: Residual vibration of the second mode
ZV	: Zero vibration input shaping commands
ZVD	: Zero vibration and derivative input shaping commands
ZV:fft	: Objective function using Fast Fourier Transform
ZZ	: Array removed from the search space in the genetic algorithm code
c	: damping of the system
cthd	: Expression for the equation of the angular acceleration of the pendulum
cxd	: Expression for the equation of the acceleration of the cart
Fft	: Fast Fourier Transform
finalangle	: The angle of the pendulum after the last input step
finalanglvel	: The angular velocity of the pendulum after the last input step
finalpos	: The position of the cart after the last input step
finaltime	: the time of the last input step
finalvel	: The velocity of the cart after the last input step
k_d	:The derivative gain of the system
k_i	:The integral gain of the system
k_p:	:The proportional gain of the system
m_b	:Mass of the block

t_{step}	: time step for the integration
x	:The position of the cart
x_d	: Desired position of the cart (position of the controller)
x_{dcuren}	: Current position of the controller
x_{dprev}	: Previous position of the controller
$\vec{xn}_i$	: Point from the population of the genetic algorithm code
x_{in}	: Locally optimized point in the genetic algorithm code
θ	:Angle of the pendulum
μ_k	:Dynamic friction
μ_s	:Static friction
ω_d	: Damped frequency
ω_g	:Angular velocity of the motor
ω_n	: Natural frequency
ζ	: Damping ratio of the system

CHAPTER 1

INTRODUCTION

This chapter gives a brief review of the current input shaping practice, the motivations behind the presented research, the approach followed during the research, the scientific contributions and an overview of the thesis.

1.1. REVIEW OF INPUT SHAPING PRACTICE

One of the interesting problems in control and dynamics fields is the time response of flexible structures (lightly damped structures). These structures have been used for a long time in applications such as tower cranes, overhead cranes, robot manipulators and large structures in space. Ship decks floating on sea surfaces can also be treated as flexible structures during loading and unloading, where large oscillations are induced. The flexible structures offer many advantages since they have less mass, thus lighter weight, which is especially useful in robot and spacecraft applications. Moreover, due to its high flexibility, it induces lower stresses in the material, thus increasing the durability of the machine. By decreasing the components and mass of flexible structures, the cost is decreased also.

However, some problems arise from the high flexibility of these structures including their sensitivity to external disturbances, large amplitude oscillation, and long settling time. Many techniques were developed in order to reduce or eliminate such drawbacks. Two broad control schemes can be applied, which are feedback and feedforward control. The former is useful in case of reducing the effect of disturbances on the system (structural model under

two responses. However, this type of control is not useful in reducing the oscillations of the system for a given input command (impulse, step, ramp) due to its delay in response. In such a case, feedforward control is more useful, since it provides a series of input commands that will result in anticipation of oscillation and elimination of their occurrence. One of these forward methods is input shaping in which a desired input command is broken into steps that cancel the vibration out.

Input shaping can be illustrated by the simple cart and pendulum example shown in Fig. 1-1

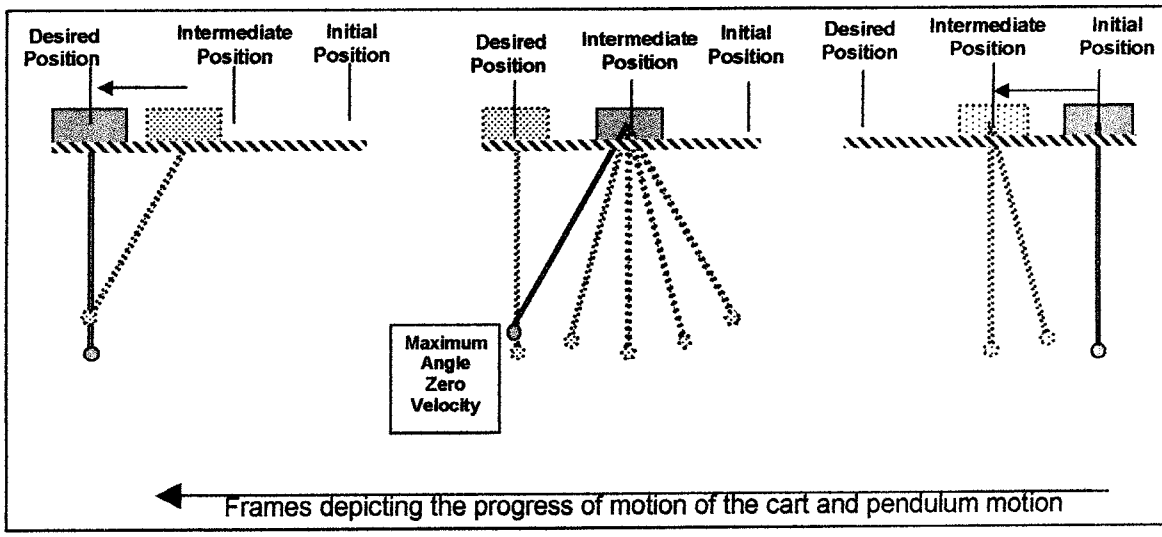

Fig. 1-1: Illustrative drawing of the application of input shaping to a cart and pendulum model

The cart should be moving between an initial and a desired position, while minimizing the oscillations of the attached pendulum. Instead of displacing the cart instantaneously (step input command) to the desired position, the cart is subjected to a series of instantaneous displacements at specific timings that will cancel the pendulum oscillations. The cart is subjected to a step input at the initial position that is only sufficient to move it to the

1.2. MOTIVATION

There exists a constant need to suppress the oscillations of the different flexible structures. In most cases these structures have a non-linear behavior. Moreover, in many applications, high positioning accuracy is required. There are several approaches in practice that can be used to suppress such oscillations. One of these approaches is input shaping, which presents an easy, simple and cheap way for the achievement of such goal. Recently there has been some research in hybridizing input shaping with conventional controllers (such as proportional-integral (PI) and proportional-derivative (PD) controllers). However, this seminal work is confined to linear systems, where only the system's natural frequency and damping ratio are considered. There are other parameters that need to be taken into consideration in order to properly describe the systems such as friction and saturation. Therefore, there is a need for an input shaping algorithm that will take into consideration such extra non-linear parameters.

1.3. OBJECTIVES AND APPROACH

The objective of the research reported in this thesis is to develop a procedure for determining the optimal input shaping command set for non-linear systems. This goal is achieved in this thesis using the following approach:

1. The equations of motion of an exemplary system composed of a cart and pendulum are developed, including the effect of non-linear parameters such as friction and saturation.
2. A numerical integration algorithm using the Runge Kutta method is developed to obtain the system response. The developed algorithm ensures compatibility between the

3. System identification experiments were applied on an experimental setup of a cart and pendulum system to determine its parameters that include friction and damping coefficients.
4. An optimization algorithm is developed to find the optimum input command set for the cart and pendulum system. The optimization algorithm is based on the hybridization of genetic algorithm and direct search methods.
5. Verification experiments are performed to compare the actual system response with the simulation response.

1.4. CONTRIBUTIONS

The research presented in this thesis makes the following contributions in the area of input shaping:

1. Optimized input command sets can be developed for different nonlinear systems. To date, no optimization method have been developed for command input shaping for nonlinear systems.
2. A novel hybridization of the optimization of input shaping commands and the conventional feedback controllers, especially the integral controllers, has been developed. This hybridization offers the chance of benefiting from the property of the integral controller to eliminate the steady state error of the system, while canceling out the extra oscillation induced by such controller.

1.5. THESIS OUTLINE

The thesis is divided into six chapters and two appendices:

1. Chapter one includes the introduction, motivation, research objectives, approach, and the list of contributions to input shaping field.
2. Chapter two presents a literature review about feedforward control, input shaping, the different hybridization schemes, and the combination of command input shaping with optimization and nonlinear systems.
3. Chapter three addresses generally optimization as a tool for the solution of the input shaping problem, and Genetic Algorithm as the optimization tool used in this thesis. This chapter is a prelude to the work done in the consecutive chapters.
4. Chapter four presents the one degree of freedom system composed of a cart and a controller. The chapter introduces optimization of the input shaping commands with the inclusion of nonlinearities in the system, and compares the final response with that of a linear system. In the chapter, the equations of motion, and the objective function for the different models are developed. The sequence of solution and implementation to the actual experimental set is presented. System identification process is described and the simulations as well as the experimental results are presented.
5. Chapter five describes the two degree of freedom system composed of a cart, a pendulum and a controller. Modifications to the Genetic Algorithm code will be explained and the system identification process will be briefly discussed. Simulation and experimental results will be compared.
6. Chapter six concludes the thesis and provides suggestions for future research.

CHAPTER 2

LITERATURE REVIEW

2.1. INTRODUCTION

There are many types of strategies that are mentioned in the literature dealing with vibration suppression of flexible structures such as optimal control approaches, and optimal feedback control which usually are difficult to calculate and implement for many systems (Singer and Seering, 1990). Some of these commands will be discussed, while input shaping will be carefully surveyed. The research in the input shaping field assumed two main directions: the first deals with theoretical formulations of the input shaping commands in order to provide a general solution that can be applied to most linear cases. The second is concerned with applying these results with either modification to the system to which they are applied or modifications of the commands themselves.

2.2. FEEDBACK CONTROL

Feedback control is one of the widely used types of control, where a feedback command is developed based on the difference between the actual response of the system and the desired response. In the case of flexible structures, such a broad type of controller wasn't successful to cancel the vibration of the system during its transient response. Feedback control proved to be successful in system disturbances rejection (Mohamed and Tokhi, 2003), yet limited oscillation suppression was achieved using this technique in displacing flexible structures due to the delay in its feedback commands (Singer and Seering, 1990).

2.3. FEEDFORWARD CONTROL

Feedforward control is based on priori information of the system under consideration. Based on this information, the input command set anticipates the future oscillations, and cancels them out. The benefit of such type of control is that it doesn't wait for an error to occur in the system in order to take an action, but rather estimates any deviation before hand. Many types of feedforward control can be applied including inverse dynamics, input shaping, and time optimal control.

2.3.1. INVERSE DYNAMICS

In inverse dynamics, input commands are designed based on the desired output of the system. Given a desired output response function for the system, the function coefficients are deduced by backward solution of the system equations. In order to apply such method, the desired function has to be differentiable and continuous (Singer and Seering, 1990). Examples of output functions include the third order exponential function. In addition to being limited to a specific number of output functions, the method suffers from disadvantages that include the restriction of the speed by the actuator limits and inapplicability at high speeds. Nevertheless, the method has an advantage of high robustness (Sahinkaya, 2001).

2.3.2. INPUT SHAPING

The development of input shaping was done by breaking the input command into several delayed steps that cancel out the vibrations (Smith, 1958). For a one degree of freedom system, a two-impulse command was developed by setting the residual vibration equations (2-1) equal to zero, and solving the equation for the impulses amplitudes and

$$V(\omega,\zeta)=e^{-\zeta\omega_n}\sqrt{[C(\omega,\zeta)]^2+[S(\omega,\zeta)]^2} \tag{2-1}$$

where

$$C(\omega,\zeta)=\sum_{i=1}^{n}A_i e^{\zeta\omega t_i}\cos(\omega_d t_i)$$
$$S(\omega,\zeta)=\sum_{i=1}^{n}A_i e^{\zeta\omega t_i}\sin(\omega_d t_i) \tag{2-2}$$

ω_d is the damped frequency of the system described by the following expression

$$\omega_d=\left(\omega_n\sqrt{1-\zeta^2}\right) \tag{2-3}$$

This type of command is called the zero vibration shaper (ZV). The main variables in this model are the impulses A_i and their timing t_i. The response of a model subjected to this impulse is described in Fig. 2-1 (Singh and Singhose, 2002). The solutions to this problem include the trivial one of impulses of zero amplitude, which will cause no motion. In order to avoid this case, another condition has to be specified which sets the sum of the normalized amplitudes equal to zero (equation (2-4)) to ensure that the desired position is reached.

$$\sum A_i=1 \tag{2-4}$$

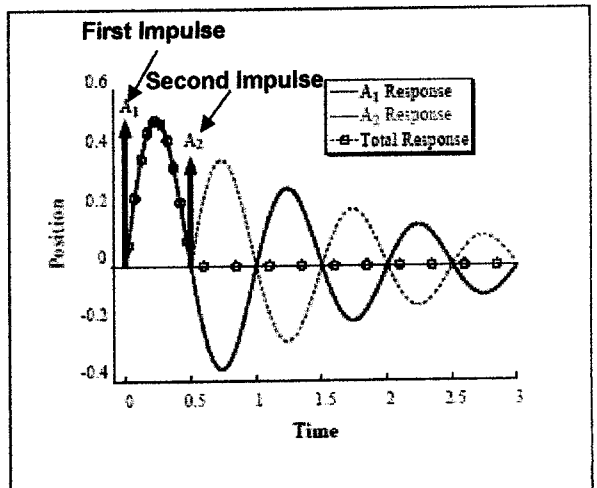

An expression of the first impulse and the timing of the second impulse are shown in equation (2-5).

$$A_1 = \frac{e^{\frac{\zeta\pi}{\sqrt{1-\zeta^2}}}}{1+e^{\frac{\zeta\pi}{\sqrt{1-\zeta^2}}}} \qquad t_2 = \frac{\pi n}{\omega_d} \tag{2-5}$$

Systems in real life are usually subjected to step and ramp response rather than simple impulses. Thus in order to obtain the desired shaped step, the obtained impulses could be superimposed on the desired step response in order to obtain the final command as shown in Fig. 2-2 (Singh and Singhose, 2002).

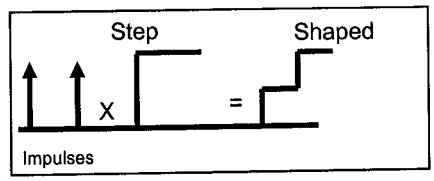

Fig. 2-2: Convolution of impulses with a step command

It was found that this type of shaper is rather sensitive to system parameter variations. To improve the robustness of the input command, another method, called zero vibration and derivative (ZVD) shapers is developed. A ZVD shaper has an additional constraining equation, which sets the derivative of the vibration equation with respect to the natural frequency of the system to zero (Singh and Singhose 2000):

$$\frac{\partial}{\partial\omega}V(\omega,\zeta)=0. \tag{2-6}$$

With equations (2-1), (2-4) and (2-6)

, it is possible to solve for five variables considering that the initial time is set a free choice.

timings of the second and third impulses (t_2 & t_3). It was shown that this type of command produces much less vibration than the ZV shaper as shown in Fig. 2-3 (Singh and Singhose, 2000)

More robust shapers can be designed by increasing the number of impulses. These shapers are called the *extra insensitive* (EI) shaper. In the single hump extra insensitive shapers, the vibration level is constrained to a limit value V, at the model frequency, and is set to zero at two other locations around the model frequency (single hump EI). This leads to higher robustness that minimizes the vibration level below V for a variation of frequency of ±20% as shown in Fig. 2-3 (Porter et al., 1995).

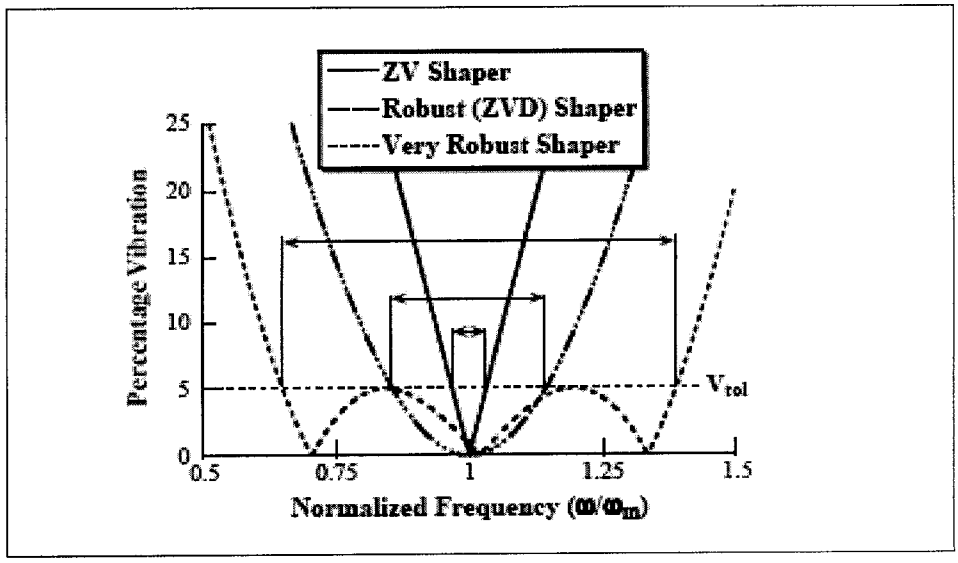

Fig. 2-3: Comparison of ZV, ZVD & Extra Insensitive shapers (Singh & Singhose 2000)

However, in many systems there exist model nonlinearities related to either large motions of the system, presence of friction or input limits of the actuators. As the system nonlinearities increase, these types of shaping commands sometimes fail to reduce the vibration level considerably. Thus more robust shapers were designed by increasing the

vibration level is equal to zero. This comes at the penalty of increasing the time delays (Porter et al.,1995).

It was shown that for multi mode systems; input shaping can be applied by the convolution of the different steps of each mode (Singer and Seering, 1990). This encouraged many researchers to apply this concept to flexible link by using the previously discussed shapers (ZVD, EI) in order to damp the vibration of flexible links.

2.3.3. TIME OPTIMAL CONTROL

Time optimal control is based on setting the values of the input parameters of the system to their maximum, in order to either accelerate or decelerate it. Such a way ensures that the optimum performance of the system is achieved. Pao and Singhose (1997) developed a time optimal control shaper (constant amplitude input commands) for the zero-vibration (ZV) and the zero-vibration-derivative (ZVD) cases. They compared its performance to that of a standard shaper (variable amplitude input commands). It was shown that no general expression could be provided for the time optimal control shaper. Moreover, a comparison of the behavior of the variable amplitude shaper and the time optimal control shaper shows that the former excites less higher-mode oscillations and has higher robustness. Yet, it is slower than the latter (Pao and Singhose, 1995). One of the applications in which ZV, ZVD and time optimal control shapers were tested is the motion of cranes with and without hoisting. (Kension and Singhose., 2000). It was shown that time optimal control for a rigid body leads to large swing angles, while time optimal control of a flexible body reduces the vibrations. However the time optimal control of flexible bodies is sensitive to modeling errors. Moreover, its calculations are to be found for each displacement size, and the implementation

reduce the transient vibration when compared to optimal control commands. If negative impulses are used in the case of variable amplitude input shaping, shorter time delay is achieved, with larger transient oscillations.

2.4. Hybridization of Input Shapers With Controllers

As shown previously, input shaping is a useful method in suppressing the vibration of flexible systems. Hybridization of input shaping with different types of controller yield better results than simply using these controllers. The main concept behind such hybridization is that the input shaping commands are designed to suppress the vibration, while the different controllers are responsible for accurately positioning the system. Many types of controllers were used with input shaping including a proportional-derivative controller, low pass and band pass filters and other types of controller.

2.4.1. Proportional and Derivative (PD) Controller

A PD controller is a feedback controller that takes action based on the rate of change of the system's error. A method was suggested for the design of both input shaping and PD controllers simultaneously. The simulation results showed that the analytical solution developed yielded better results with less overshoot, settling time and sensitivity than for a PD control alone, yet the only disadvantage of this method is the higher disturbance amplification (Kension and Singhose, 2000). Input shaping combined with PD and lead controllers were applied to a single flexible link in order to reduce residual vibrations (Kuo and Kuo, 1992). By computer simulation, it was shown that this method was effective in reducing such vibration and improving tracking properties of the system.

2.4.2. Low Pass and Band Pass Filters

Filters are devices that determine the range of signal that is allowed to reach the system. For low pass filters, only low frequency signals are fed to the system while the higher frequency signals are cancelled. For the band pass filter, signals with specific range of frequency are allowed to pass. Input shaping with two and four impulses was used in combination with low pass and band pass filters in order to reduce vibrations of different modes, where the filters were applied to the input command to ensure that the imposed frequency is different from the natural frequencies of the different modes of the system (Mohamed and Tokhi, 2002). It was shown that the input shaping command have high robustness toward errors, while low pass filter was shown to perform better than band pass filters.

2.4.3. Other Types of Controller

Hybrid control schemes and input shaping were applied to a flexible manipulator model. Proportional-derivative PD, proportional-integral-derivative PID and the combined PD and PID controllers were used for the input tracking of the manipulator and a four impulse shaper was used for the vibration suppression (Mohamed and Tokhi, 2003). It was shown by simulation that PD controller with input shaping performed better than PD controller with PID controller in terms of vibration reduction at the end point tracking of the manipulator. Other works include the combination of input shaping to reduce modes vibration of flexible links and sliding mode tracking control to overcome friction problems (Romano et al., 2002).

2.5. Input Shaping of Non-linear Systems

Nonlinearity presents a major problem in the design of the input shaping command. The effect of friction as a nonlinearity in the system, was introduced by Lawerence, et al. (2002) who analytically solved a one degree of freedom model with a PD controller in the presence of Coulomb friction. They compared the results of the new input commands with the conventional input shaping commands. The former gave the system a better response by accurately positioning the mass and by eliminating the need for a large derivative controller that causes higher overshoot.

Moreover, some research was done in the case of multi-degree of freedom systems (Banerjee and Singhose, 1998). The objective was to determine an analytical solution for an input shaping command for a two link flexible robot in order to dampen two modes of oscillation of its links. This was combined with nonlinear feedback control. Simulation results showed that an improved response was obtained.

2.6. Input Command Optimization

One of the useful ways in determining new input commands is optimization where nonlinearities could be included. A trajectory optimization problem using recursive quadratic programming algorithm was implemented to a single flexible link in order to reduce vibrations. A numerical model was made taking into account the flexibility of the link and the friction. An optimized trajectory was calculated in order to eliminate two modes of vibrations of the link, in addition to the use of a PD controller for the angle of the link. It was shown that the optimization method offered a solution that reduced the tip vibration of the link, and

dampen further vibrations induced in the system due to model inaccuracies (Wilson and Starr, 1996). As the nonlinearities increase, this optimization method could fail in finding the global optima especially for large variations in the natural frequency of the system.

2.7. CONCLUSIVE REMARKS

From the above literature review the following areas of research present vacant gaps that need further studies in the subject of input shaping commands of flexible structures:

1. Hybridization of input shaping with proportional-integral (PI) controllers for nonlinear systems: PI controllers have the advantage of eliminating the steady state error of the system as opposed to PD controllers. One of the major challenges is to hybridize input shaping with PI controller in nonlinear systems since there is no analytical solution for the optimum input command needed to suppress the vibration such system.
2. Large nonlinearity effect in flexible systems: One of the major sources of nonlinearity is saturation. An example of saturation is in the case of DC motors. If large input voltages are applied, these voltages will be down scaled to the maximum allowable voltage of the motor. Saturation has an effect equivalent to altering the natural frequency of the system. This feature represents a major nonlinear factor that is not included in the design of input shapers.
3. Global optimization for nonlinear two degree of freedom systems: The optimal selection of input commands to minimize oscillations, have been approached with optimization techniques that linger in local minima. However, due to the highly nonlinear nature of the oscillation function, it is expected that it would contain several minima. Therefore a global optimization method should be used.

The previous research gaps are addressed in the present thesis. A new approach for the determination of the input command for nonlinear systems is developed and applied to two models. This approach models the system numerically, and then genetic algorithm is used to optimize the input commands by varying their amplitudes and timings. A one degree of freedom system is modeled. This system, with a PD controller, is modeled to verify that the new approach for determining the input commands produces the same results as in the literature. The system will then include a PI controller in the presence of both friction and saturation for the sake of studying the hybridization of input shaping with PI controllers in nonlinear systems. In addition, a two degree of freedom system is modeled including two nonlinear terms representing the effects of friction and saturation. An optimized input command set is developed for such a model using genetic algorithm as a global optimizer to escape the expected local minima. The results for both systems are verified experimentally.

CHAPTER 3

GENERAL METHODOLOGY

This chapter shows how optimization theory can be used in general to find optimum input shaping commands. This basic presentation is imperative to the understanding of the work done in the consecutive chapters. Section 3.1 presents the layout that is used in order to use optimization with input shaping. Sections 3.2 will briefly discuss the genetic algorithm as a global search method and how it is introduced in the solution scheme.

3.1. OPTIMIZATION OF INPUT SHAPING COMMANDS

It is clear that a simple analytical solution could be found for linear model. However, when different types of controllers are included in the model and with the presence of friction and saturation, the closed form solution is tedious to find, and sometimes it is not possible to find one. While analytical solutions are difficult to obtain, numerical modeling can predict the system response with high accuracy. Moreover, the input shaping problem presents itself as an optimization problem where the main constituents are the objective function to be minimized, the system variables that are substituted in the objective function and a set of constraints that have to be satisfied. The way to conform the input shaping problem to these optimization points are different. In some cases the objective is to produce the shortest amount of an input command sequence, and in this case the constraint is to set the vibration level equal to zero. In this thesis, this problem layout is inappropriate, since the presence of a zero vibration level as a constraint is not assured in the case of the different types of

constraints are specified. First the time should be less than a limiting value depending on the system natural frequency thus minimizing the time instead of including it in the objective function. Second, the sum of the impulses is scaled to unity in order to reach the desired position. Third, All the impulses are positive in order to decrease the search space for the optimization problem since the use of the negative impulses is not applicable in all systems. The decision variables are the impulses amplitude and the corresponding timing.

The problem is set to be solved as an optimization problem where the values of the variables are fed into the numerical model of the system, and the corresponding objective function value is evaluated. The next step is to choose which optimization technique to be applied. Since the function is highly oscillatory, the local optimization method could not be applied directly. Instead, a near global optimization method is applied, such as genetic algorithms and then the solution is used as an initial guess for the local optimization method.

The sequence in the design, modeling and calculation is based on two main codes. The first code is the optimization code, which is responsible for producing results depicting the optimum solution. This code calls the second one, which is the objective function code. The latter code involves the numerical model of the system response. In the schematic diagram in Fig. 3-1, the relation between the codes is presented.

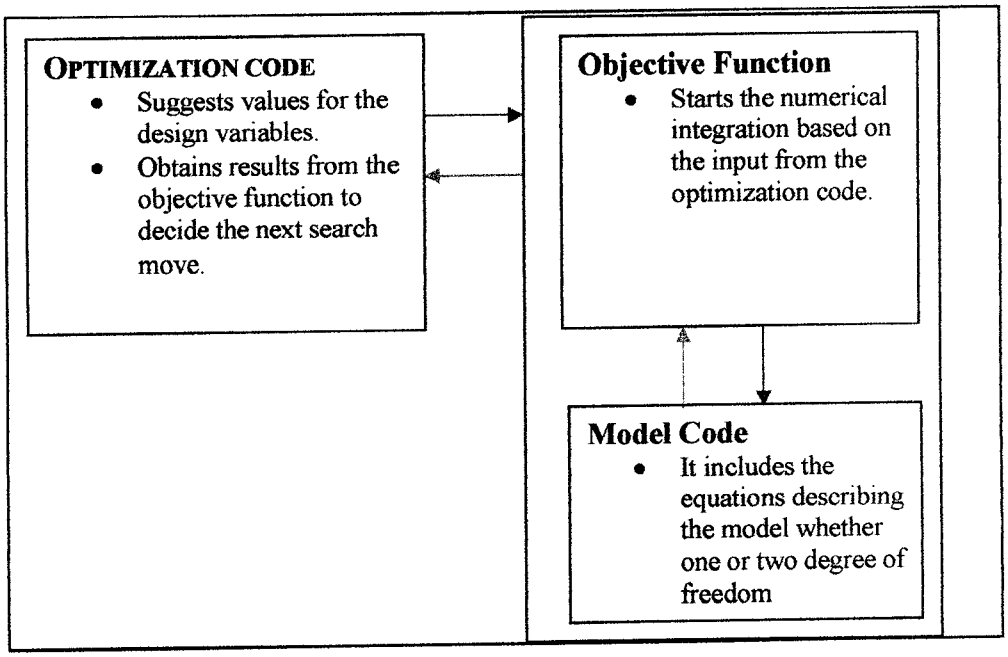

Fig. 3-1: Schematic diagram for the sequence of code steps

3.2. GENETIC ALGORITHMS

In the following chapters, genetic algorithms will be the global search method used in the optimization of input shaping commands. Since the input shaping optimization is a continuous variable optimization problem, a special kind of genetic algorithms is adopted. This is the real-coded genetic algorithm. The method is reviewed in this section in addition to some search features that suit the problem at hand.

The genetic algorithm (GA) is a global optimization method that is based on using multiple points in its search in order to find a near global optimum solution. The structure of the GA's differ from one problem to the other depending on the complexity of the problem, the number of variables, the shape of the objective function and other factors. However, the main components of the optimization problem in this thesis are:

The decision variables in case of the ZV input command set were the amplitude of the first step A_1 and the timing of the second step t_2. For the ZVD models the four variables were the amplitude of the first and second step A_1 & A_2 and the timing of the second and third step t_2 and t_3. In case of the two degree of freedom system they were three amplitudes and three timings in the case of the four step command.

- Constraints

Step timings:

The timings of the input commands should have values greater than zero ($t \geq 0$), and they should not exceed a value equal to the period of oscillation of the system.

Amplitudes:

The normalized amplitudes should satisfy equations (2-4) and (3-1).

$$A_i \geq 0 \text{, for } i=1,2,3 \tag{3-1}$$

The constraint of equation (2-4) can be satisfied by using decision values that represent ratios of the amplitudes (between zero and one), instead of the direct use of the amplitudes themselves. This guarantees that the amplitudes will sum up to be equal to 1.

- Objective Function

The objective function in this thesis is the minimization of the vibration level, as will be described in sections 4.3 and 5.2.

REAL CODED GENETIC ALGORITHM

Traditional genetic algorithms converted the decision variables from their real domain to a binary code. This code was used in turn in the search process. However, such coding was found unsuitable for continuous domain optimization, and was replaced with the real-coded

version of genetic algorithms (Herrera et al., 1998). The general algorithm for a real-coded genetic algorithm is as follows:

- Randomly initialize a population of points within the boundaries of each decision variable. Each decision variable is assumed to be ranging between an upper and a lower bound.
- For the generated points, the objective function has to be evaluated. These points represent the initial population of the GA.
- Such step is the start of the generation loops where every step including this step will be repeated for a specified number of generations.
- The generated points are to be ordered based on their objective function value, depending whether this is maximization or a minimization problem. In this case (minimization), the points are ordered in ascending order of the objective function.
- Then a fitness function for each point has to be defined in order to rate the probability of selecting this point to survive in other generations. This fitness function will help selecting the different points probabilistically. Another option that was used in the GA's is to use geometric probability distribution in order to choose probabilistically the best points. This guarantees that even if the size of the population size is increased, still the best chromosomes (points) will remain on the next generation.
- Create a temporary population in which new points and points from the previous generation are put. The way to fill this temporary population is by the following operators:
- Selection

A number of points are selected from the population of the previous generation without any modifications. The selection process is either based on the fitness function previously defined or on a random variate from geometric distribution. In the case of a single degree of freedom system, 20% of the population was selected. In the two degree of freedom system 70% of the population was selected. This selection operator ensures that the high fitness chromosomes are present in further generations.

- Cross Over

  This general type of operator is based on a two point averaging method. Such averaging leads to two new search points, which are referred to as the children of the old ones. This cross over is sometimes intended to randomize the search so as to break off one of the local optima and sometimes it is a selective operator that improves the actual solution. The following types of cross overs where used (Michalewicz and Fogel, 2002) including arithmetic cross over, simple cross over, and heuristic cross over.

- Mutation

  The mutation operator modifies one point either randomly or in a specific search direction. In many cases, the mutation could help in breaking off local optima. The role of the mutation depends on its type. The mutations that are used in the genetic algorithm code in this thesis are (Michalewicz and Fogel, 2002) including uniform mutation, whole uniform mutation, boundary mutation, non-uniform mutation and Gaussian mutation.

CHAPTER 4

ONE DEGREE OF FREEDOM SYSTEM

In this chapter, input shaping is applied to a one degree of freedom model. The main contribution in this model is that it combines input shaping, with a PI controller in the presence of nonlinearities. Section 4.1 describes the general model. Section 4.2 introduces the previously researched one degree of freedom model with PD controller and Coulomb friction, and the new model with PI controller in the presence of friction and saturation. Section 4.3 defines the objective function for these two types of models for the zero vibration (ZV) input command set and the zero vibration and derivative (ZVD) command set. Sections 4.4 describes the sequence of solving the model and applying it to the experimental set up and the system identification procedure. Finally, in section 4.5 the simulation and the experimental results are presented and compared.

4.1. DESCRIPTION OF THE MODEL

The first model that was used in the application of input shaping is a one degree of freedom model consisting of a mass, a damper and a controller. Although this model is simple, yet the presence of nonlinearities such as the Coulomb friction and saturation complicates it. This model was based on an experimental device produced by Quanser Consulting Inc[1]. Fig. 4-1 is a schematic representation of the actual model present in the lab:

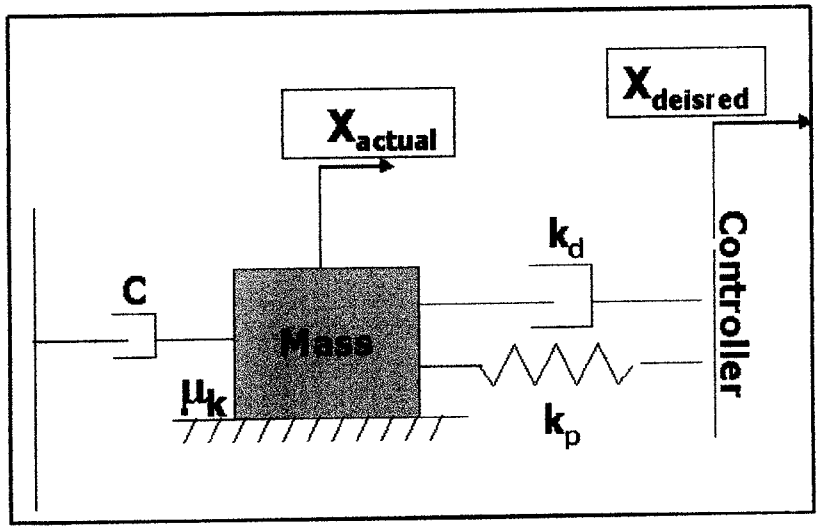

Fig. 4-1: Schematic drawing of One degree of freedom model

The mass block represents a cart subjected to both static and dynamic friction depending on the status of motion of the mass. The friction applied to the cart is both sliding friction and rolling friction. The front of the cart is held on two small rods to which a gear and a pinion are attached that allow the motion of the cart on a linear rack (see Fig. 4-2). The gear acts as an encoder that allows the measurement of the position of the cart. The back of the cart is held on a long rod that causes the sliding friction of the cart. There is an extra weight added to the cart to prevent it from being lifted off the track. The cart is driven by a motor that delivers the motion to the gear thus causing the motion of the cart to the right and left.

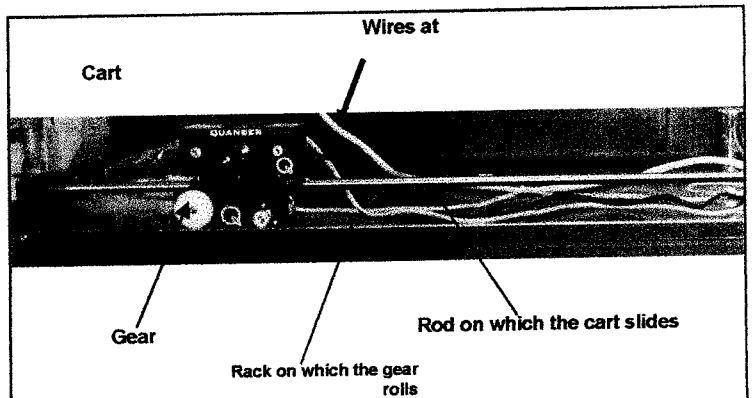

The controller is mainly designed in a computer program and communicates with the cart through a board and wires connected to it. The wires represent another type of friction that affects the motion of the cart. Depending on the position of the cart the wires increase or decrease the friction. In Fig. 4-1, the controller is represented by physical components such as a spring for the proportional controller (k_p) and a damper for the derivative controller (k_d). The position of the controller is the desired position of the cart ($X_{desired}$), while the actual position of the cart is X_{actual}. The damper on the left is a physical representation of the back EMF of the motor. The expression for this term will be developed in the section 4.4.

4.2. ONE DEGREE OF FREEDOM MODEL WITH PD AND PI CONTROLLERS

In this section, the equations describing two models are presented. The first model is the one with a PD controller, which was researched by Lawerence, et al. (2002). The second is the same model with a PI controller.

4.2.1. PD MODEL

The first model that is used simply expresses the schematic diagram in Fig. 4-1. This case of PD controller has been solved previously, and also analytical results were obtained for such model whether with friction (Lawerence et al., 2000) or without friction (Singer and Seering, 1990). However, it is essential to demonstrate at this stage the possibility of using optimization together with numerical integration to prove that the new approach for the determination of the input command is capable of producing same results as the analytical solution, and that it is general since it can include any nonlinearity in the system, which is sometimes difficult to include in case of analytical solution.

The model is presented in state space equations on which the numerical integration is based. In this case there are two state space variables which are the position of the cart and the velocity. The equation describing the model is:

$$m_b \ddot{x} = \left(F_{CONT} - \mu_K N \bullet sign(\dot{x}) - k_p x - (c + k_d)\dot{x} \right) \tag{4-1}$$

where F_{cont} is the controller force represented by the following expression

$$F_{cont} = k_p x_d + k_d \dot{x}_d \tag{4-2}$$

where $x_d, \dot{x}_d$ are respectively the desired position and velocity of the controller. Since the controller is digital, the velocity of the controller is calculated based on the rate of change of position using the same time step as the one used in the integration code.

$$\dot{x}_d = \frac{x_{dcur} - x_{dprev}}{t_{step}} \tag{4-3}$$

where x_{dcur} is the current position of the controller, x_{dprev} is the previous position of the controller and t_{step} is the time step. The time step shouldn't be less than the sampling time of the controller. The numerical integration used is Runge Kutta RK_4 where the two equations to be solved are:

$$\begin{aligned} &for: x1 = x, x2 = \dot{x} \\ &\dot{x}1 = x_2 \\ &\dot{x}_2 = \frac{1}{m_b}\left(F_{CONT} - \mu_K N \bullet sign(\dot{x}) - k_p x - (c + k_d)\dot{x} \right) \end{aligned} \tag{4-4}$$

Two conditions are to be specified which deal with the maximum input voltage to the system

$$V_{in}(voltage) = k_d\left[\frac{(x_d - x_{dprev})}{t_{step}} - x_2\right] + k_p(x_d - x_1) \tag{4-5}$$

A condition is specified to set the velocity and acceleration equal to zero when the force applied is less than the static friction force, and the velocity is less than 0.001 m/s. By developing the Runge Kutta integration code, with appropriate time step, a response for the system is developed. The structure of the code is as follows:

1. Determine the input to the system: impulse or step
2. Apply it by varying the value of the desired position of the controller at the required time of the input application. In order to calculate the velocity of the controller, the previous value of the position has to be recorded. For the first step, the value of the previous position (x_{dprev}) is equal to zero.
3. Perform the calculation for the constants of the RK4. In each calculation, the function with the equations describing the model (Model Code) is called.
4. Then the value of the velocity and acceleration is determined for this time step, and are used as the initial point for the next integration step.
5. Steps 3 and 4 are repeated until the end of the period of integration.

4.2.2. PI MODEL

This model is an extension of the previous model where instead of a PD controller, a PI controller is used. In this case all the sequence of equations will be the same as the PD model, except for the controller equation which will be:

$$F_{cont} = k_p x_d + k_I\left(\sum error\right)t_{step} \tag{4-6}$$

In equation 4-6, the integral controller gain is multiplied by the integration of the error function. In this case, the integration code will include an extra expression for calculating and recording the cumulative error at each time step in order to feed it to the model code.

4.3. OBJECTIVE FUNCTIONS FOR THE MODEL WITH PD AND PI CONTROLLERS

The definition of the objective function varies with the type of the model and the type of the input command. There are two main types of input commands that are investigated which are the zero vibration (ZV) and the zero vibration and derivative (ZVD) input commands. Thus, objective functions will be defined for four models:

- Model with PD controller and ZV input command.
- Model with PD controller and ZVD input command.
- Model with PI controller and ZV input command.
- Model with PI controller and ZVD input command.

For the ZV shaper with PD controller case, the goal was to reach the desired position with zero velocity, thus the objective function is:

$$Objfun = |x - x_d| + |\text{velocity}| \tag{4-7}$$

The above function has two terms, and since each term has to be minimized, the function yields itself as a multi-objective optimization problem. However, when there are several objectives at hand, they should be having the same order of magnitude, otherwise one of the objectives will dominate the other during the search. Therefore the velocity term is scaled by dividing it by the natural frequency of the system, which is a constant value. This was found to keep both terms in the same order of magnitude. Moreover, an undamped system with an

$$Objfun = |x - x_d| + \left| \frac{\dot{x}}{\omega_d} \right| \tag{4-8}$$

For the ZVD shaper with PD controller, the objective function is composed of two main parts which sets the vibration equal to zero and the derivative of the vibration with respect to the natural frequency equal to zero. In order to obtain an expression for the derivative of vibration level function with respect to the natural frequency of the system, numerical differentiation with three points forward differencing will be used. For a function f to be differentiated with respect to one of its variables x, the first derivative will be computed as follows:

$$f' = \frac{1}{2}\left(\frac{-f(x) + 4f(x+dx) - 3f(x+2dx)}{dx} \right) \tag{4-9}$$

where dx is the change in the variable x. In the case of the model, x is be the natural frequency, and dx and 2dx represent 2.5% and 5% changes in the natural frequency respectively. The computer code will calculate the response for these extra two values of the natural frequency at each time step. Central differencing method was not suitable for this kind of application because of the symmetry in the sensitivity graphs of the ZV and ZVD shapers. In Fig. 2-3 it can be seen that around the designed value of the natural frequency, both ZV and ZVD have zero vibration level. Moreover, at any two symmetric points at the frequency axis, the level of vibration is the same. Thus, in order to be able to distinguish between the response for ZV and ZVD input commands, two successive non symmetric points will be used, which favors in this case the use of either backward differencing or the forward differencing method. The terms used in defining the objective function are:

$$Term_1 = |x - x_d| + \left| \frac{\dot{x}}{\omega_n} \right| \tag{4-10}$$

$$Term_2 = |x_2 - x_d| + \left| \frac{\dot{x}_2}{\omega_n + d\omega_n} \right| \tag{4-11}$$

$$Term_3 = |x_3 - x_d| + \left| \frac{\dot{x}_3}{\omega_n + 2d\omega_n} \right| \tag{4-12}$$

where the subscript 2 & 3 designates the values of position and velocity obtained by increasing the gain by 2.5 % and 5% respectively. Thus the objective function becomes

$$Objfun = term_1 + \left(\frac{-term_1 + 4term_2 - 3term_3}{2d\omega_n} \right) \tag{4-13}$$

In the case of PI controller, the objective function definition is modified because of the presence of the integral controller. The input shaping commands dampen the oscillations of the system. However, by definition, the integral controller takes action based on the summation of the error function. Thus it cumulates the error in the response at each stage, and feedbacks a signal based on this error summation. Although the system response might reach the desired position, yet, the integral controller still inputs further signals to the system leading to further oscillations. This is seen in Fig. 4-3 where the response obtained from the linear ZV input command set reaches the desired position, then starts to oscillate again. This is the same for the response obtained from the input command optimized using the previous objective function. In other words, the integral controller adds another pole to the system,

yet the third pole of the integral controller which is an overdamped one had not settled yet. The current definition of the objective function (traditional function)^2 doesn't include the settling of this last pole. Another objective function is defined based on the Fourier series of the response. By obtaining the Fourier transform of the response between the end of the final step and an extra oscillation period, the frequency of the oscillations in the response. By minimizing this function, all the oscillations should cancel out.

Some oscillations remain because the command that executes the Fourier transform is based on summing the responses at each point. The oscillations of the two underdamped poles are superimposed on the settling curve of the third pole. It is necessary to separate these two types of responses in order to apply the Fourier transform effectively. This is done by assuming that the settling curve of the over damped pole is a straight line connecting the start point after the final input step and the end point after a period of oscillation. This line is subtracted from the total response of the system after the final input step, and then the Fourier transform is applied.

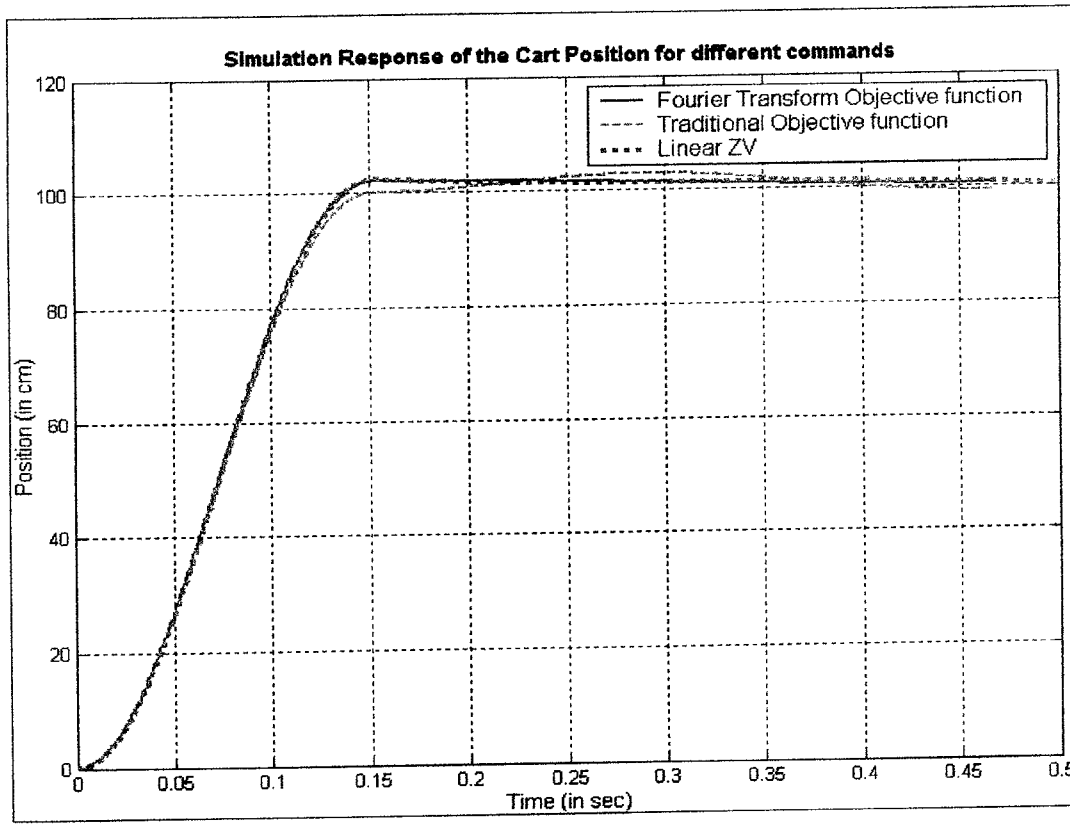

Fig. 4-3: Comparison of the simulation response for the linear ZV command, and the commands generated by the traditional objective function and the new objective function.

By comparing the linear ZV command (described in the literature review), the traditional objective function and the new objective function, it can be noticed that the latter leads to zero oscillation (see Fig. 4-3). It slightly overshoots; however, it reaches the desired position without vibrations. It also gives the same response as that of the linear ZV command. Moreover, as shown in Fig. 4-4 and Fig. 4-5 , the mesh plot for the variation of the traditional objective function versus the step amplitude and timing for a ZV command has several local optima as compared to the new objective function.

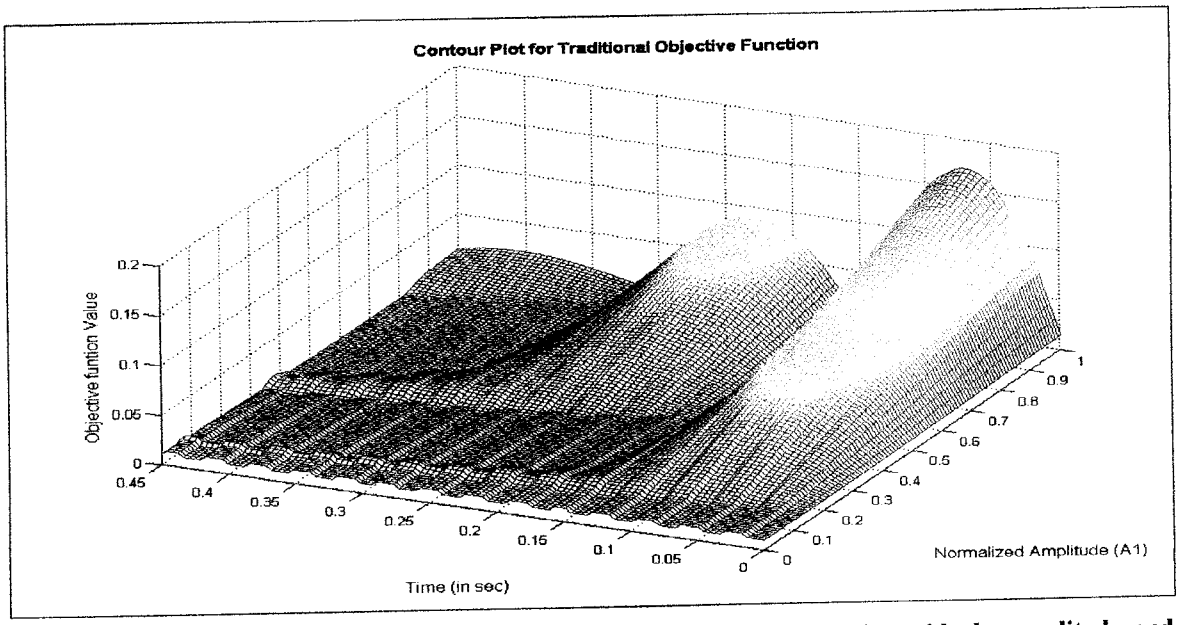

Fig. 4-4: 3D mesh showing the variation of the traditional objective function with the amplitude and timing of a two step command for a zv shaper (step size :1cm)

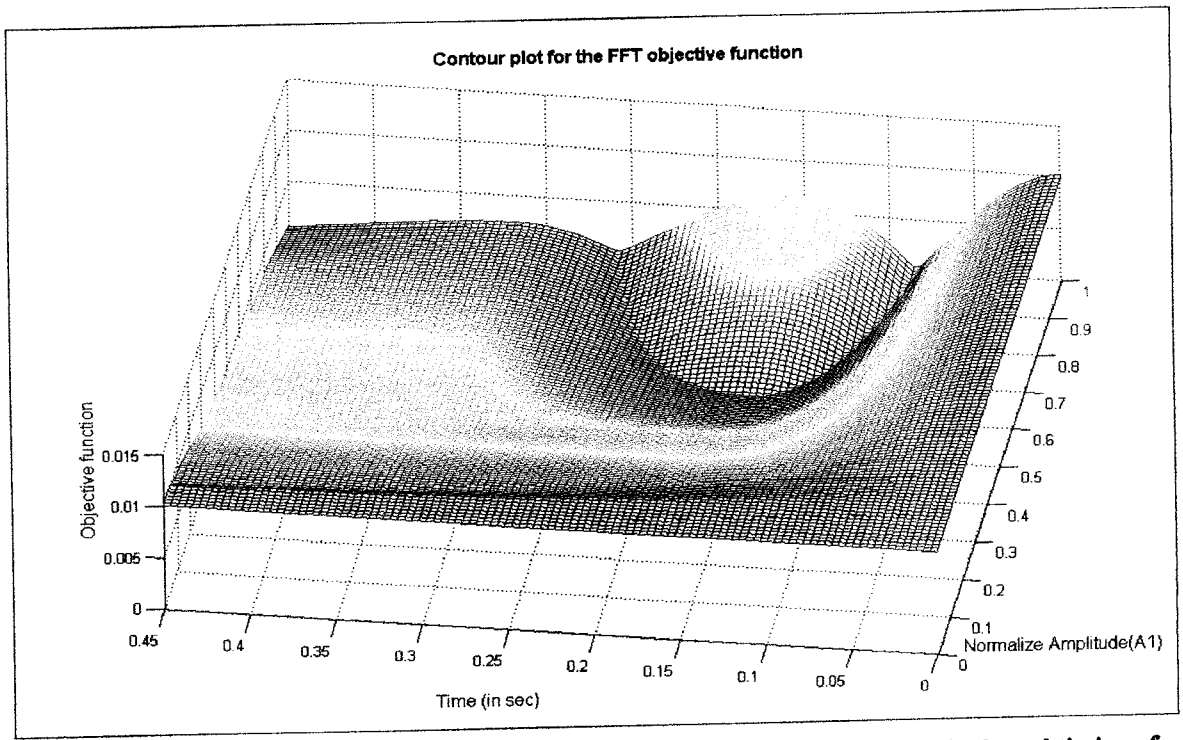

Fig. 4-5: 3D mesh showing the variation of the FFT objective function with the amplitude and timing of a two step command for a zv shaper (step size :1cm)

This definition is extended in the case of ZVD input commands in order to set the

is done by computing the Fourier transform for the two other frequencies, and performing the forward differencing differentiation as previously described. This method gives better results, yet a problem remains since the final position is not accurate. Thus another term comparing the final position of the cart to the desired position is added. For the ZVD case, two objective functions were applied; the first takes the derivative of the Fourier transform part with respect to the natural frequency, without taking the derivative of the error in the final position. The second takes the derivative of the total error function. The reason for that is to test different objective functions, and their corresponding command.

With these variations, the PI system with ZV input command has two choices of objective functions, one setting the error in position and velocity equal to zero (Traditional ZV objective function), and the second (ZV/fft) taking the Fourier transform of the oscillatory response. The PI system with ZVD input command has also two choices of objective functions: the first one (Objfun1: (4-14)) using the Fourier transform and it derivative with respect to the natural frequency, and including the error in position only.

$$\left(1+\frac{\partial}{\partial\omega_n}\right)fft(response)+|x-x_d| \tag{4-14}$$

The second function (Objfun2: 4-15) uses both the Fourier transform & the error in the final position and their derivatives.

$$\left(1+\frac{\partial}{\partial\omega_n}\right)\left(fft(response)+|x-x_d|\right) \tag{4-15}$$

4.4. IDENTIFICATION AND VERIFICATION OF THE MODEL

In this section, a general sequence is presented to show how to apply a given set of input on to the experimental set up, showing how the voltage is transferred to a force applied to the machine.

The desired controller is designed on SIMULINK using the parameters previously calculated. The model is built by a C code provided by the supplier in order to be able to communicate with the physical device. The newly built code is run giving a signal for the motor to start. The motor equations which are depending on the voltage are as follows[3]:

$$V = I_m R_m + K_m K_g \omega_g = I_m R_m + K_m K_g \frac{\dot{x}}{r} \tag{4-16}$$

The torque and Force generated by the motor are

$$\begin{aligned} T &= K_m K_g I_m \\ F &= \frac{T}{r} \end{aligned} \tag{4-17}$$

By developing the above equation, a final expression of the force can be generated based on the voltage:

$$F = \frac{K_m K_g}{R \times r} V - \frac{{K_m}^2 {K_g}^2}{R \times r^2} \dot{x} \tag{4-18}$$

The coefficient of $\dot{x}$ represents the back EMF of the motor and this is represented on the schematic drawing by a damper (Fig. 4-1). Equation 4-18 offers a theoretical formula to calculate this damping factor. However, the actual damping and the friction force are determined in the lab in order to recalibrate the device. Once the machine starts to move, the encoder in the gear starts to measure the position of the cart and feeds it back to the computer

in order for the controllers to produce the next set of signals. Real time graph plots are developed on the computer describing the motion of the mass.

The next step is to define the different parameters of the system. The main parameters that need to be determined are the dynamic friction of the model and the damping coefficient. These parameters are defined by performing a series of experiments where the input is a ramp with different values. The input voltage is compared to the desired velocity value (ramp value), and by linear regression, a line is fitted to these points. The steps to determine the friction and the damping of the system start by inputting a ramp command and its opposite one to the system such that it covers the whole track of the cart back and forth. From the velocity graph of the cart, an average value of the velocity for the forward and backward travel of the cart can be obtained. The previous steps are repeated for 40 different input voltages. After obtaining the 40 points, a linear line is fitted where the x-axis is the velocities of the cart, and the y-axis is the input voltages (see Fig. 4-6). Finally, from the intercept and the slope, the friction voltage and the damping of the system can be determined respectively.

It should be noted from the results that the friction is not exactly the same in the forward and the backward travel; however, an assumption is made that they are the same since the difference is very small. The friction is not the same all over the travel track due to the wear in the different parts of the track. Moreover, the presence of the wires at the back of the track affects the friction. When the cart is at the beginning of the track, the wires are in a position of pulling the cart in its direction of motion, which decreases the effect of friction. At the end of the track, the wires are pulling the cart in the reverse direction to its motion, which increase the effect of friction. For this reason, an average value of the friction is calculated by

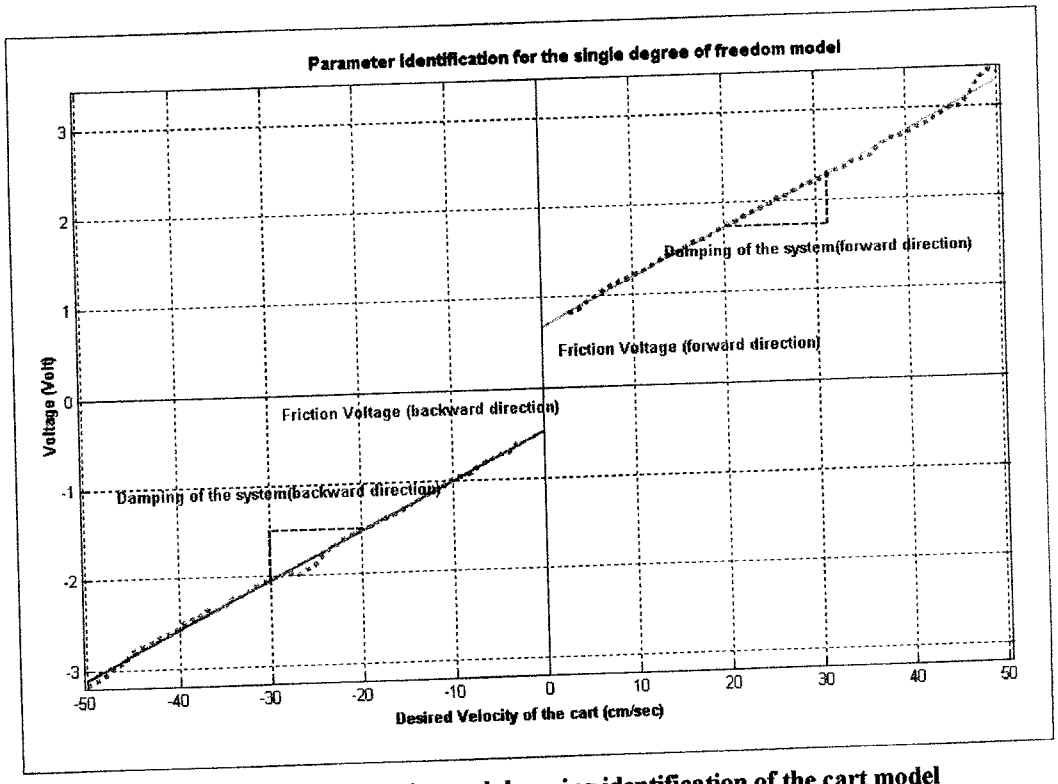

Fig. 4-6:Plot for the friction and damping identification of the cart model

After determining the required parameters of the model, the computer simulation of the model was compared to the actual motion. This was done by inputting different step sizes to the actual system, and comparing it to the computer simulation results. Correction factors are used in order to adjust the differences in the natural frequency and the damping of the simulated and the actual system. By using these correction factors, it is shown that the two responses are quite close with small difference at the end of the step due to the difference in the modeling of the friction as seen in Fig. 4-7.

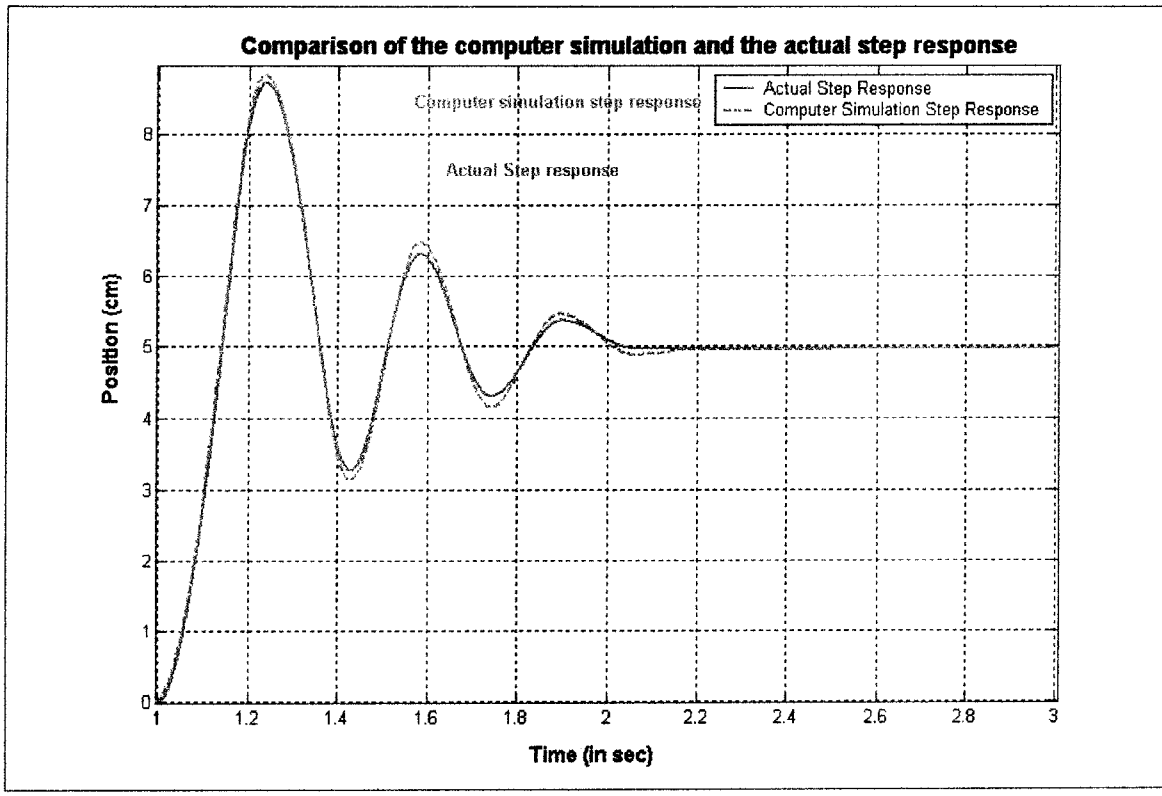

Fig. 4-7: Comparison of the computer simulation and the actual responses

4.5. DISCUSSION & COMPARISON OF COMMANDS AND RESPONSES

For the one degree of freedom model, several comparison scenarios were developed in order to obtain comprehensive results that could be later used without restrictions. All the scenarios that were developed were based on expected performance of the system under the specified conditions. The main factor that determined these scenarios is the effect of nonlinearities on the different responses of the system due to different input commands. These cases, with its corresponding input command will be presented briefly in order to clarify the objective of each one.

The first case is the linear system ZV input command, which was presented in section 2.3.2. As was seen, this type of command was able to set the vibration level to zero, in case of

reduction in oscillations will still take place; however, it is expected that oscillations will be induced. This command will be referred to as *theoretical ZV command*. The second case is a normal step response, but with higher damping (*damped step*). This type of command is frequently applied to systems when no oscillations are desired. Yet the main problem of such command is the high overshoot after this step, which is not desirable in many cases, in addition to the delay that it causes in the settling time of the system. The third case, which is similar to the previous case, is for an S curve input with high damping. This command eliminates the discontinuity in the input command set as compared with a step input. However, due to the fact that the input time is small, still the effect of such input will lead to high overshoot. The results of this type of command are listed in Appendix A for all step sizes. For these three cases, two optimized input commands will be compared. These two commands are based on the optimization of the model with PI controller and ZV input command set using the two objective functions previously specified. The first objective function (*Trad.Obj*) is the traditional objective function that sets the error in position and the velocity equal to zero. The second objective function (*ZV:fft*) is the one that uses Fourier transform to describe the oscillations of the system response.

Considering the ZVD models, the comparison will focus on the theoretical ZVD command that is developed for linear system (*Theoretical ZVD*). As compared with the ZV inputs, this command is more robust when dealing with variations in the system, thus less vibrations are expected. Yet, as the nonlinearities increase, more oscillations are induced. This theoretical command is compared to two commands developed by optimizing the model with PI controller and ZVD input command using also the two objective functions previously

the response, its derivative and the position error. The second objective function (*Objfun 2*) is defined by taking the Fourier transform of the system response, the error in position and the derivative of both terms. This latter objective function is expected to yield more robust results. A comparison of the robustness of such command will be developed by varying the K_p and K_I of the controller by 15%, and considering the corresponding changes in the response.

In order to facilitate the comparison between these different cases, some response parameters are used. The first is the percent overshoot of the final step. This parameter is a key parameter in describing the ability of the system to eliminate extra motion. Second, the settling time required to reach a response within the limits of 5% of the desired position reflect the speed of the response. It is desired to decrease this parameter. The rise time, which designates the time it takes the cart to reach the desired position for the first time, is another measure of the speed of response. The difference between the rise time and the settling time is a good indication of the speed of the response. For fast responses, the settling time and the rise time are the same. Finally, the percent deviation in the final position measures the error in the final position of the response with respect to the desired position. The main essence of this parameter is to ensure that the error in position is within a small percentage. It is shown that these deviations are very small in all cases (see Appendix A)

These different parameters will be used in order to compare the response of the system when the values of the controller are changed. The discussion will focus on cases based on the step size first, than a general comment will be made summarizing all the cases.

STEP SIZE: 1CM

At this step size, the main nonlinearity is the effect of friction on the system. As previously mentioned, the effect of friction on the final position of the cart is cancelled by the integral controller that eliminates the steady state error. The responses of the ZV and the ZVD case are presented in Fig. 4-8 and Fig. 4-9 respectively. For all the cases, the cart reaches the final position with a maximum error of 0.87% for the theoretical ZVD and a minimum of 0.04% for the optimized ZV (Trad. Obj).

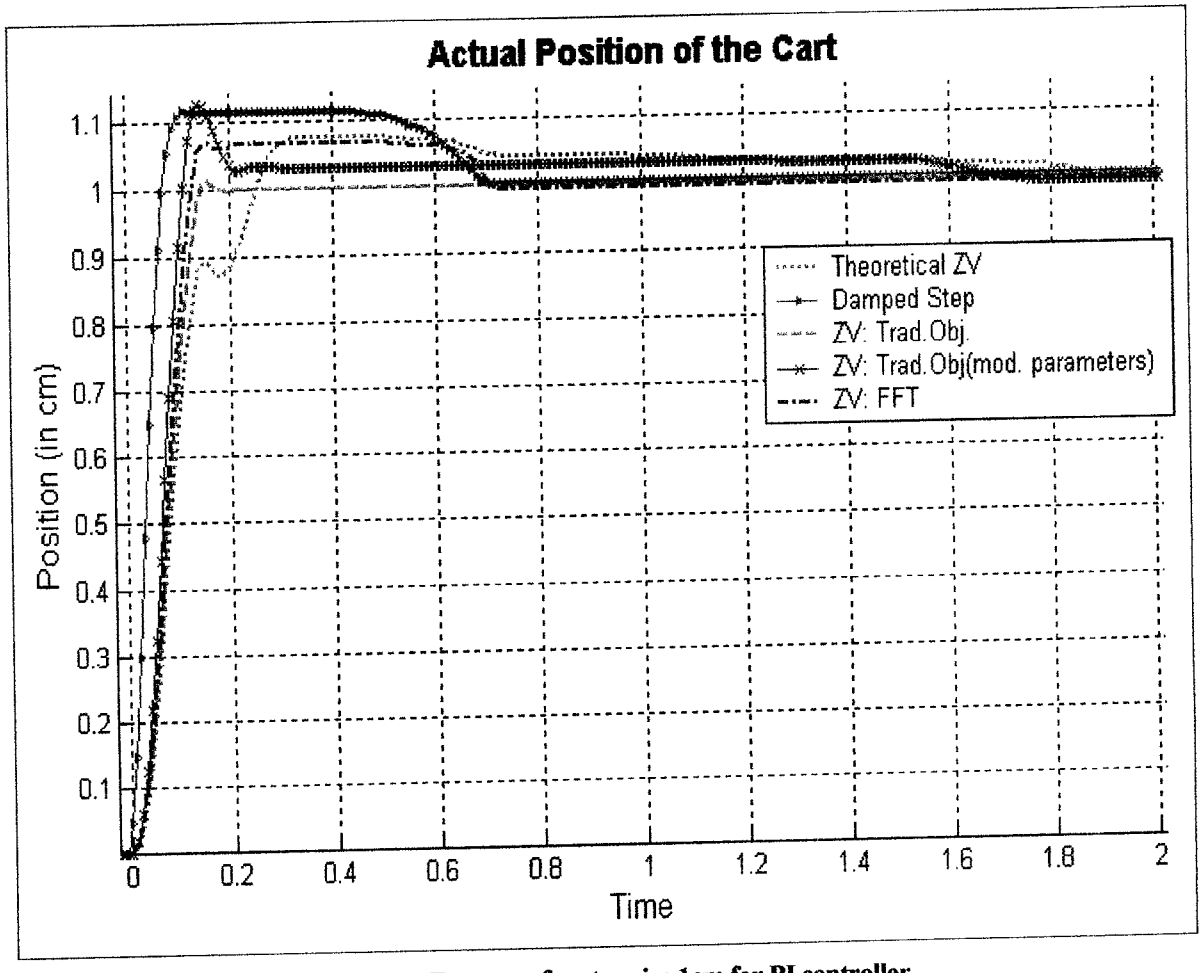

Fig. 4-8: ZV Response for step size 1cm for PI controller

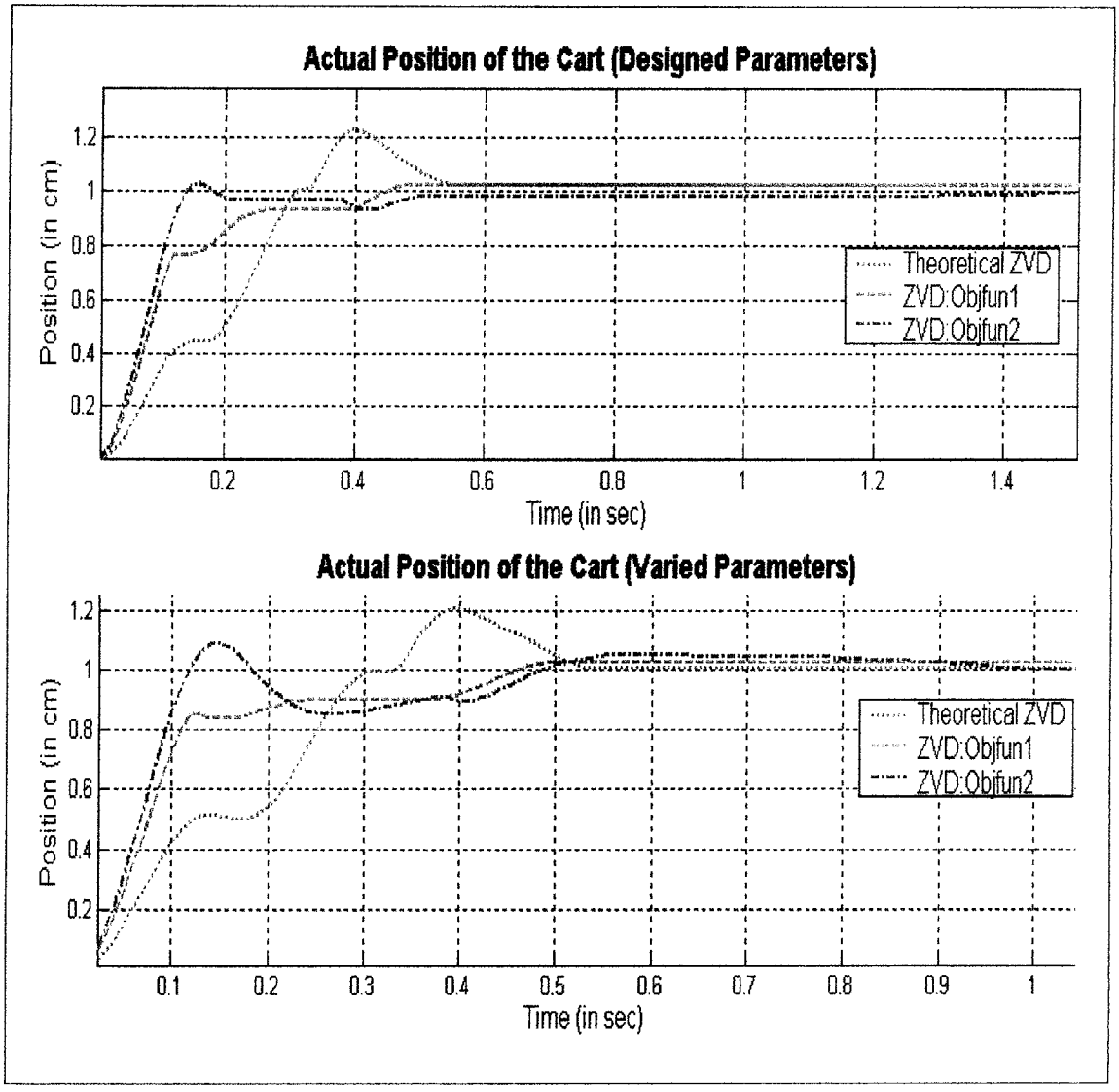

Fig. 4-9: ZVD responses for step size: 1cm for PI controller

The S-curve results were eliminated from the comparison because of the high overshoot it causes to the system (see Fig. 4-10). Fig. 4-11 summarizes the results for the different input command sets. The details of the results are shown in Table A-2, where the amplitudes of the incremental step sizes, and the cumulative times are included.

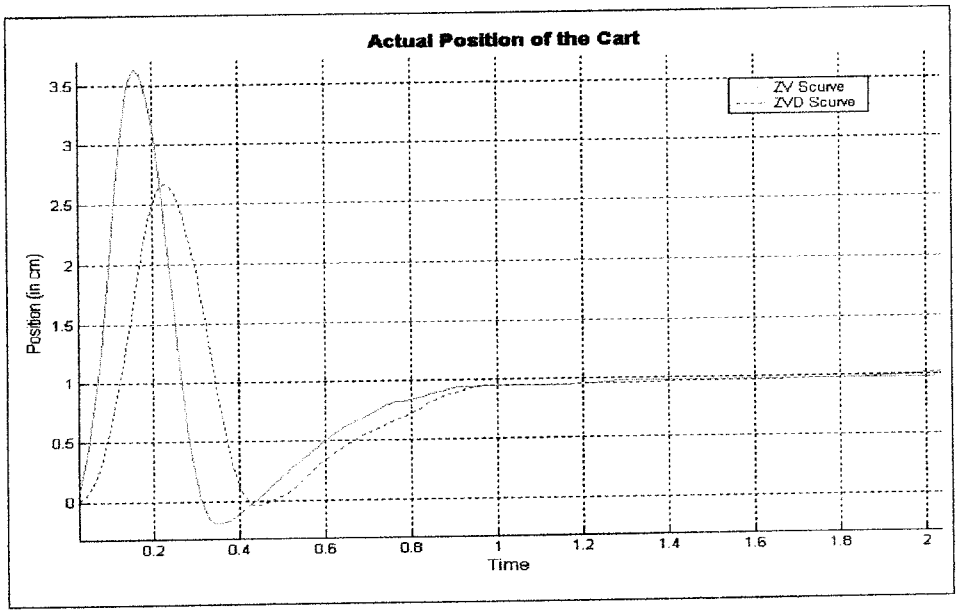

Fig. 4-10: Actual Response for Scurve commands for ZV and ZVD cases

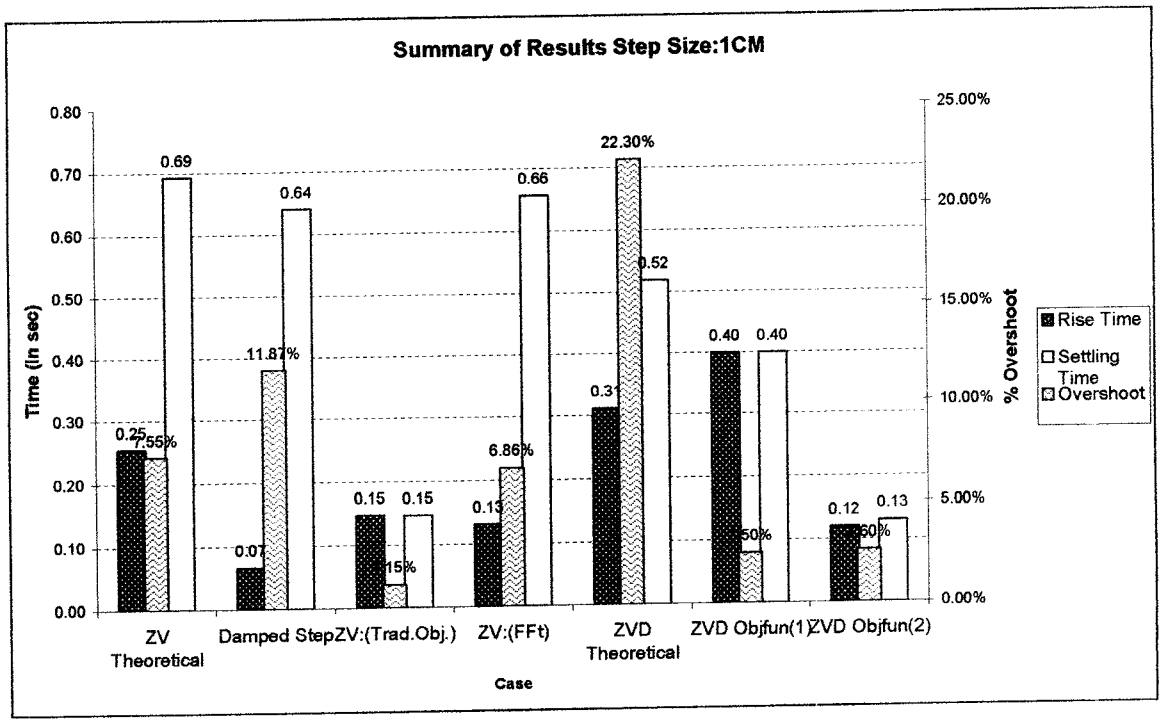

Fig. 4-11: Comparison of results for step size:1cm for PI controller

Overshoot:

The theoretical ZV command minimized the overshoot considerably if compared to

respectively 7.66% & 11.87%. The theoretical ZV command, which is only based on the damped frequency of the system and damping ratio, ignores the effect of friction on the system. Thus when comparing the optimized commands with the theoretical ZV, it is clear that the former ones lead to a smaller overshoot. The command obtained from the traditional objective function (Trad.Obj: setting the error in position and velocity equal to zero) results in 1.15% overshoot, while the ZV:fft objective function is 6.86%. It was expected that the traditional ZV objective function would result in further oscillation. As previously explained, this objective function provides a set of input commands that damp the two complex poles, while not taking into consideration the third overdamped pole. Yet, due to the fact that the displacement is small, the vibrations induced by this third pole are damped by the presence of friction, and thus don't appear neither on the simulated nor the actual response. Unexpectedly, the theoretical ZVD command resulted in higher overshoot than the theoretical ZV. The reason for that is the presence of friction for a small step size, which substantially magnifies the effect of nonlinearity in the system. For the optimized command using objective function 1 or 2, the overshoot was 2.5%, which is considerably low as compared to the (ZV: fft) case.

Rise & Settling time:

The rise and the settling time of the theoretical ZV are respectively 0.3 and 0.7 seconds, while the results of the optimized command (ZV: Trad.Obj) are respectively 0.1 & 0.1. It can be seen that for this command that the position is reached directly, thus offering a fast response as compared with the theoretical ZV. Although the damped step response has a small rise time (less than 0.1), yet the high overshoot increased the settling time to 0.6 seconds. As can be seen, the optimized command (ZV: fft), lead to fair results in terms of the

the rise time is higher than the case of the ZV, which is attributed to the delay in the command by half a period. Yet, the settling time of the theoretical ZVD (0.5 seconds) is less than the theoretical ZV. For the optimized commands, the settling times of Objfun1 & Objfun2 are respectively 0.4 and 0.1. It can be noticed that these two commands settle quickly, thus the settling and rise time are the same, thus leading to a fast response.

Variation of Parameters

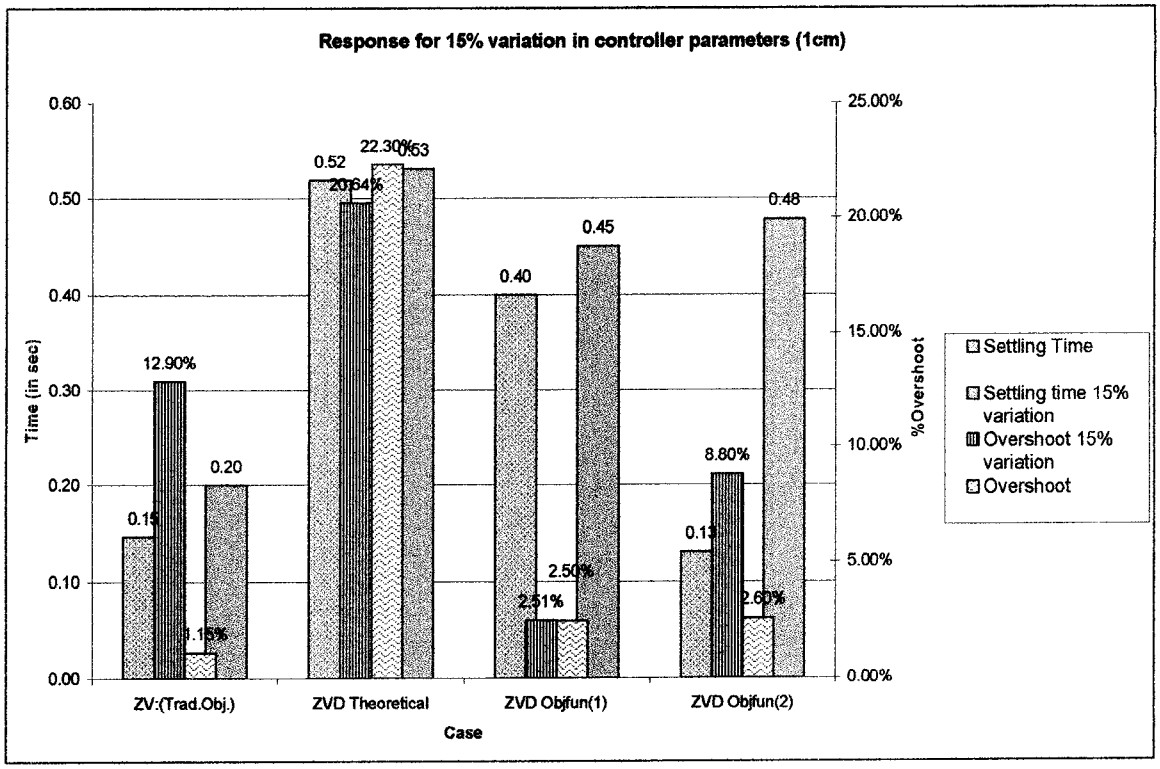

Fig. 4-12: Effect of controller parameter variation on the different commands (1cm) for PI controller

The variation of the controller parameters is applied to the best ZV optimized command (ZV: Trad.Obj) and the three ZVD commands. This change leads to a considerable increase in the overshoot percent of the ZV command to reach 12.9%, an the settling time (0.2 seconds) while for the theoretical ZVD command, the overshoot decreased to 20.6%, and the

seen that the ZVD optimized command maintained some robustness to variation as compared to the ZV optimized command (see Fig. 4-12). From the computer simulation responses, the ZVD 2nd objective function was expected to have higher robustness as compared to the first one, yet it showed increase in overshoot and settling time. This is mainly attributed to the presence of some modeling error.

Thus for this step size, the theoretical commands lowered the vibration level as compared to a step response. However, due to the presence of nonlinearity, the optimized commands offered lower overshoot % and faster settling time. The robustness of the theoretical ZVD and the optimized ZVD using the second objective function were highest compared to the other remaining cases, yet the optimized ZVD commands still lead to lower vibration level for the designed and the varied cases.

STEP SIZE: 5CM

As the step size increases, the friction force becomes less effective as compared to smaller step sizes. The effect of saturation starts to affect the efficiency of the theoretical commands. Moreover, the overdamped pole of the system induces further vibrations that are not cancelled by the effect of the friction. The S-curve input command with high damping results in very high overshoot for the ZV and the ZVD case, thus it will be eliminated from the comparison (see Appendix A). The comparison of the results is presented in Fig. 4-13 (for result details see Table A-3).

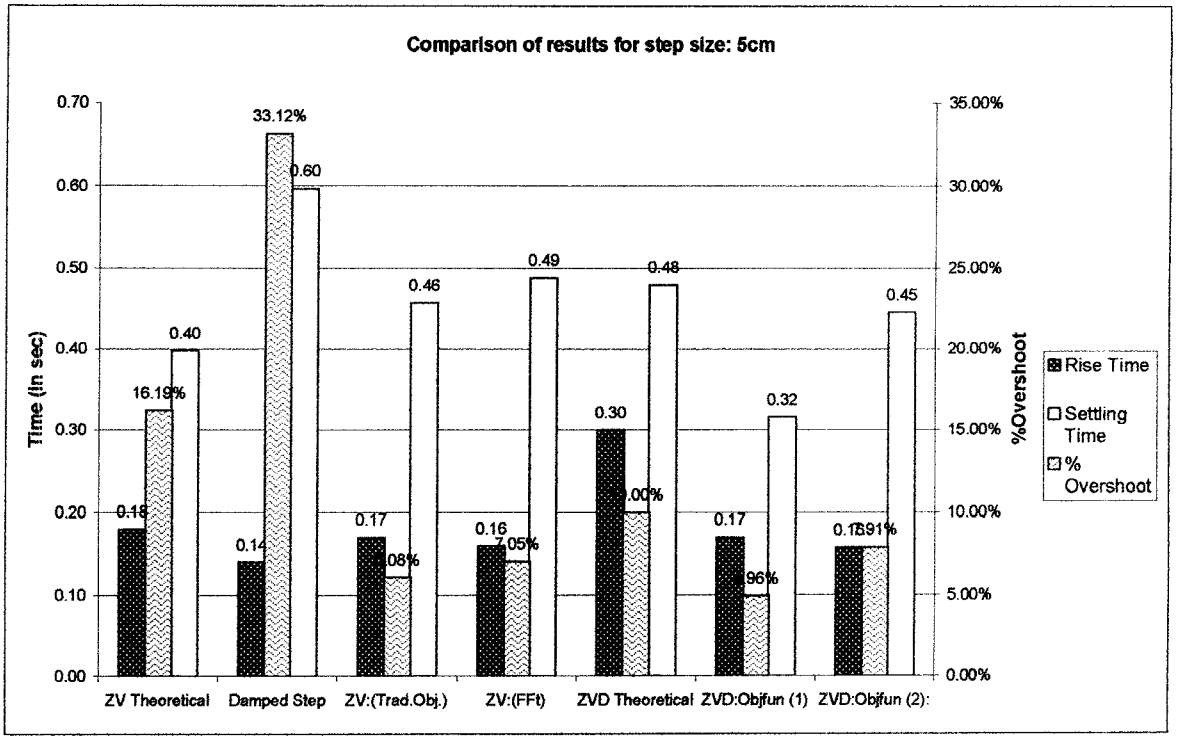

Fig. 4-13: Comparison of results for step size: 5cm for PI controller

Overshoot:

The highest overshoot result from the damped step command to reach 33% of the step size, while the theoretical ZV command is 16%. This shows the effect of applying input shaping to minimize vibration. However, the theoretical ZV command was expected to further reduce the vibration, but due to the presence of the saturation and friction, it still produces a higher overshoot. The two ZV optimized commands offer a lower overshoot ranging from 6% for the traditional objective function (ZV:Trad.Obj) to 7% for the ZV:fft objective function. The oscillations are still low (Trad.Obj) due to the presence of friction, which is still not negligible at this step size. The overshoot decreases considerably by using the ZVD commands. The values of the overshoot of the theoretical ZVD, ZVD (objfun1) and ZVD (objfun2) are respectively 10%, 5% and 8%. As expected, the theoretical ZVD is able to

overshoot especially using the 1st objective function (fft+ derivative (fft) + the final position error). The decrease in the overshoot is 50% when comparing the optimized command (objfun1) and the theoretical ZVD.

Rise and settling time:

Although the rise time of the damped step is the lowest, yet the settling time is large due to the high damping and the large overshoot. While the overshoot of the theoretical ZV command is high compared to other commands, and so is the rise time (0.2 sec), yet the settling time (0.4 sec) is lower than the optimized ZV commands (0.5 sec). The settling time for the optimized ZV command using the traditional objective function (Trad.Obj) is close to theoretical ZV command. For the ZVD theoretical commands, the rise time and the settling time is higher than the theoretical ZV which is expected. As for the optimized ZVD commands, the rise time (0.2 sec) is nearly the same as the optimized ZV. This might lead to slight decrease in the robustness of these commands. However, it can be noticed that the settling time of the command (Objfun1) are the smallest (0.3 sec) as compared to all other responses.

Variation of Parameters

By varying the controller parameters by 15%, it can be noticed that slight variations in the parameters of the response changed. However, the response could be qualitatively judged to have more oscillations. For the optimized ZV command using the ZV:fft function, the overshoot increased from 6% to 7.5%, and the settling time slightly increased. The intermediate oscillations are higher in this case. For the theoretical ZVD command, the

response, while (Objfun2) maintained higher level of robustness. The response for the different cases is presented in appendix

STEP SIZE 10CM

At this step size, the effect of friction can be considered as negligible, and the main source of nonlinearity is the saturation of the system and the presence of the overdamped pole that will cause further oscillation by exciting the other two complex poles. By closely examining the results shown in Fig. 4-15, the following can be noticed (for result details see Table A-4):

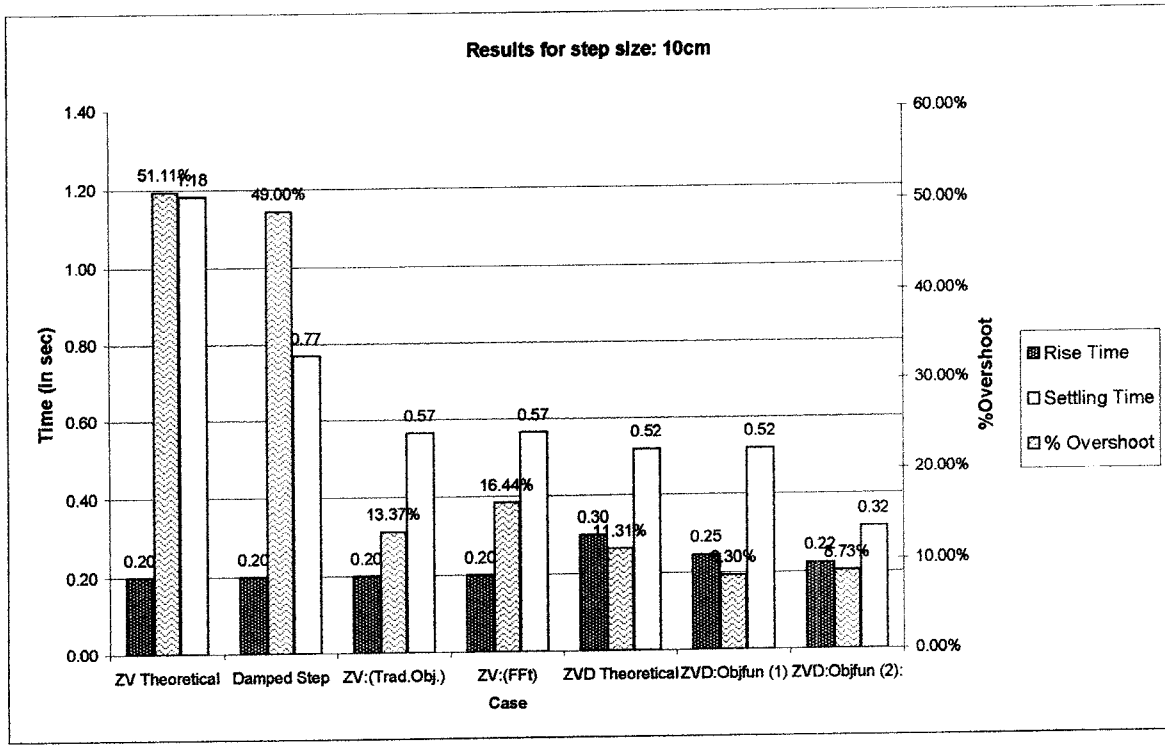

Fig. 4-15: Comparison of results for step size: 10cm for PI controller

Overshoot:

The theoretical command whether the ZV one or the damped step, will result in an overshoot of 49% to 51%, which is certainly very high. The main factor that leads to the

and objfun2 the overshoot was 8.5%. The optimized ZVD commands reduce vibration considerably as compared to all other commands.

Rise time and Settling:

The rise time for all ZV commands varies with a limit of 0.2 (sec), while for the ZVD commands it ranges from above 0.2 in the optimized cases, to 0.3 in the theoretical case. As the overshoot of the theoretical ZV and the damped step is high, their settling times (1.2 and 0.8 seconds respectively) are high. For the optimized ZV commands, the settling time is much lower (0.6 seconds). As for the ZVD commands, the optimized command offers the smallest settling time (0.3 seconds)

Variation of Parameters:

As shown in Fig. 4-17, by varying the controller's parameters by 15%, slight increases in the overshoot and settling time occurred.

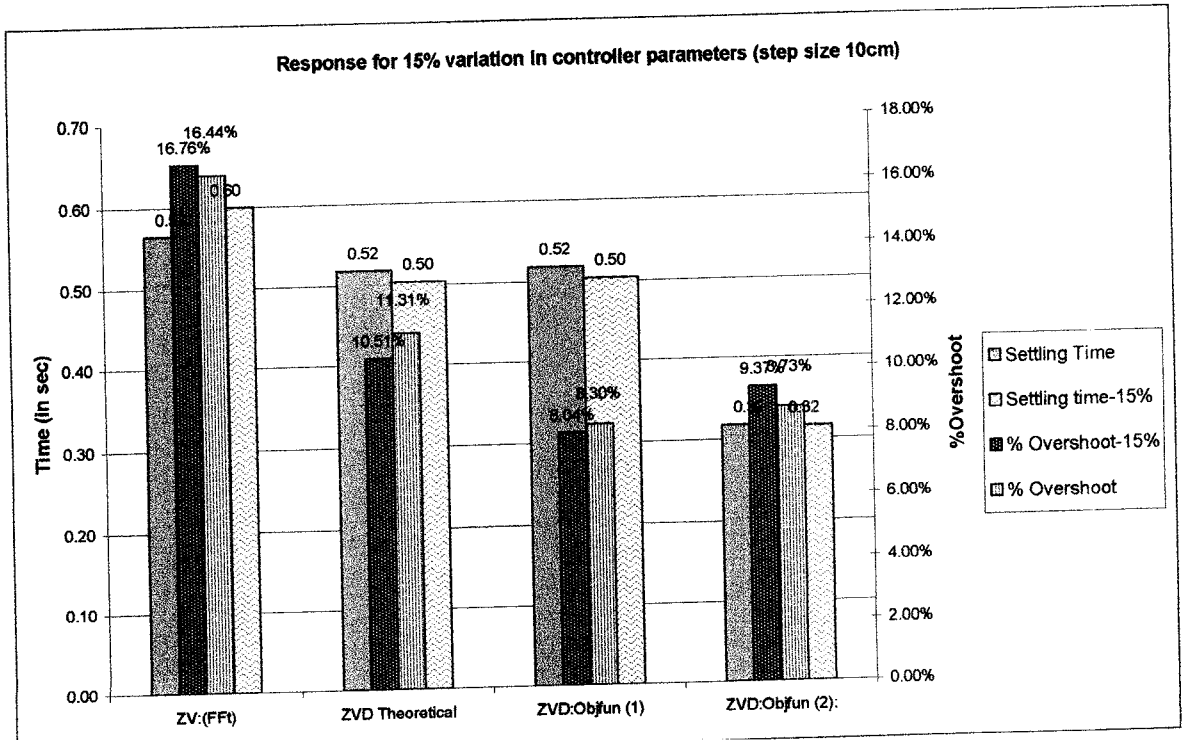

It can be seen that the main variation is in the response shape in the case of the ZV commands where more oscillatory response is depicted, whereas the ZVD commands still maintain nearly the same shape. It can be seen that the optimized ZVD commands perform better that the optimized ZV command and the theoretical ZVD commands.

Thus, for this step size, the optimized ZVD commands provide the smallest overshoot, and the fastest response in terms of settling time. Although these command have a slight delay in the rise time, but the fact that the oscillation level is minimal leads to this fast and steady response.

STEP SIZE 20CM

Similar to the previous step size, the same nonlinearity effects are present with are larger pronounced effect of the saturation and the extra pole in the integral control. The results in Fig. 4-18 show the following (for result details see Table A-5):

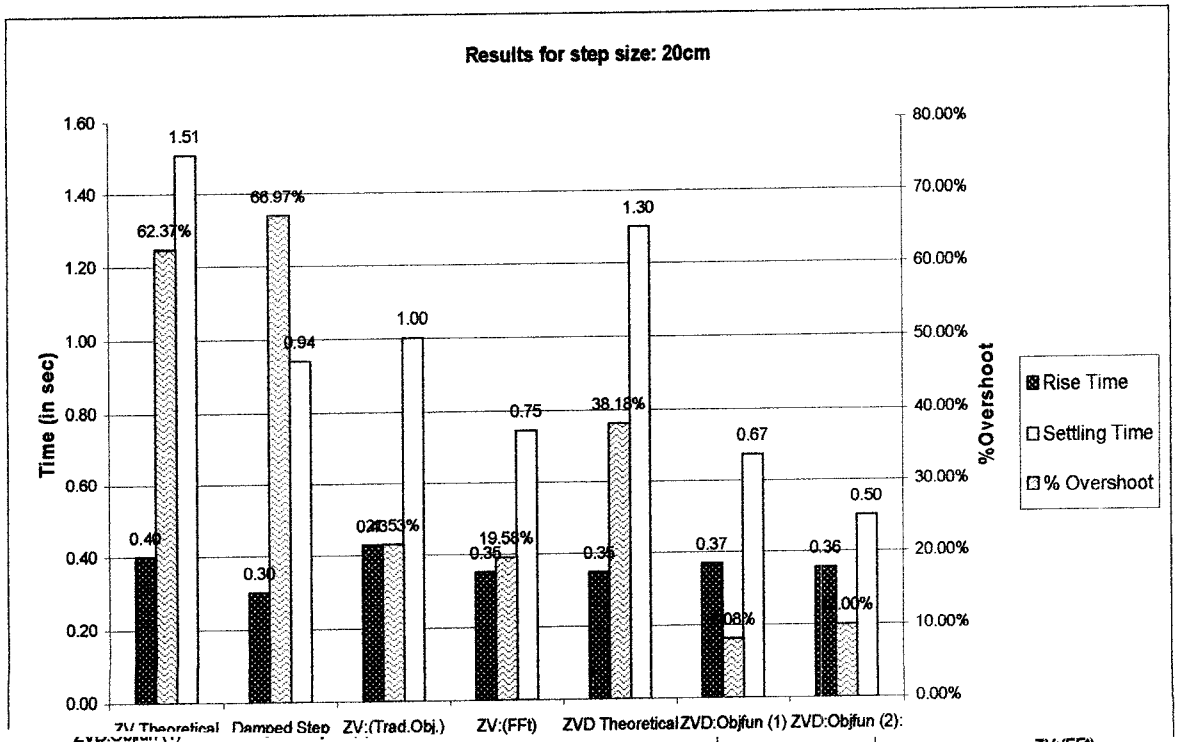

Overshoot

In the case of the theoretical ZV command and the damped step, the overshoot percent reaches 62% and 67% respectively. By considering the optimized command, the overshoot increased as compared to the previous step sizes, yet its values are far less than the theoretical command. The ZV optimized command using the traditional objective (Trad.Obj) function leads to an overshoot of 21.5% as compared to the other optimized command (ZV: fft) where the overshoot is 19.6%. By examining the two responses, it will be found that the oscillation level for the first case is much higher than the second case where there are almost no oscillations. The theoretical ZVD command failed also to reduce vibrations since the overshoot is 38%. It is clear that at this stage, the saturation caused a considerable shift in the natural frequency of the system thus canceling the damping effect of the theoretical ZVD commands. For the optimized ZVD commands, the overshoot is within the same ranges as the previous step size cases. For the case of objfun1 and objfun2 the overshoot is 8% and 10% respectively. Moreover, the system response has slight oscillations, which is reflected in the low settling time.

Rise time and settling time

The rise time for all commands falls within the same range of 0.3 to 0.4 seconds. It is worth mentioning the substantial variations in the settling times of each command. The theoretical ZV command and the damped step have a settling time of 1.5 and 0.9 sec respectively, while the settling time for the optimized commands using the traditional objective function Trad.Obj and the ZV:fft function are 1 and 0.7 (sec) respectively. While these numbers differ by fraction of seconds, however, the variation increased considerably for this step than

of 1.3 (sec). The optimized ZVD commands have settling times of 0.7 and 0.5 (sec) for objfun1 and objfun2 respectively.

Variation in parameters

At this step size, the variation in the controller parameters slightly affects the parameters of the ZVD commands. The main considerable change is a decrease in the overshoot of the optimized command (objfun1) from 8% to 6.6%. However, all other parameters are the same. For the ZV command, the overshoot decrease from 21.5% to 19 %, and the settling time from 1 sec to 0.7 sec, thus indicating more variation in the response. Although these variations show less vibration level, however, it can be seen that it shows that this type of command is more susceptible to changes than other types of ZVD set of commands (see Fig. 4-19).

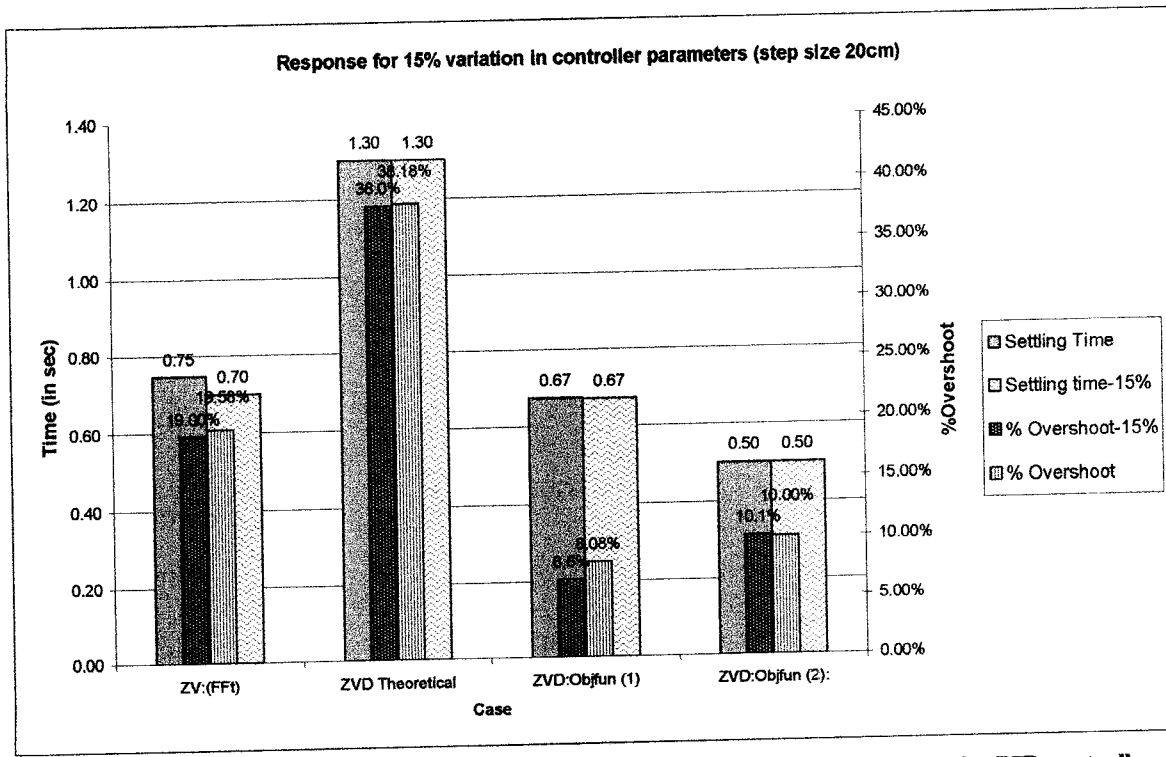

Fig. 4-19 Response variation on the different commands (20 cm) for PID controller

Thus the ZVD optimized commands maintain an overshoot value and a settling time comparable to previous steps. At the same time, the optimized ZV commands lower the vibration level when compared to the theoretical steps; however, it can be noticed generally that the overshoot values are higher than previous step. The response induced by the traditional objective (Trad.Obj) function is more oscillatory than the one obtained by using the ZV:fft function.

STEP SIZE: 30CM

Overshoot:

As expected from the previous results, the theoretical commands will lead to a high overshoot while the optimized commands will keep the same range of values for the overshoot. As shown in Fig. 4-20, for the ZV theoretical command, the damped step and the ZVD theoretical command the overshoots are 69%, 75% and 50% respectively.

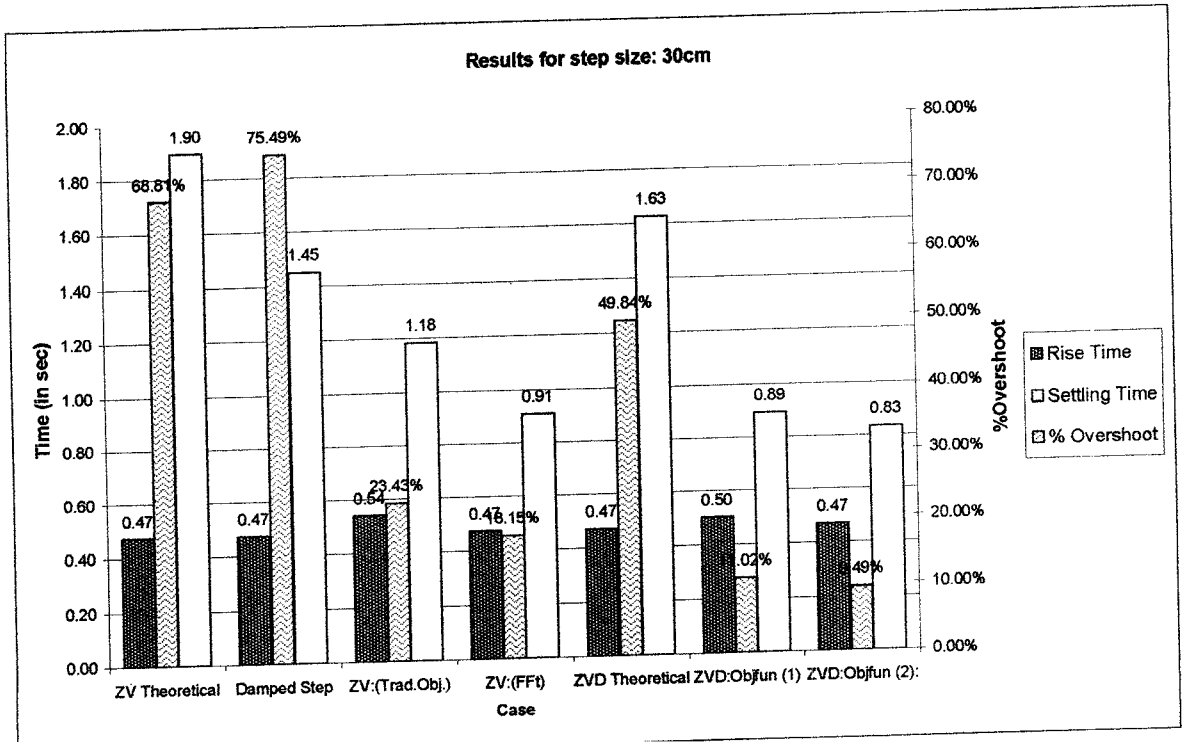

The corresponding values for the ZV optimized values are 23% for the traditional objective function (Trad.Obj) and 18% for the ZV:fft function. Similar to the previous step size, the ZVD optimized commands have the lowest overshoot of 11% for Objfun1 and 9% for Objfun 2 (for result details see Table A-6).

Rise and settling time:

The rise time varies within the same range for all the types of command; however, the settling time varies greatly from the theoretical command to range from a minimum of 1.5 seconds to 1.9 seconds, whereas the optimized commands have a maximum settling time of 1.2 in the case of the traditional ZV objective function to a minimum of 0.8 seconds for the ZVD optimized cases.

Variation in parameters:

As mentioned for the previous step size, the parameters that depict the percent overshoot and the settling time will result in the same value for all cases (see Fig. 4-21).

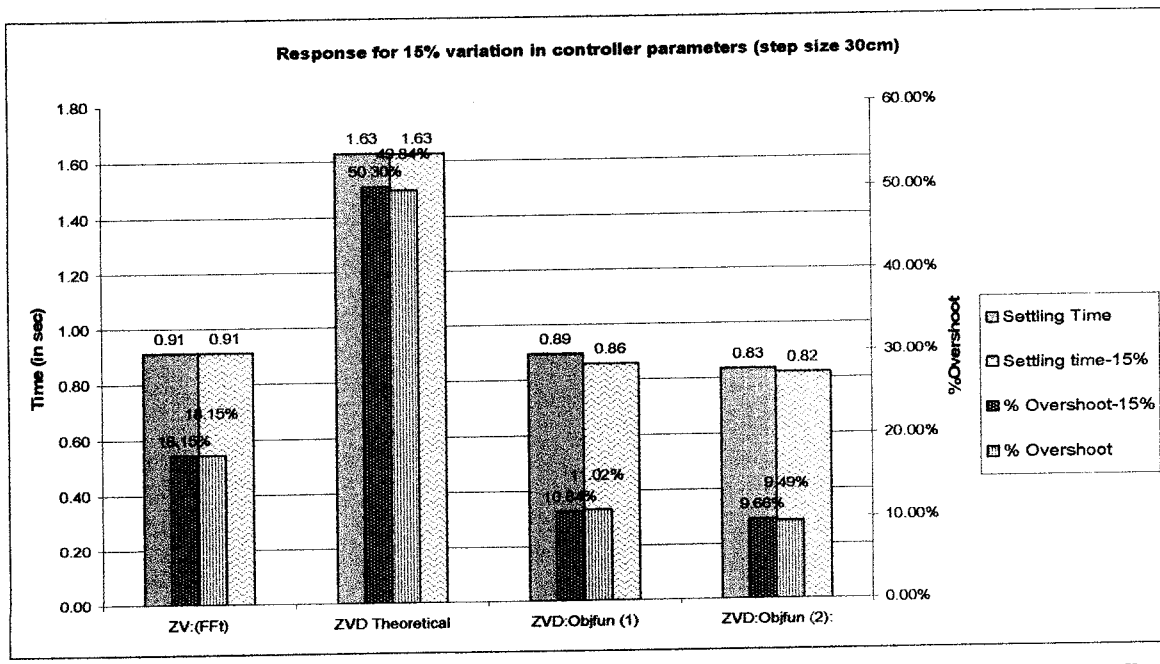

However, during the intermediate response, there are some variations in the case of the ZV command when compared with the ZVD commands. It can be noticed that as the step size increases, the effect of these variations decreases due to the fact that the nonlinear terms are more pronounced.

The responses that describe the motion of the cart for the different input commands are shown in Fig. 4-22 and Fig. 4-23

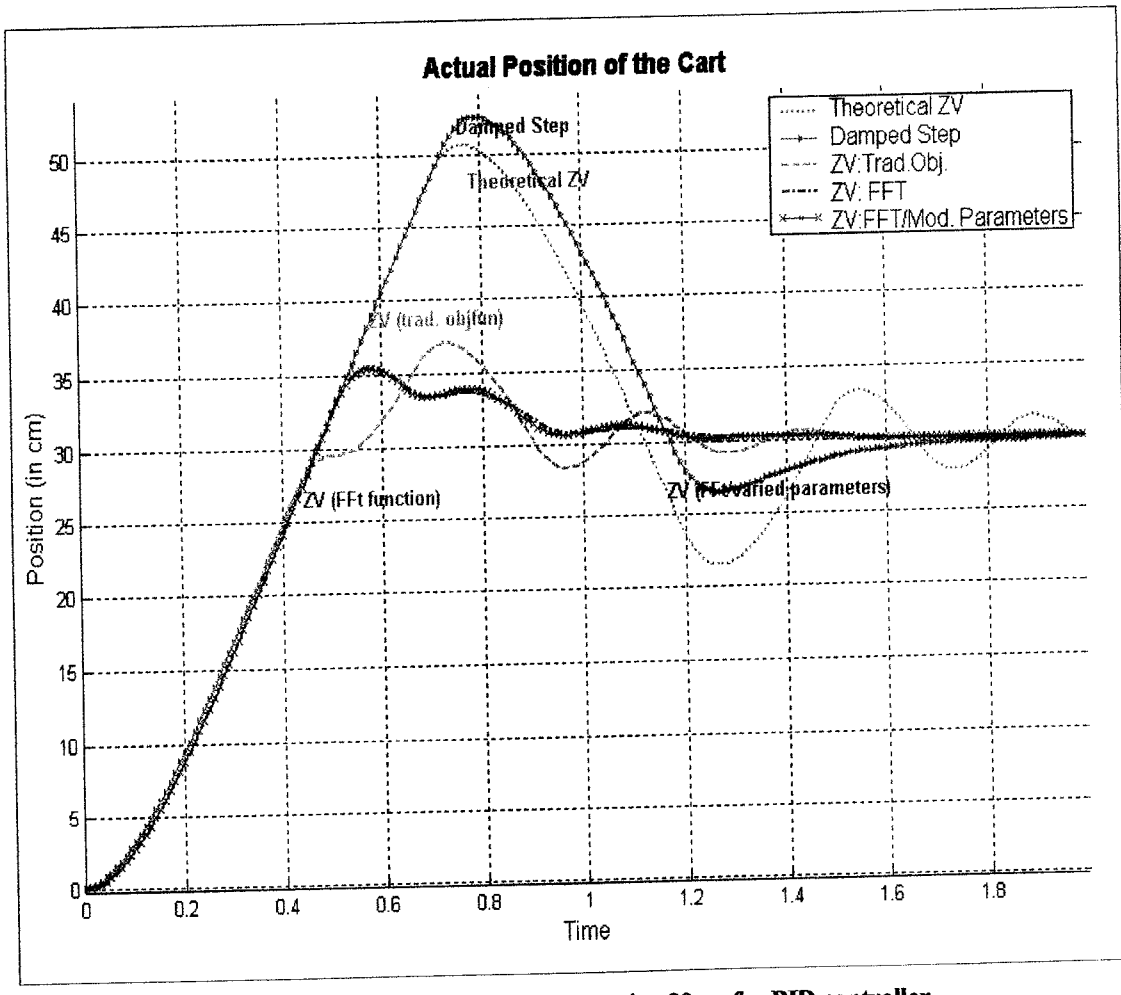

Fig. 4-22: ZV response for step size:30cm for PID controller

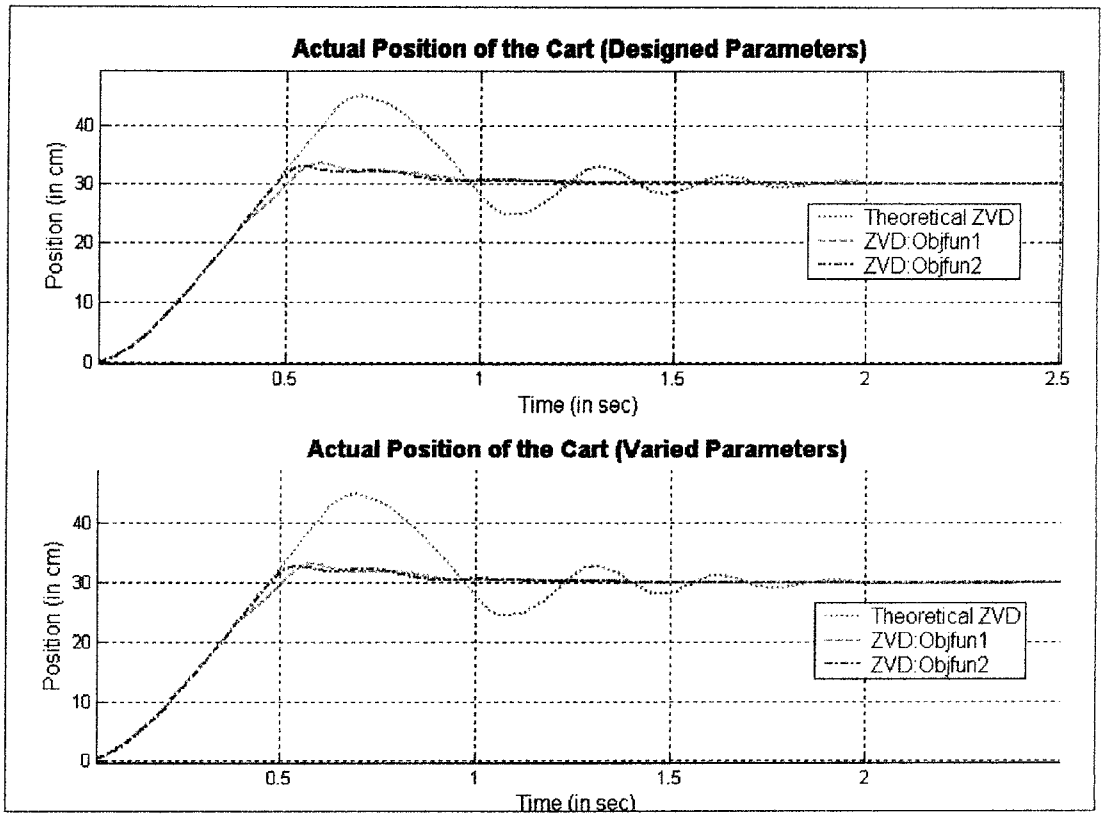

Fig. 4-23: ZVD response for step size:30cm for PID controller

SUMMARY OF RESULTS

From the above results, it can be shown that the theoretical input shaping command fail to reduce the vibration in the case of nonlinear models. The effect of these nonlinearities varies with the step size of the motion of the cart. For small step sizes, the friction plays the main role as a nonlinear factor in the model. As the step size increases, the friction effect diminishes while the effect of the saturation of the system is more pronounced. It was also shown that the traditional objective function (Trad.Obj) that settles the error in position and velocity to zero is not effective for the case of the integral controller, since this controller adds an extra pole that takes longer time to settle, thus exciting the two complex poles. This is apparent for large step sizes where the oscillations are higher. A comparison of the

overshoots and settling time for the different commands is presented in Fig. 4-24 and Fig. 4-25 respectively.

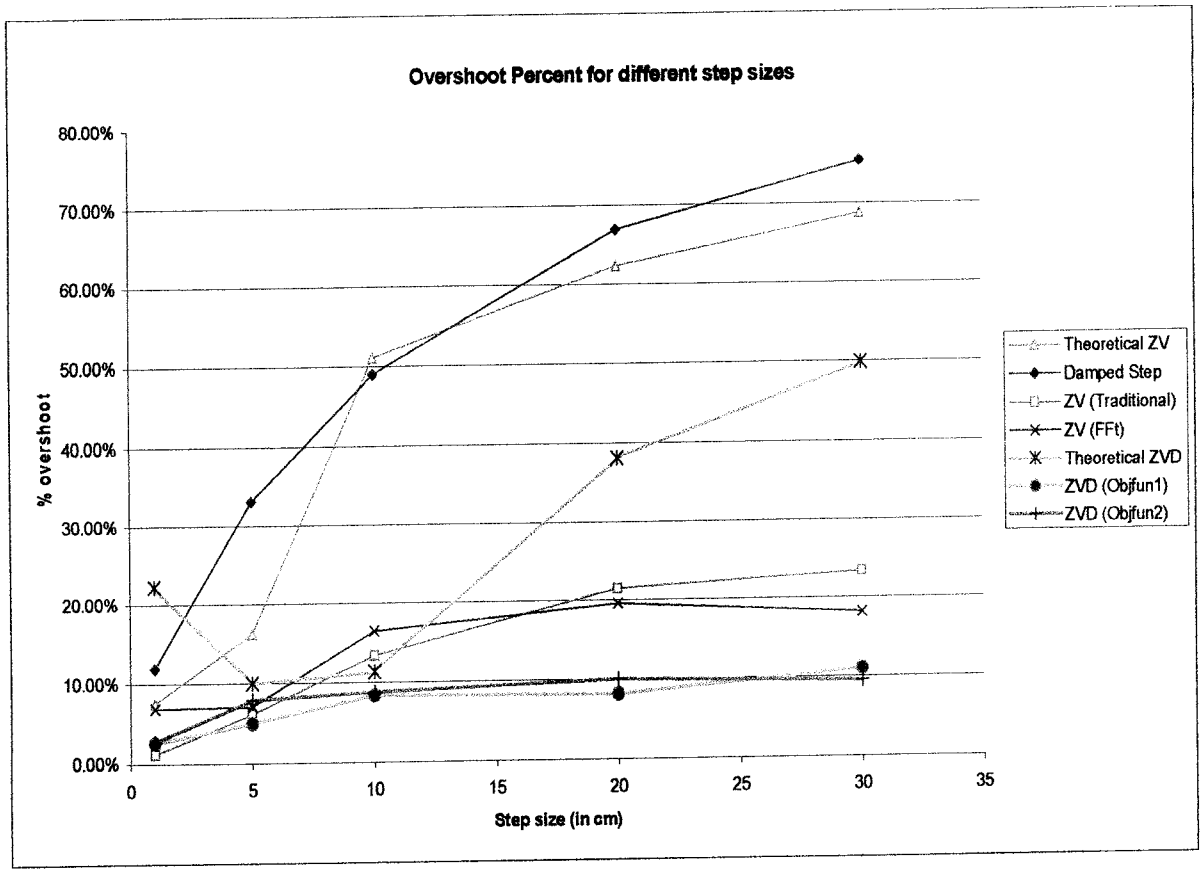

Fig. 4-24: Comparison of overshoot percent for different command & different step sizes

For the settling time, the optimized ZVD commands offer the smallest settling time as compared to all other commands. By comparing the optimized ZV commands with the theoretical ZV commands, it is found that the settling time in the first case is in general smaller than the second case especially for the extreme cases of nonlinearities (very small step size and very large step sizes).

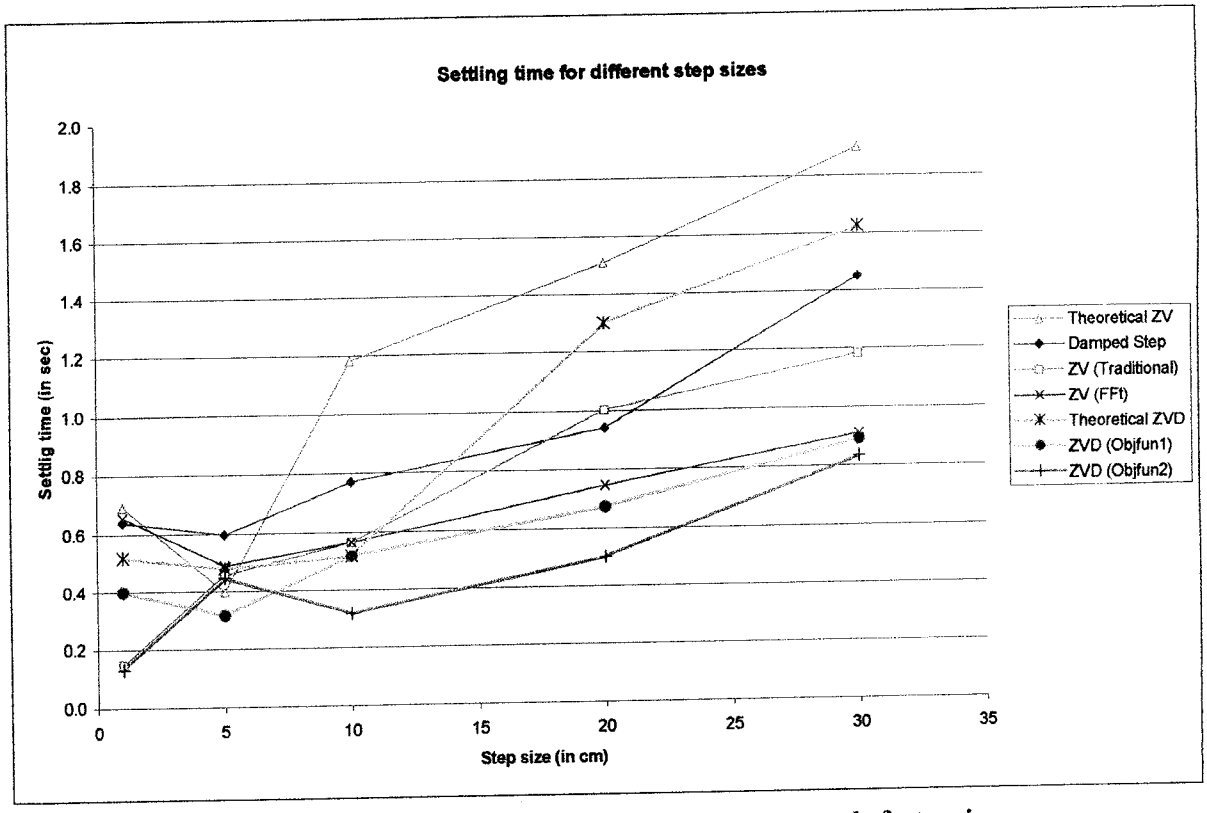

Fig. 4-25: Comparison of settling time for different commands & step sizes

By comparing the robustness of the different commands, it was shown that the ZV commands, although might show small variations in the overshoot and settling time, yet changes in the intermediate response values are more apparent than in the ZVD cases. Moreover, the optimized ZVD commands showed better responses than the theoretical ZVD ones. As expected, the optimized ZVD commands using the second objective function (Objfun 2) was more robust than all other commands except for the step size of 1cm.

It is necessary to compare the trends of the amplitude and timing of the different input steps for the different commands. For the traditional objective function, the amplitude of the first and second input step follows a near constant line for all step sizes except for the 1cm step size. For this step size, the friction effect is high, thus a higher values of A_1 is required to

displacement step size. This is attributed to the effect of saturation of the system (see Fig. 4-26).

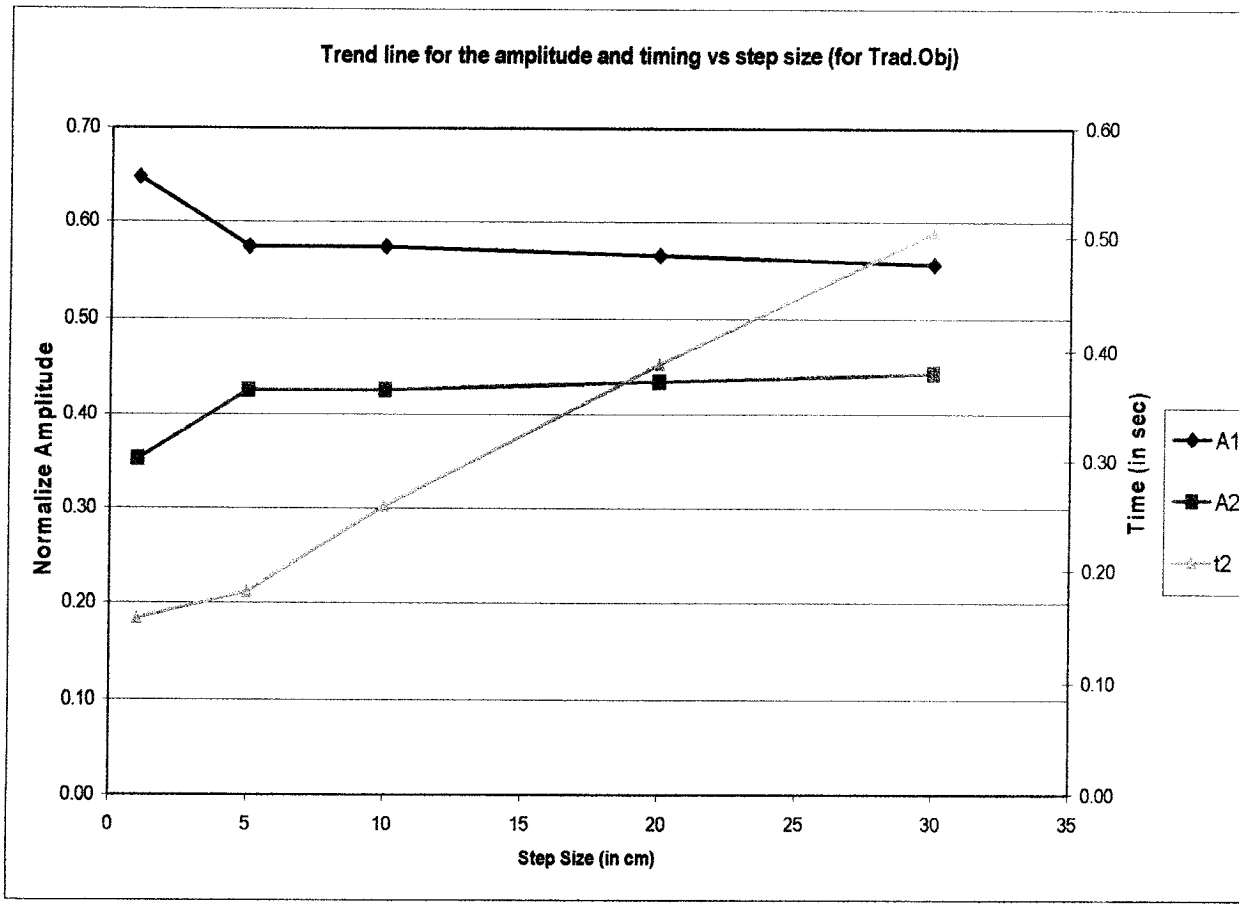

Fig. 4-26: Trend for the amplitudes of the two step and the timing of the second step for a ZV command for the traditonal objective function versus step size.

For the fft objective function, the amplitudes of the first and second step are constant, except for the step size of 5cm. The timing of the second step also increases linearly with the step size (see Fig. 4-27)

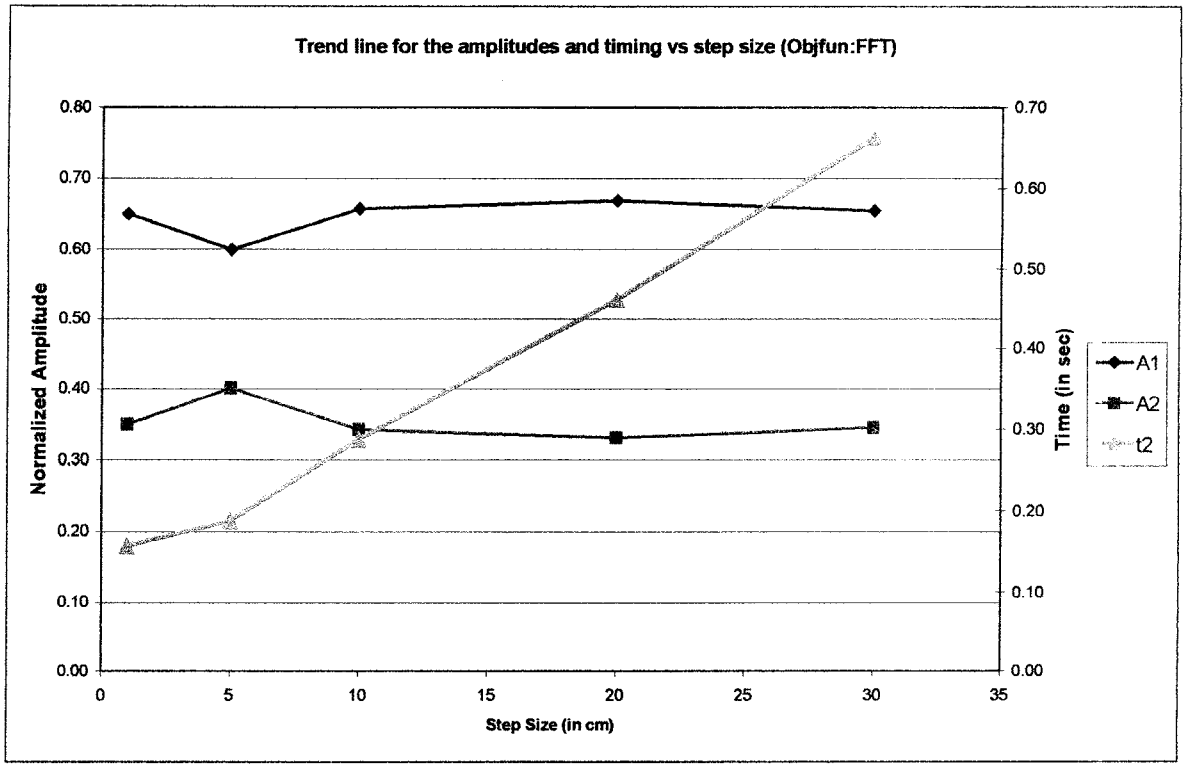

Fig. 4-27: Trend for the amplitudes of the two step and the timing of the second step for a ZV command for the fft objective function versus step size.

For the ZVD case using Objfun1, the amplitude of the third step decreases linearly with the step size. For the smallest step size (1cm), the amplitude of this step is small, which indicates that the amplitude of the first two steps is high in order to overcome the friction effect. As shown in Fig. 4-28, no trend is identified for the amplitude of the first or second step. This indicates that the derivative part of the objective function (4-14) is not completely optimized. The scaling of this term has to be modified. The timing of the second and third input steps increases linearly with the step size of the displacement. This is due to the effect of saturation (see Fig. 4-29).

not optimizing the derivative of the objective function (see equation 4-15). The time of the different steps increases linearly with the step size. As shown in Fig. 4-31, the timing of the input steps does not follow the same trend. This is attributed to the effect of friction.

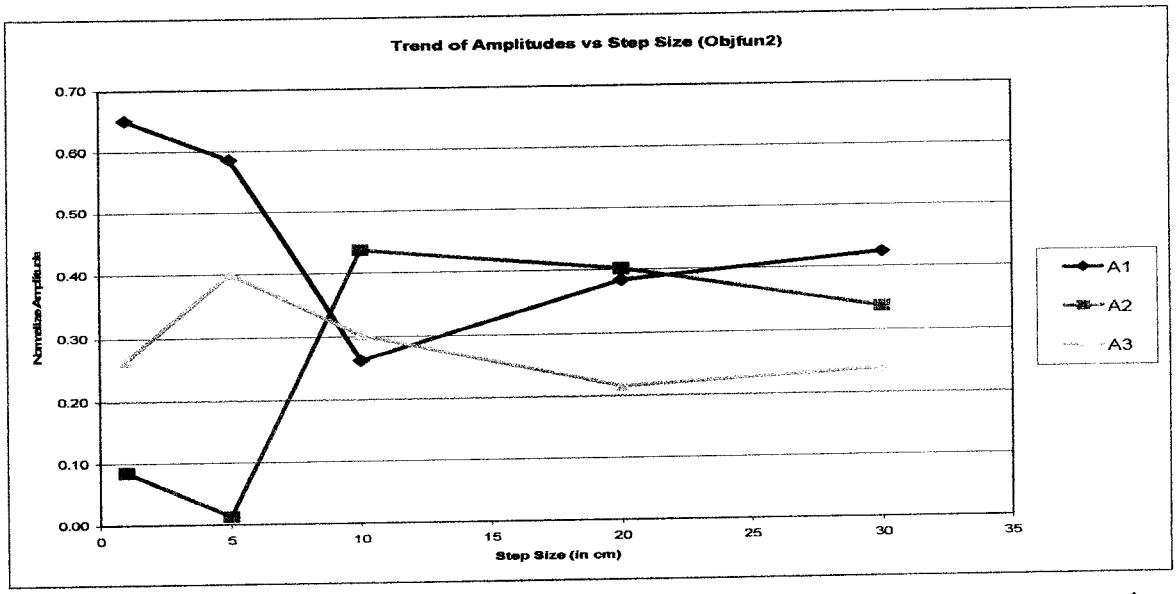

Fig. 4-30: Trend for the amplitudes of the three steps of the ZVD command for Objfun2 versus step size.

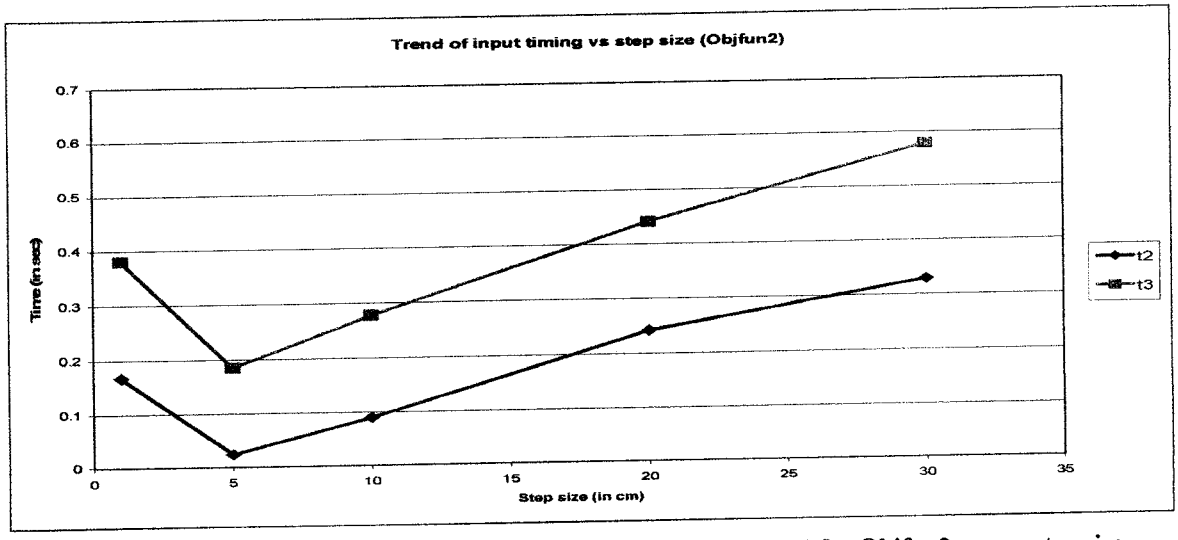

Fig. 4-31: Trend for the timing of the two steps of the ZVD command for Objfun2 versus step size.

Thus, it is shown that for the ZV objective function a trend for the amplitude and timing can be detected. Moreover, for the ZVD objective functions the timing of the input steps

to be done for the objective function in order to ensure that the different terms are properly scaled.

LIMITATIONS

Although the optimized results offer better responses than the conventional types of input steps, there are some limitations in the model that affected these results. The modeling of the friction presents one of the limitations of the model. As shown in the system identification parameters, the friction is not constant all over the track. Moreover, it was shown that the backward friction is different from that of the forward direction. The presence of the wires at the back of the cart affected also the motion of the cart. In the comparison between the different commands, the same starting position for the cart was used. In the model, the friction was specified as a constant value at all positions. Thus more refinement in the model could be included in order to obtain higher accuracy.

Some differences were noticed between the response of the actual model and that of the simulation. These differences result from the fact that the parameters of the model are slightly different from the actual ones.

It was desired to use smaller step sizes; however, the minimum size of the displacement was limited to 1cm in order to have accuracy in the measurement.

CHAPTER 5

TWO DEGREE OF FREEDOM SYSTEM

In the previous chapter, the focus was on a one degree of freedom system with friction and saturation. This chapter is concerned with a two degree of freedom model with low damping where the effect of input shaping will be examined. In this case, there is an extra mass added to the previous system where the vibration level of this additional mass is affected by and affects the vibration level of the first mass.

In the coming sections, section 5.1 presents the equations for a linear model without friction in order to show the procedure for the calculation of the theoretical input command. Section 5.2 develops the equations of motion for the nonlinear two degree of freedom model and defines the objective function. Section 5.3 describes the modifications made to the Genetic Algorithm code to escape possible genetic drift phenomena that arose during the test runs. Section 5.4 will briefly describe the system identification process for this model which is similar to the previous model. In section 5.5, the results are compared for different cases and input command sets.

5.1. LINEAR TWO DEGREE OF FREEDOM MODEL WITHOUT FRICTION

The problem of command input shaping that cancels out the vibration for a two degree of freedom system is already solved in the literature for linear systems. The solution can be obtained by different methods. In this case, there are four main equations that need to be equal to zero which are the two equations for the vibration levels of the first mass and the

respectively, are unknown together with t_2 and t_3 the timings of the second and third step respectively. The response of a mass subjected to three impulses, where their sum is equal to 1 is:

$$\begin{aligned} &for: t > t_3 \\ &x(t) = e^{-\zeta_1\omega_1(t-t_1)}e^{i\omega_1(t-t_1)} + e^{-\zeta_1\omega_1(t-t_2)}e^{i\omega_1(t-t_2)} + e^{-\zeta_1\omega_1(t-t_3)}e^{i\omega_1(t-t_3)} \end{aligned} \tag{5-1}$$

For the two degree of freedom model, it is required that the residual vibration of the first and the second modes be set to zero. By referring to (5-1), the expression of the residual vibration of the two modes at t_3 is:

$$\begin{aligned} V_1 &= A_1 e^{(-\zeta_1\omega_1 t_2)}e^{(i\omega_1 t_2)} + A_2 e^{(-\zeta_1\omega_1(t_3-t_2))}e^{(i\omega_1(t_3-t_2))} + A_3 \\ V_2 &= A_1 e^{(-\zeta_2\omega_2 t_3)}e^{(i\omega_2 t_2)} + A_2 e^{(-\zeta_2\omega_2(t_3-t_2))}e^{(i\omega_2(t_3-t_2))} + A_3 \end{aligned} \tag{5-2}$$

where A_1, A_2 & A_3 are the amplitudes of the three steps and t_2 & t_3 are the timings of the second and third step respectively. ω_1, ω_2, ζ_1 and ζ_2 are the damped frequency and the damping ratios of the system respectively. The objective is to set $|V_1| + |V_2|$ equal to zero. For this equation, there are many solutions depending on the period of time through which the system should stop vibrating. As can be seen this equation is applicable to any system that is modeled linearly.

Another way to obtain a set of input commands is done by finding the command needed to set the vibration of the first mode shape equal to zero, and similarly for the second mode. Then the two sets are superimposed on each other. In this case there will be four main steps. For a linear system, this solution is feasible. The calculations are the same as described in section 2.3.2, which determine the appropriate input shaping command for a one degree of freedom system, and then the procedure is extended for the two degree of freedom model.

These two methods of obtaining an input command that will set the vibration level to zero will be used in order to check the model formulation and calculation (without friction), as well as the ability of the optimization procedure to give same results.

5.2. CART AND PENDULUM SYSTEM

The model that is used in this chapter is a further extension of the one degree of freedom model in which a cart connected to a PD controller moves on a track. A rod is linked to the cart by a joint (see Fig. 5-1). The experimental setup used is shown in Fig. 5-2.

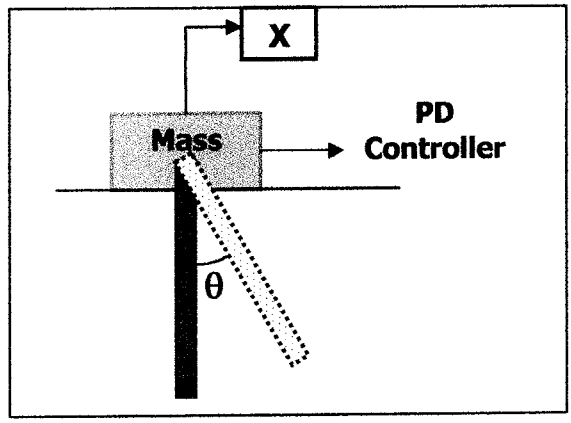

Fig. 5-1: Schematic diagram of the two degree of freedom system

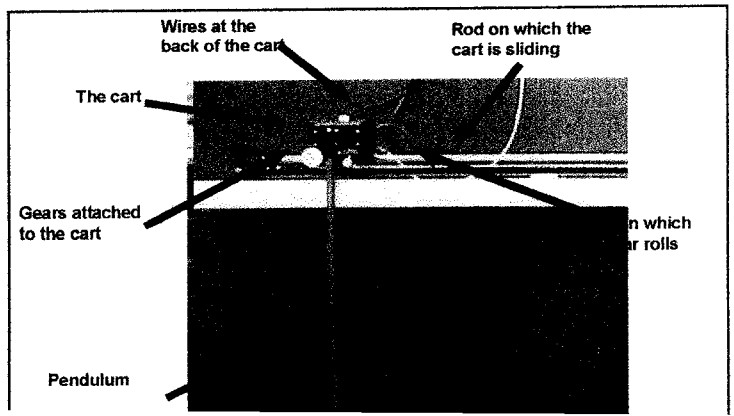

The objective is to position the cart at a certain point with no vibration of the cart and the pendulum. In order to achieve this, the same procedure that was used in the one degree of freedom system is used in this case. The equations describing the model are specified, then rearranged in a way to be able to apply numerical integration. The genetic algorithm code is adjusted accordingly in order to find the optimum solution.

The equations for the model are the block and rod translation in x direction, y direction and rotation (see equations 5-3, 5-4 and 5-5).

$$(m_b + m_r)\dot{x}_2 + m_r l\cos(\theta)\dot{\theta}_2 = k_d \dot{x}_d + k_p x_d - (c + k_d)x_2 - k_p x_1 + m_r l\sin(\theta_1)\dot{\theta}_2 - \mu_k N sign(x_2) \quad (5\text{-}3)$$

$$N = (m_b + m_r)g + m_r l\dot{\theta}_2^{\,2}\cos(\theta_1) + m_r l\dot{\theta}_2\sin(\theta_1) \quad (5\text{-}4)$$

$$J_r\dot{\theta}_2 + m_r\dot{x}_2 l\cos(\theta_1) + m_r l^2\dot{\theta}_2 = -m_r \lg\sin(\theta_1) \quad (5\text{-}5)$$

The nonlinearities in the model are several. Some of them are included while others are ignored depending on the relevance of each to the models.

The model has to include both the static and dynamic friction in order to be able to obtain an accurate representation of the experimental setup. Moreover, the saturation of the system which greatly affects the efficiency of the generated input command had to be incorporated in the code.

The structure of the code is as follows:

- Input the parameters of the model: m_c, m_r, l, J_r, k_d, k_p μ_k and c
- Define the input variables of the model function, which are the angle θ_1, position x_1, angular velocity θ_2 and velocity x_2.
- Calculate the state variables based on the equations previously described with the

1. The nonlinear terms of the angles will be linearized since there effect is minimal on the system response. The linearization will be done by assuming that:

   $\cos(\theta) = 1$, $\sin(\theta) = \theta$, $\theta^2 = 0$ (for small θ);

   The equations will be as follows:

$$V_{in}(voltage) = k_d\left[\frac{(x_d - x_{dprev})}{t_{step}} - x_2\right] + k_p(x_d - x_1)$$

$$cthd = \frac{-J_o(m_b + m_r)}{m_r l} + m_r l$$

$$cxd = \frac{m_b + m_r - (m_r l)^2}{J_o}$$

$$\dot{\theta}_1 = \theta_2 \qquad (5\text{-}6)$$

$$\dot{\theta}_2 = \frac{V_{in} - cx_2 - \mu_k N sign(x_2) + (m_b + m_r) g\theta_1}{cthd}$$

$$\dot{x}_1 = x_2$$

$$\dot{x}_2 = \frac{V_{in} - cx_2 - \mu_k N sign(x_2) + \frac{(m_r l)^2 g\theta_1}{J_o}}{cxd}$$

2. In practical applications, the allowable voltage of the system is limited, which usually causes saturation. Thus a limit was put on the absolute values of the voltage in order not to exceed 5 volts.
3. The initiation of the motion requires the cart to overcome static friction. Similarly, at the end of the motion, where the vibration supposedly should be set near to zero, there is a point where dynamic friction changes into static friction. This was applied in the model through the following condition:

$$F = \frac{k_d(x_d - x_{dprev})}{t_{step}} + k_p(x_d - x_1) - (c + k_d)x_2 + \frac{(m_r l)^2 g\theta_1}{J_o}$$

$$Conditions: F < \mu_S N \;\&\; x_2 < 0$$

$$\dot{\theta}_1 = 0 \tag{5-7}$$

$$\dot{x}_1 = 0$$

$$\dot{\theta}_2 = \frac{k_d\left(\frac{x_d - x_{dprev}}{t_{step}} - x_2\right) + k_p(x_d - x_1) - F + (m_b + m_r)g\theta_1}{cthd}$$

The code for the numerical integration will be the same as for the one degree of freedom model with the only difference that there are four equations, which are put in a matrix form in order to decrease the computational time. At the beginning of this code, the input command applied to the controller is defined with the amplitudes and timing. At the end of the integration code, the objective function has to be evaluated. For the analytical solution of the model without friction, two equations have to be satisfied in order to achieve zero vibration which consists of setting the vibration of the pendulum equal to zero, and so for the cart. This leads to four equations, two for each component of the system. Thus the command that can be generated consists of three steps. Thus, the minimum number of steps needed in order to set the vibrations of a two degree of freedom to zero is three. However, the difference between the natural frequencies of the system causes some problems especially with the presence of nonlinearities to the system. The small natural frequency (pendulum) required two steps with large timing, while the larger natural frequency (cart) required two successive steps with much smaller time in between. This could not be solved with the three step command since some oscillation for the cart will be induced at one of the intermediate commands due to the difference between the frequencies of the cart and the pendulum. A four

step command will be required to set the vibration of both elements of the system equal to zero. Thus two unknowns will be added which are A_3 and t_4.

The next step in the integration code is to define the objective function that will set the vibration equal to zero (near zero). The definition of the objective function is more complicated since the terms that describe the level of vibration are numerous. Several objective functions were suggested:

The first objective function consists of simply setting the different terms of position and velocity equal to zero. This is achieved by the following equation:

$$Obfun = |finalpos - x_d| + |finalvel| + |finalangle| + |finalanglvel| \quad (5\text{-}8)$$

where the first term refers to the error in the final position of the cart, the second term refers to the final velocity of the cart, the third term refers to the final angle of the pendulum and the fourth term refers to the final angular velocity of the pendulum.

It was noticed that this function led to the development of a larger number of local minima which rather prevented the program from finding the near global optimum. Thus a modification was done to the objective function. The final time of the command was included in the objective function, taking into consideration that it will be scaled by multiplying it with one of the terms of the objective function. It was noticed that the optimization code failed to find a consistent solution or even a solution that will lead to low level of vibration. This is explained by the fact that it is not recommended that any of the decision variables of the optimization (which is the time in this case) be included in the objective function (5-9).

$$Obfun = (1 + finaltime) \times |finalpos - x_d| + |finalvel| + |finalangle| + |finalanglvel| \quad (5\text{-}9)$$

It was noticed that the number of terms in the objective function is large. Only three of

Thus an extra term was added in order to achieve no vibration of the cart after the first two steps. The new objective function became:

$$Obfun = \sum_{t=t_2}^{t=t_3} |x - x_{d1}| + \sum_{t=t_4}^{t=2t_4} |x - x_{d2}| + \sum_{t=t_4}^{t=2t_4} |\theta| \tag{5-11}$$

where t_2 is the timing of the second input step, t_3 is the timing of the third input step.

The previous equation gave better results, yet it was noticed that at time t_4, which is the timing of the final step, the actual position was still far from the desired position. This is the same for the position of the first two steps. This definition still created some undesired local optima by not including the fact that by the time the final step is applied, the cart or the pendulum should be near their desired position. In the current definition, the cart or the pendulum is at its position after the command is done. Moreover, the summation term continued until a long period after the final step, which hid the substantial overshoot at the timing of the final step. The final objective function was as follows:

$$Obfun = \sum_{t=t_{2^-}}^{t=t_3} |x - x_d| + \sum_{t=t_{4^-}}^{t=1.4t_4} |x - x_d| + \sum_{t=t_{4^-}}^{t=1.4t_4} |\theta| \tag{5-12}$$

where, t_2^- is one time step before the second input step, and t_4^- is one time step before the final input step.

All of the previously described objective functions describe responses with zero vibration; however, the method of defining the objective function is essential in changing its shape, thus leading to less local optima, which decreases the chances of drifting in the search for the global optimum.

5.3. MODIFIED GENETIC ALGORITHMS

At this stage of the programming of the genetic algorithm code, it was noticed that a drift towards local optima was happening. This problem occurs when the objective function values of the local optima are close to each other, which can cause a premature convergence of the code (see Fig. 5-1).

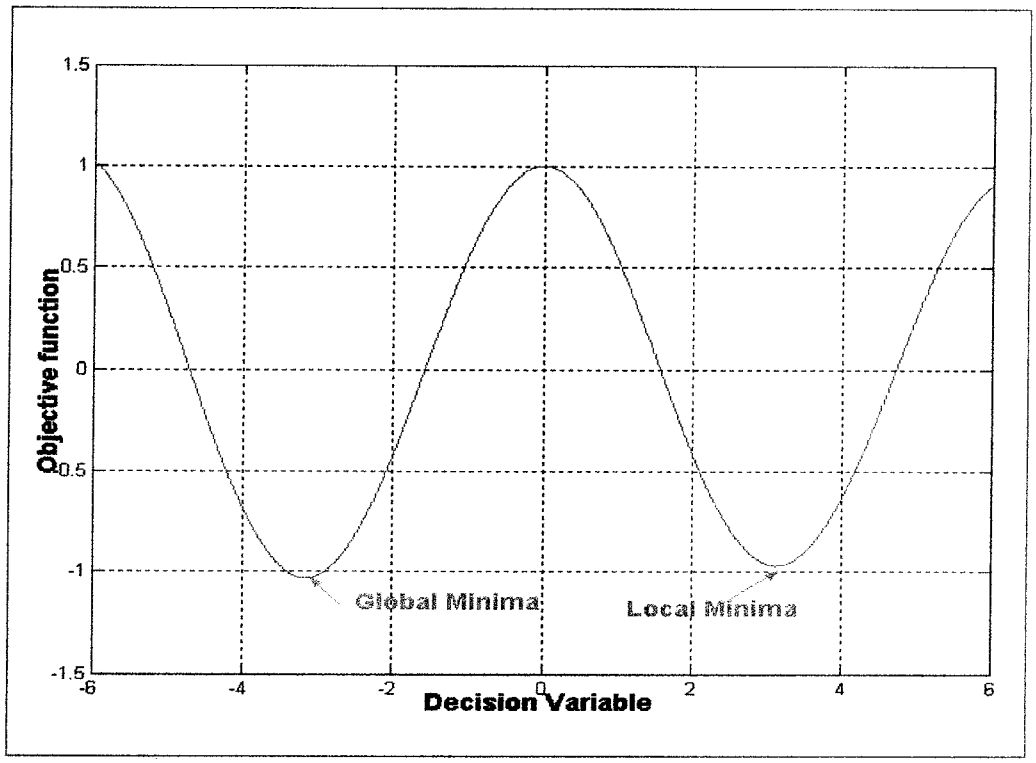

Fig. 5-4: Illustration of the genetic drift

This problem is highly dependent on the definition of the objective function. As was explained in the previous sections, the objective function for the one degree of freedom system required some modifications. However, the normal GA's perform well in such problems. For the two degree of freedom model, the case is different, since the number of

code. The solution suggested for such a problem is the use of a modified GA code, in order to avoid the occurrence of such phenomena.

The modification to the GA mainly consists of investigating completely some search area and then removing them from the total search space. It is desired that as the number of generations increase, the search space decreases, thus focusing the search on smaller areas. Thus the best point of each subregion is saved in an array and the search proceeds in the remaining area. The method of coding such a concept required the following modifications in the GA code.

Local optimization mutation

An extra operator was added which is applied to the point with the highest fitness in each generation. After sorting the points based on the normal fitness function, this point is locally optimized. As a new local optimum is found, a Cartesian region is created around this point, which is a prohibited area to search in (see Fig. 5-5).

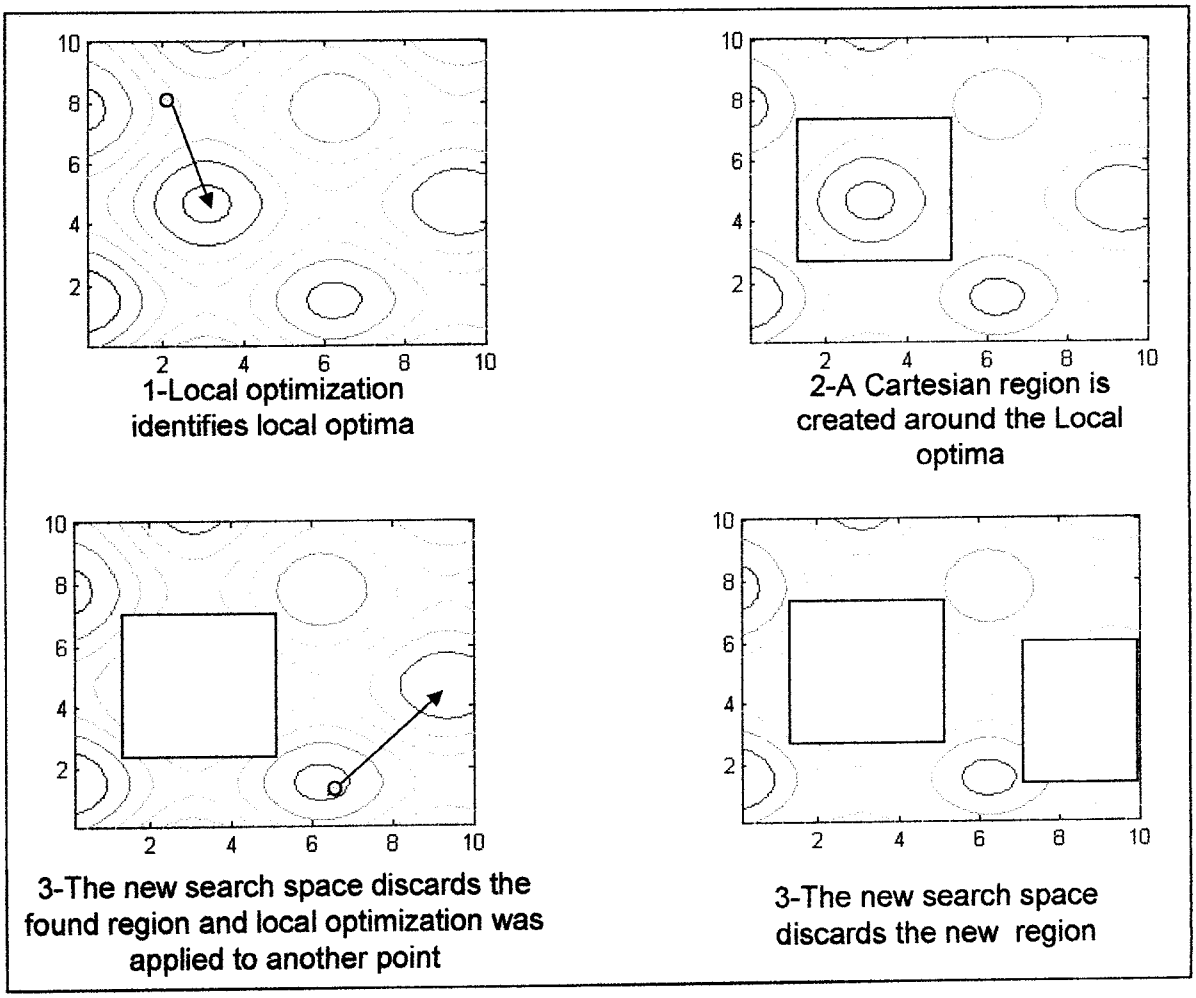

Fig. 5-5: Illustration of the effect of the local optimization mutation

This is imposed in the selection, crossovers and mutations. The formulation of this step is done as follows:

For the best point of an generation i $\bar{x}_i = \{x_{i1}, x_{i2}, x_{i3}, \ldots, x_{in}\}$,

the locally optimized points is $\bar{x}n_i = \{xn_{i1}, xn_{i2}, xn_{i3}, \ldots, xn_{in}\}$, and the region that is removed from the search space is defined by the following two column array:

$$ZZ_i = \bar{x}n_i \pm \bar{x}_i \tag{5-13}$$

In this case a condition has to be imposed in order to guarantee that this region does not

This method created an array with i rows (number of generations) with boundary limits in each row that are not to be searched. Thus this newly optimized point is removed from the population list and put in the candidate array points in order to be compared to other generated points from later local optimization in order to find the global optimum.

Selection

For the selection operator, caution should be made in order not to fall into a drift of local optimum. This could be due to the fact that the high fitness points are usually close in value to the best point of the current generation. Thus although this point was eliminated from the search space with a region surrounding it, the following points in the sorted list could be very close in value to it. This leads to a long and ineffective computational time. The reason is that any point found in one of the prohibited regions, it will only be moved to the boundary of the region. This will create a high density of points around this current local optimum that will be attached to it all over the generations. Thus the selection is based on a uniform probability instead of a geometric distribution.

Other Operators

The crossovers and mutations are applied normally without modification. The only change that will be done is that if a newly generated point falls in between the limits of the prohibited array (Region), it should be moved to the boundary of this row on this area. The boundary, to which the generated point will be moved, will be chosen randomly. It can be seen that as the number of generations increase, the search area decreases, leading to more effective search. The comparison of the results of the normal and modified GA's is shown in Table 5-1.

Table 5-1: Comparison of results for the normal and modified GA

	A_1	A_2	A_3	T_2	T_3	T_4	Objective function value
Normal GA Results	0.483	0.793	0.853	0.963	0.884	0.620	0.912
	0.972	0.501	0.473	0.636	0.095	0.651	0.846
	0.916	0.560	0.934	0.658	0.106	0.934	0.643
Modified GA Results	0.489	0.727	0.751	0.286	0.356	0.286	0.609
	0.498	0.800	0.747	0.312	0.334	0.283	0.433
	0.500	0.823	0.829	0.306	0.340	0.332	0.306

It can be seen that the normal GA's yield different results, while the modified one yields nearly the same results. There are two disadvantages to such method. First, for large number of variables, the computational time will be very high. Second, the assumption that the region around the locally optimized point is symmetric is not always true.

However, since the number of variables did not exceed 6, then the computational time was appropriate. As for the second disadvantage, this is solved by the fact that points at the boundaries of the locally optimized point can still be selected, which includes the probability of choosing them for local optimization. Moreover, this method offers reliable and consistent results which were applied on the experimental apparatus and gave appropriate results.

LOCAL OPTIMIZATION METHODS

The local optimization is an essential part in the solution of the input shaping command using the GA in order to achieve a good command. Although, the command is not supposed to give fully accurate results due to modeling error; yet the command was always closely equal to the theoretical values of the analytic solution of the model without friction, and resulted in no vibration for the actual models with friction and saturation. Several local

optimization techniques were used including Nelder Mead and the sequential quadratic programming (Rao, 1996).

5.4. FRICTION AND DAMPING IDENTIFICATION

Once the genetic algorithm has been modified, the next step was to compare the actual system with the theoretical model. This required the determination of the coefficient of dynamic friction of the model and the damping of the motor due to its back EMF. This was done by inputting ramp commands with specific voltages, and comparing the actual velocity of the system with these voltages. This generated a set of points that were fitted using linear regression. The slope of the line determined the damping of the motor, while the intercept determined the friction force of the system (see Fig. 5-6).

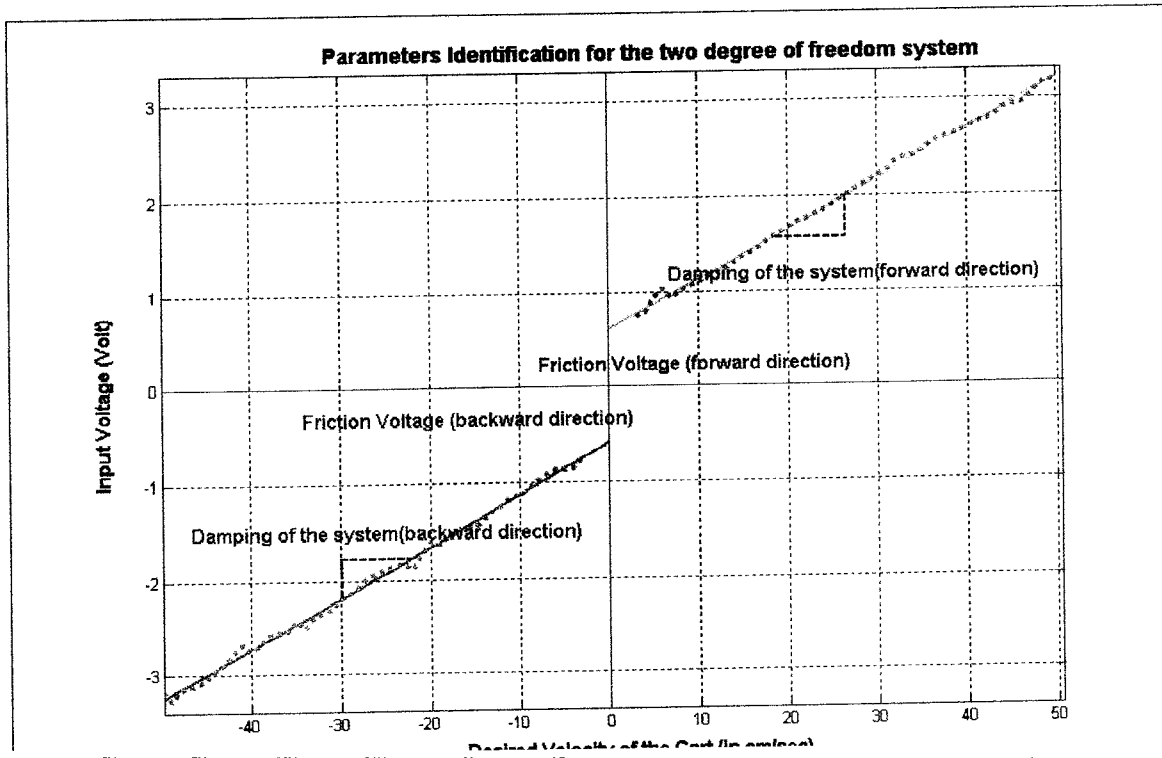

There were two methods to perform such experiment; the first was to use the cart only in order to reduce the oscillations of the system, then determining the coefficient of friction. However, this would not be representative enough for the actual system, since the effect of the pendulum on the cart won't be included in these calculations. Moreover, even if it is included in the normal reaction force, it would provide rather a theoretical representation of the effect of the pendulum rather than an actual representation. The other choice was to include the pendulum in the friction determining experiments. The drawback of this choice is that the graph representing the velocity of the cart will be more oscillatory. Thus the average velocity would be difficult to obtain accurately. However, by investigating the graph (see Fig. 5-6), it would be clear, that the points form a straight line.

The steps for these runs were the same as in the previous model. In this case, the static friction was assumed based on the dynamic friction. Higher variability in the plot points was noticed as compared with the case of the cart alone. The cause for that is the swing of the pendulum that slightly affects the results (see Fig. 5-7).

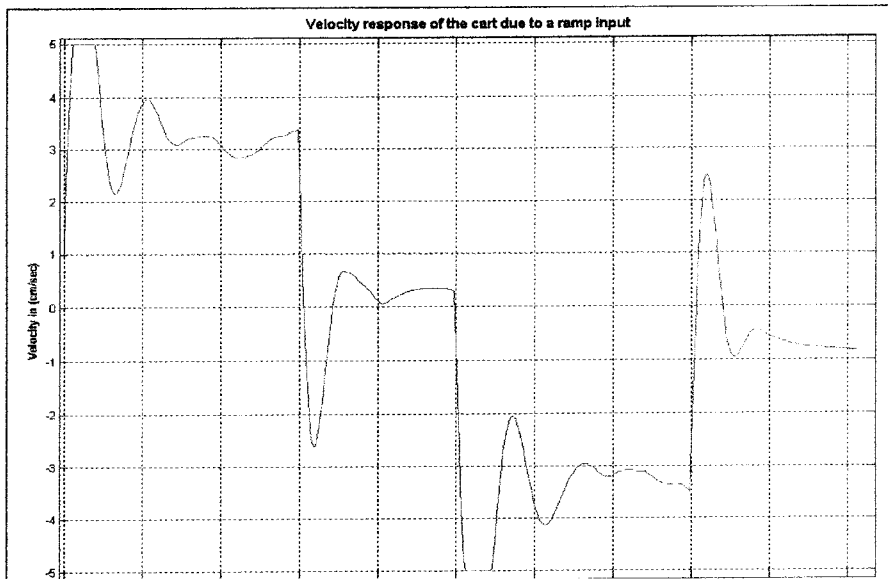

The next step was to input a step command to the actual system, and compare it to the same step command of the computer simulation (see Fig. 5-8).

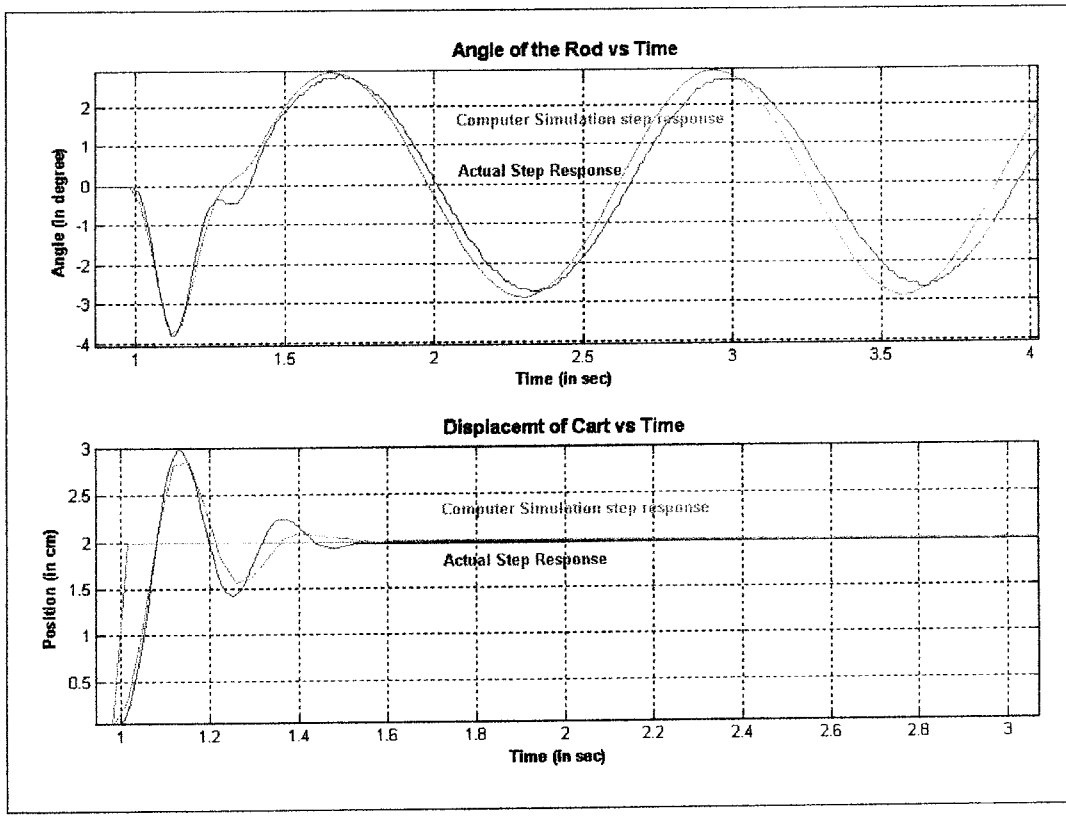

Fig. 5-8: Comparison of the computer simulation and the actual responses

At this stage, the integration code and the model code are ready to be used for optimization.

5.5. DISCUSSION AND COMPARISON OF COMMANDS AND RESPONSES

This section will present some of the results obtained for the different step sizes, highlighting the main difference between the calculated commands, the theoretical commands and the actual responses. The responses for each case are presented in detail in

Appendix B. In order to be able to evaluate the results properly, the different cases are stated and the objective of each comparison is highlighted.

There is a theoretical command input made out of two steps that can be generated for any one degree of freedom system that would result in no vibration for linear systems. The convolution of different set of steps of each mode of a higher degree of freedom system should result in the same response as for each mode separately. Thus the total response cancels the vibration of all modes in case of a linear system, while some oscillations will still be present in case of a nonlinear system. It is expected that the optimized shaper obtained by taking into account the nonlinearities of the system will perform better than the convolved step input command, and will lead to minimum vibration level. Thus a comparison between the convolved steps (*Convolved step*) of the pendulum and the cart, and the calculated shaper are compared experimentally.

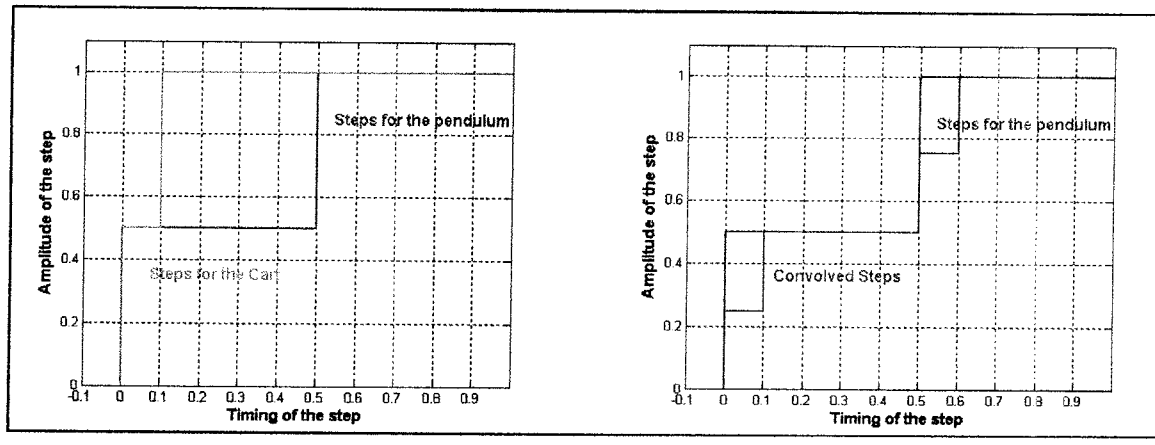

Fig. 5-9: Illustration of the convolved steps for the cart and the pendulum

For a two degree of freedom system, the current practice is to use a controller to damp the motion of the cart, and use input shaping to suppress the pendulum oscillations (low frequency). The increased damping of the PD controller has two main effects, which are a

response. For the input command obtained from the optimization, the model did not require damping in order to eliminate vibration, because the modeling of the nonlinearities in the system should result in almost no vibration. Thus a comparison is made between the optimized command and a two step command for the pendulum with high damping for the cart (*damped two step*).

By closely examining the response for a two step shaping command, it is found that it has an S curve shape. Thus, in many applications, this curve is used as an input command so as to eliminate vibrations. This is applied to the cart and pendulum system with high damping for the high frequency mode (*Scurve*).

Although the modeling was intended to thoroughly include the substantial nonlinearities; however, there are still some discrepancy between the calculated model and the actual one. Thus the response for the optimized command on the computer simulation is compared to the actual response for the same commands.

Since the friction is not constant all over the length of the track, it was expected that the response would differ slightly depending on the location of the cart track. Thus a comparison between the responses at the different locations is presented.

Thus from the previous comparison, the results will include 5 main cases which are:

1. ZV commands for each mode (*convolved step*)
2. Two step command for the pendulum with large damping for the cart (*damped two step*)
3. S curve command with large damping for the cart (*Scurve*)
4. Optimized command response based on the computer simulation and the actual

5. Optimized command response at different location on the cart track.

Several parameters where calculated in order to be able to evaluate the response in each case objectively (see Fig. 5-10).

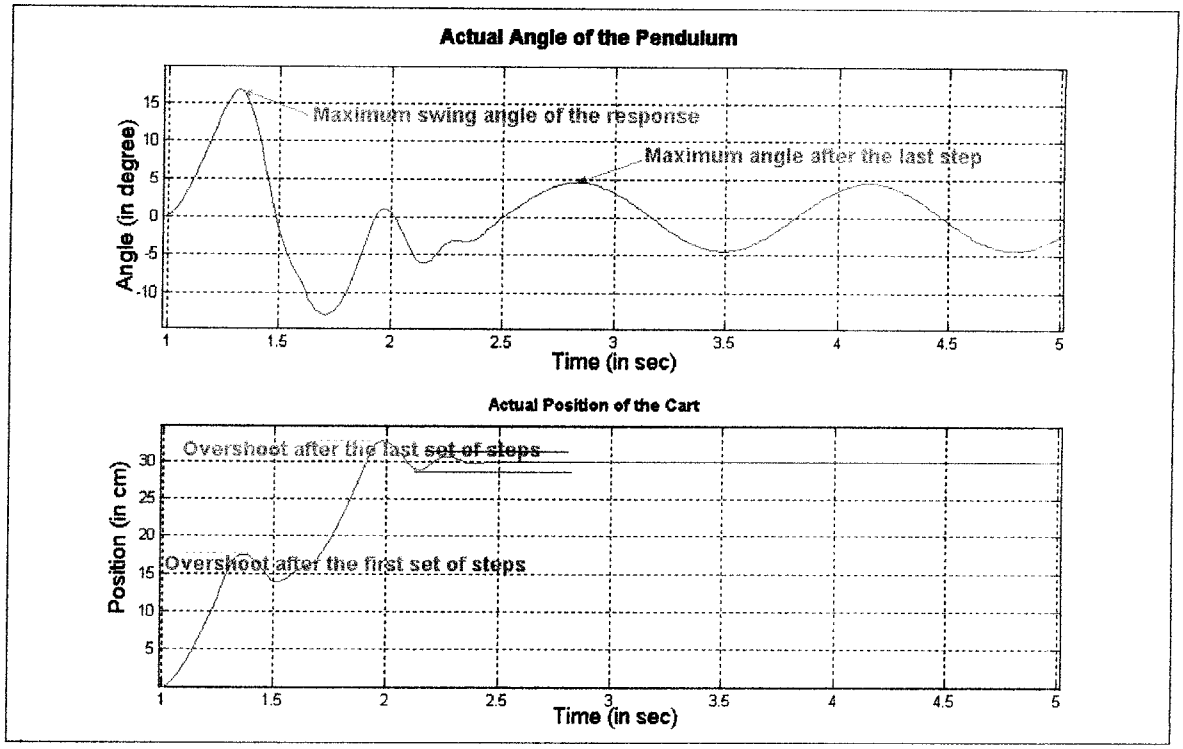

Fig. 5-10: Parameters that are used to describe the response of the cart and pendulum system

These parameters are the position and angle settling time, the maximum peak of the cart after the last and first set of steps, the final position of the cart, the maximum angle of the pendulum, and the maximum angle after the last step. The position settling time is the time it takes the cart to reach 5% of each steady state value (after the last step). The angle settling time is the time it takes the pendulum to oscillate naturally (after the last step). Both these parameters measure the speed of the response of the system. Maximum peak of the cart (after last step) is the maximum value of the position after the last step. This is used to indicate the oscillation level after the input command. In case of no overshoot, the position value will just

position. The maximum peak after the first set of steps is similar to the previous parameter, and is intended to indicate the oscillation level after the first step in case of a two step input command or the second step in the case of four step input command. The final position is the steady state position reached after all steps. This is a good indication of the effect of friction on the system response. Finally, the angles, which are measured by an encoder in the experimental setup, indicate the level of oscillation of the pendulum. The maximum angle of the pendulum is the largest angle for the whole response of the pendulum. Although this is not included in the minimization of the vibration level at the end of the steps; however, the smaller this angle is, the smaller are the extremes of the motion, which is in sometimes required in the specifications of some systems such as robots manipulators. The maximum angle of the pendulum after the last command is the angle limit after the final step of the input command is applied to the system.

For the previous types of commands and the comparison parameters, many results were obtained. The responses for a 1cm step size and a 10cm step size will be presented, while the remaining responses will be presented in Appendix B, with the amplitudes and timing of the different command steps. For each step, trend lines will show the difference between the different types of commands.

Step Size: 1cm

This case represents mainly the effect of friction on the response of the system. As was determined in the identification section of the system, the dynamic friction voltage was equal to 0.6 Volts. Since the value of the proportional gain is 5Volts/cm, then the expect deviation of the cart from its desired position is 0.12 cm, which represents 12% deviation in the case of

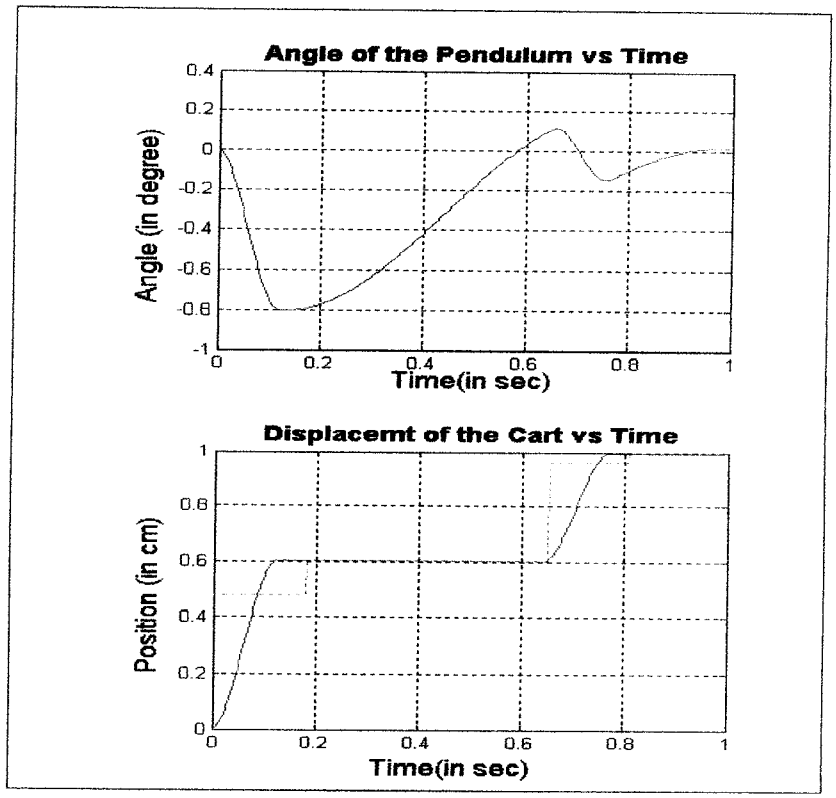

Fig. 5-11: Simulation response for Optimized command 1(step size 1cm)

As seen in Fig. 5-11, the optimized command simulation show excellent response if compared with other commands applied on the computer simulation. It has not overshoot in the position response, and the final angle after the last step (0.015°) and the deviation in the steady state position (0.5%) is smaller than other commands applied to the computer simulation. Moreover, the settling time is smaller in the case of the optimized command then the convolved steps. From the simulation response of the convolved step Fig. 5-12, it is clear that this type of command fails to position accurately the cart, and causes larger oscillations for the pendulum after the final steps. The actual response shows the same trends of the simulations (see Fig. 5-13).

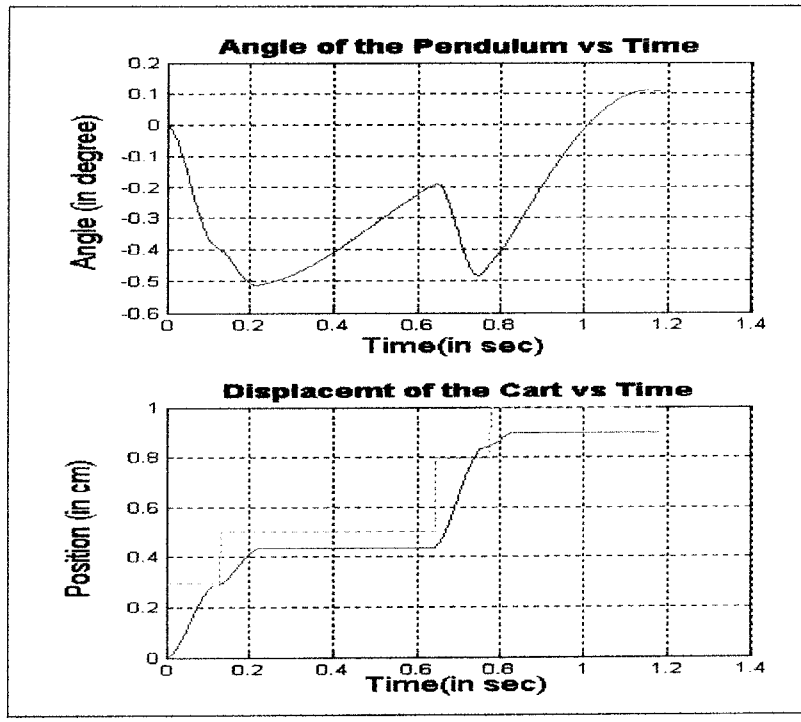

Fig. 5-12: Simulated response of the 4step convolved (1cm)

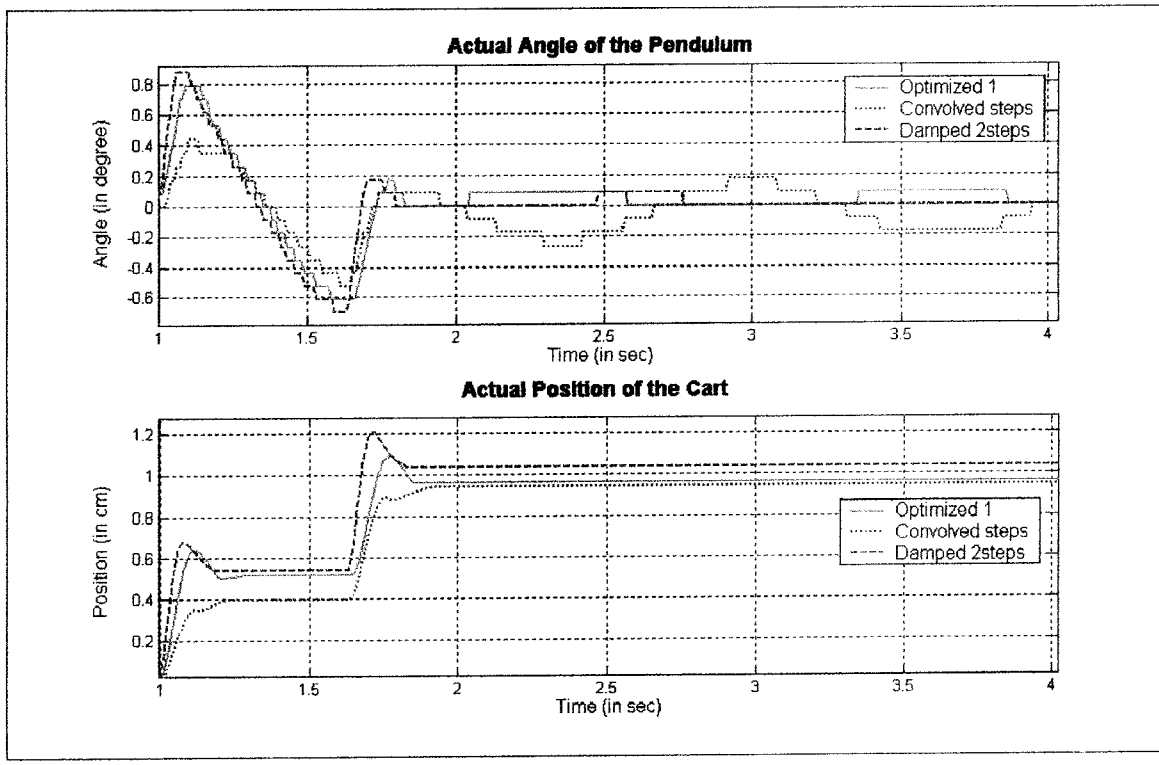

By comparing the actual results obtained from the lab, the following will be noticed see Fig. 5-14 and Fig. 5-15:

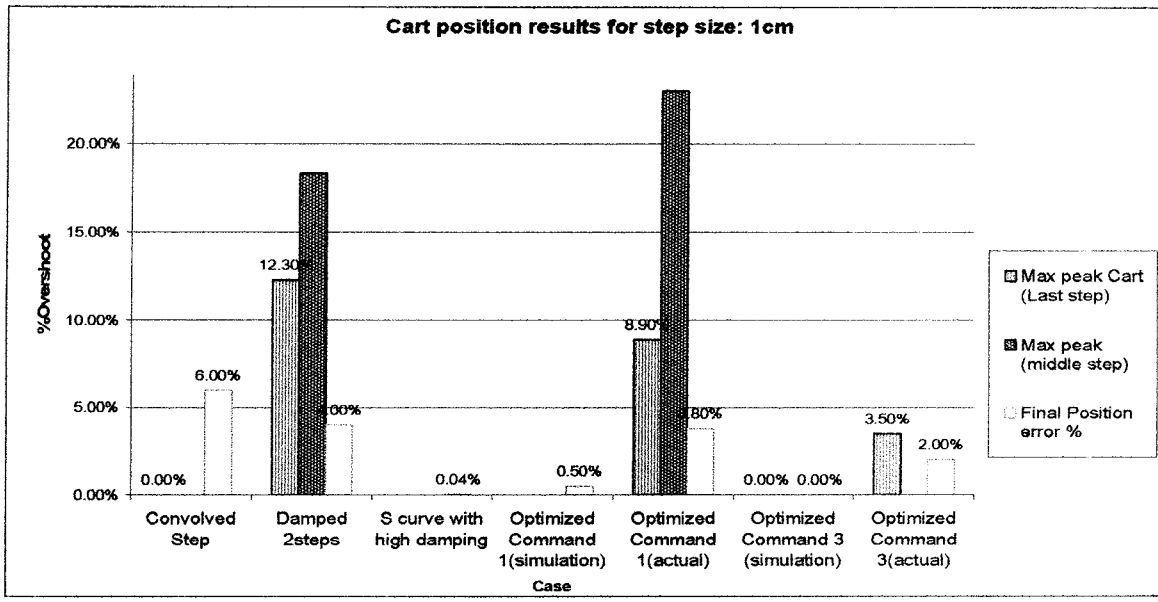

Fig. 5-14: Cart position results for step size 1cm

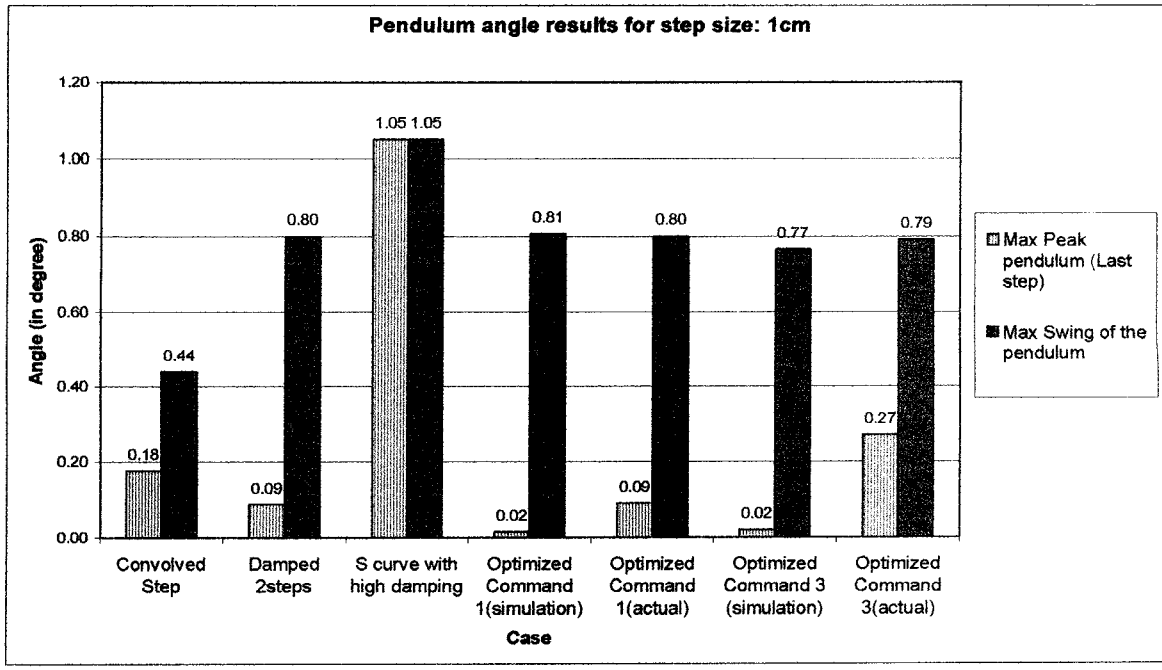

Fig. 5-15 : Pendulum angle results for step size 1cm

The convolved steps produced a steady state error in the position of 6% while the high

the steady state error is 3.8%, which is the same as the damped case. The overshoot in the high damping case (12.3%) is higher than the optimized case (8.9%). For the case of the convolved step, there was no overshoot because the cart didn't reach its desired position. For the first set of the steps, there is overshoot in both the damped case and the optimized case. For the convolved step, the cart still didn't reach its desired position, and there is no overshoot. The maximum angle of the pendulum after the final step is the same for the damped and the optimized case (0.09), which is small as compared with the convolved step angle (0.176). The maximum angle of the response is higher in the case of the damped and the optimized case as compared to the convolved step cases. However, for small displacement, this is of relatively lower significance as compared with the other parameters.

From the above results, it can be seen that the response of the optimized command is faster, with lower steady state error and vibration level after the input command as compared to the convolved step. The damped case performs similar to the optimized case with the only difference that it has higher overshoot at the final step. It can be concluded that the optimized command offers much better response than the convolved steps, and slightly better than the damped two steps. Other input commands from the optimization program set are tested. The results of these commands are compared in Fig. 5-15, and are detailed in Table B-2.

Step size: 5cm

At this displacement value, the effect of friction is smaller than the previous step size, yet it is not small enough to be ignored since it represents a deviation in the steady state position of 2%. The other non-linearity at this stage is the saturation of the system, which is not significant at this step size; however, still makes some differences especially in the final

will be seen that the problem of this command is that the final oscillations of the pendulum are high compared to the other cases. For both the convolved steps and the damped 2steps case, the maximum angle of oscillations after the final step is 0.265°, which are very small compared to a normal step response, or the response generated from an S curve input function (6.4°). For the 3rd case of optimized commands, the final angle is 0.085°, which is 67% lower than the conventional command generated.

By considering the above result, it can be seen, that the 3rd case of optimized commands optimally position the cart at the desired position with a minimum angle of oscillation as compared with other commands. The higher overshoot of the 3rd case of optimized commands compensates for the friction force, thus considerably reduces the error in the final position of the cart (for result details see Table B-3).

Step size: 10cm

For this step size, the friction plays a minor level as a nonlinear factor in the system. It is noticed that the value of the deviation of the position from the desired position is the same, but when compared to the desired position value, it represents a small percentage value. Due to the large step size of the displacement, the saturation effect is more pronounced. At this level of saturation, and with higher step sizes, the conventional input commands fail to produce acceptable results.

As seen in the table for the 10cm results (see Appendix B), there are two optimized sets of commands, which when compared to each other produce similar results. Both of the two sets have 0.8 seconds settling time and no overshoot after the final step. The overshoot after the second step for the 1st case is 3%, while for the second is 13%. The deviation of the

after the last step for the first case is 0.02°, while for the second it is 0.1°. This difference in the final angle lead to the fact that the first optimization set was chosen to be the first in the group of points locally optimized by the genetic algorithm program (see Fig. 5-18 and Fig. 5-19) . However, due to some modeling differences, it will be seen that the second optimized command will have smaller oscillations at the end of the command.

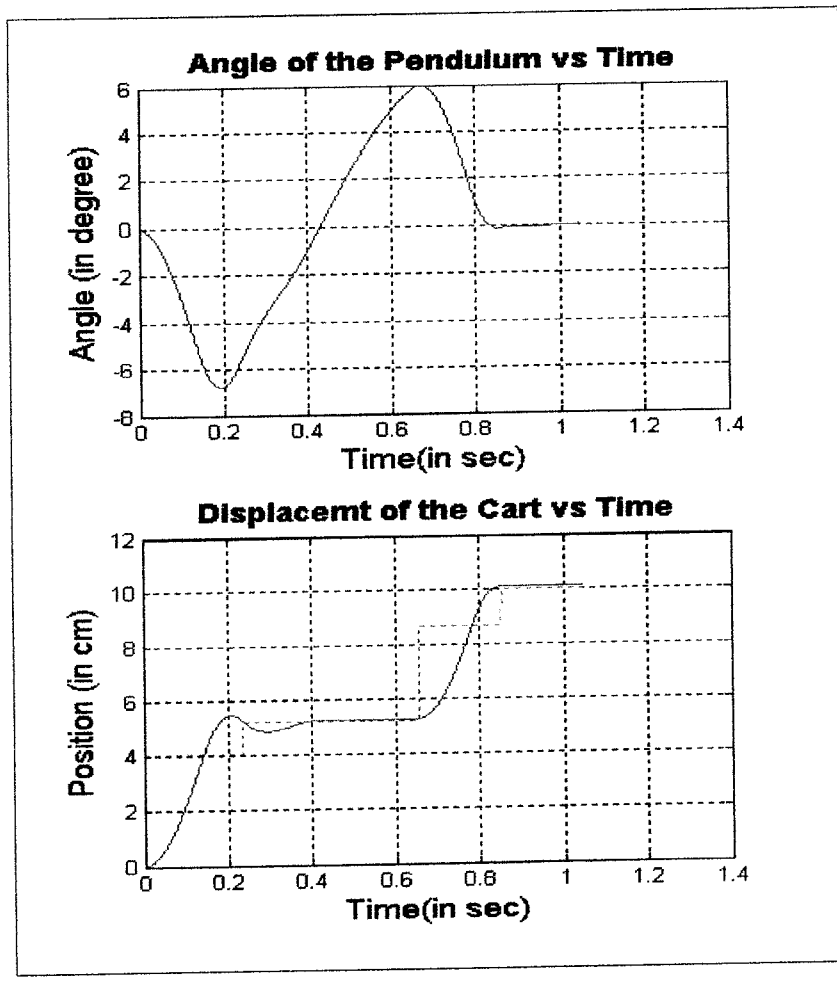

Fig. 5-18: Simulation response of the optimized command 1 (step size 10cm)

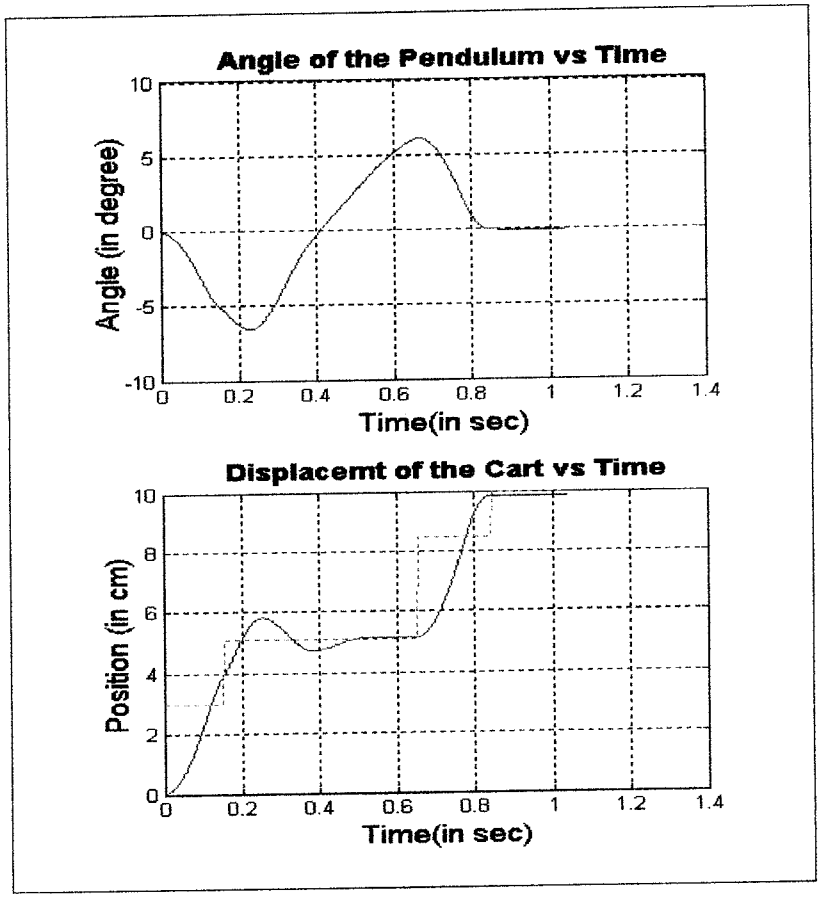

Fig. 5-19:Simulation response of the optimized command 2 (step size 10cm)

As mentioned previously, the conventional commands (convolved and the damped 2step), although will reduce vibration, but not as efficient as the optimized commands. This is shown by the following responses (see Fig. 5-20) and the following comparisons (see Fig. 5-21 and Fig. 5-22):

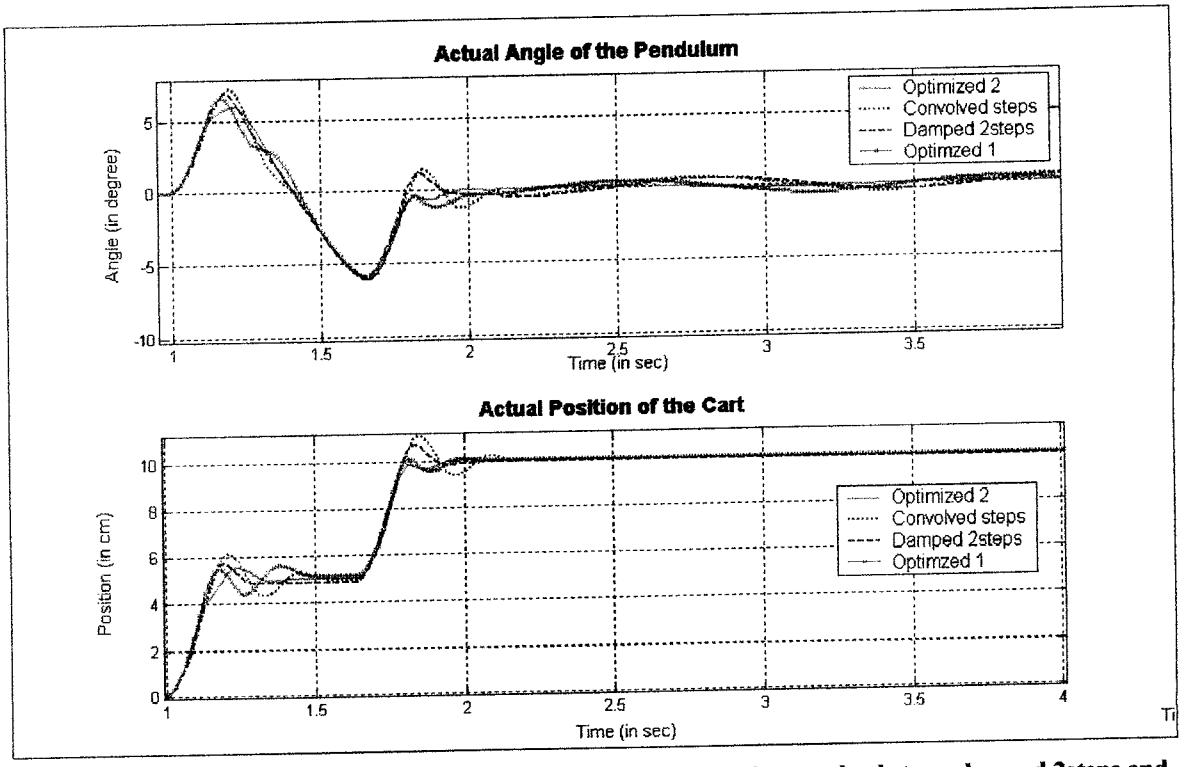

Fig. 5-20: Actual responses for the following commands: optimized2, convolved steps, damped 2steps and optimized 1 (step size 10cm)

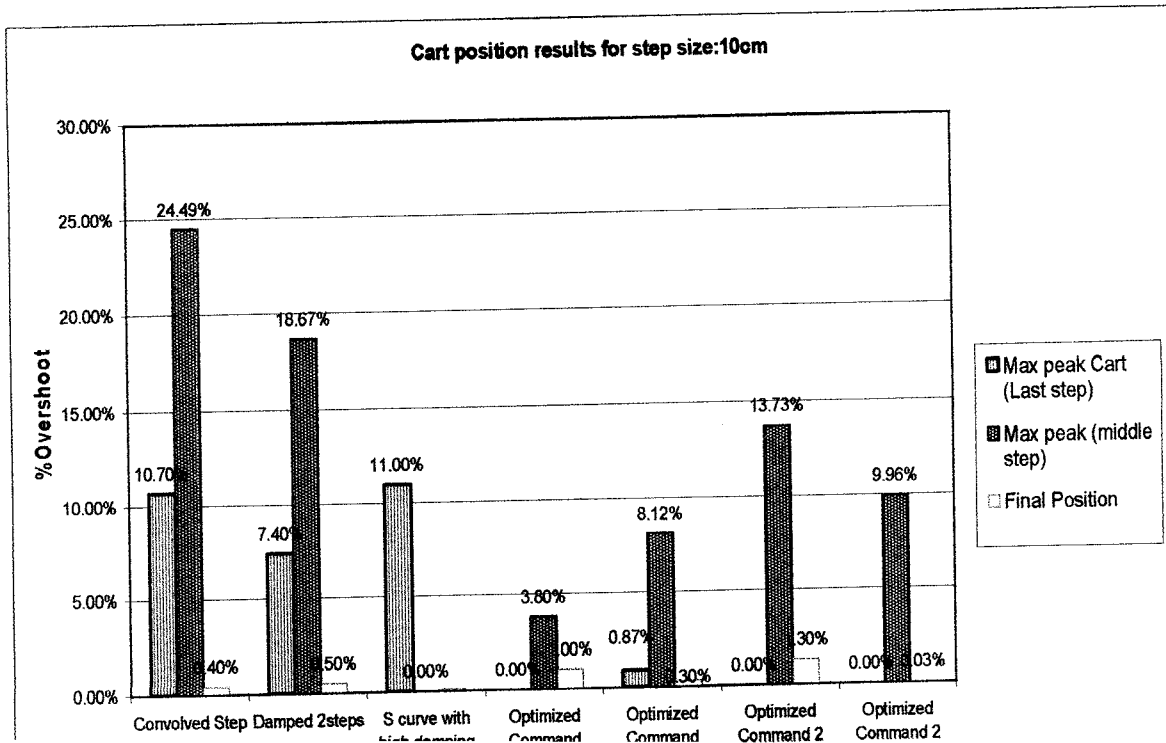

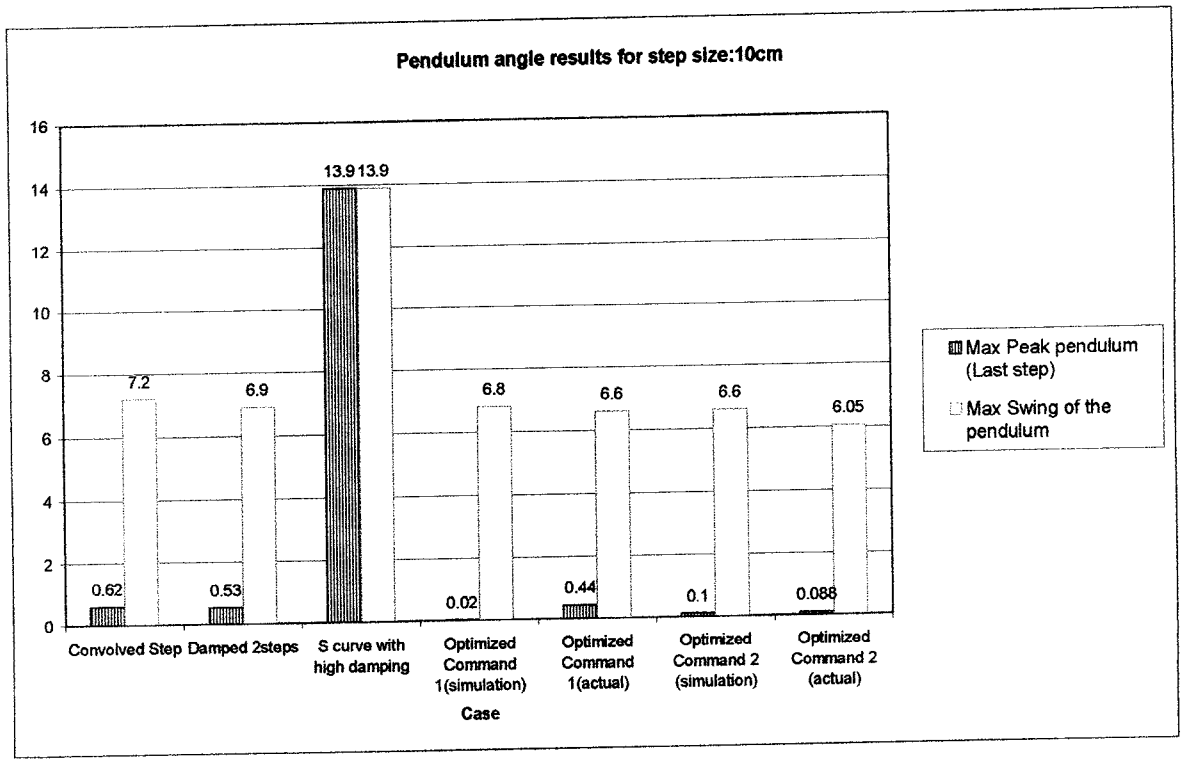

Fig. 5-22: Pendulum angle results for step size 10cm

It can be noticed, due to the presence of saturation, the settling time increased in both the convolved and the damped 2step cases to reach 1.1 and 0.95 seconds respectively. For the optimized command, the settling time is 0.8 seconds. The convolved step produces an overshoot after the last step of 10.7%, and 24.5% after the second step. The damped 2steps produce an overshoot of 7.4% after the last step and 18.67%. For the 2nd case of optimized step there is no overshoot after the last steps, and 9.9% overshoot after the second step. The deviation of the final position for the conventional command is 0.4%, while for the 2nd optimized command is 0.03%. The maximum angle after the last step for the conventional commands ranges from 0.53° to 0.62°, while for the 2nd set of optimized command is 0.088°, which is of the same order of the corresponding angle in the 1cm and the 5cm displacement. Moreover, the maximum swing angle is 6.05° in this case as compared to 7° in conventional

The commands obtained from the optimization program are far more effective in accurately positioning the cart and reducing the vibrations of the pendulum with minimum settling time.

Step size: 20cm

At this stage, the saturation highly influences the responses of the system. This will appear in the high overshoots of the cart, which has a high frequency, thus requiring large steps for small periods, and causing saturation. It will be shown that the same trend in the previous step will appear when comparing the optimized commands with the theoretical ones. Two optimized commands were chosen from the optimized command set obtained from the Genetic algorithm code. By comparing the two commands, it can be seen that both have a settling time of 0.9 seconds. while the second command has no overshoots after the final step and an overshoot of 21% after the middle step, the first command has an initial overshoot of 2.5% and a final overshoot of 0.63%. The final position of the first command varies by 0.63%, while the second command position the cart at the desired location. The final angle for the second command is 0.1° while for the first is 0.36°. From the above results, the second command shows better response in terms of all parameters except for the high overshoot after the middle steps. By comparing these commands with the theoretical command, the following can be found (see Fig. 5-23 and Fig. 5-24)

The settling times of the convolved steps command is higher than all other commands. This is due to the high oscillations induced in the cart response due to the saturation. The settling time of all other commands fall around the same value (0.9 seconds). The overshoots of the convolved and the damped commands are 12.5% and 5.5%

no overshoot after the final step. Although the saturation shouldn't affect directly the response of the pendulum since its natural frequency is low; however, the high overshoot induced by the convolved and the damped steps lead to a final angle of 1.15° and 1.75°. At the same time, the final angle for the optimized command is 0.88°. Moreover, the optimized command positions the cart accurately with an error of 0.05%. Thus it can be seen that the increase in the step size increases the nonlinearity of the system causing the theoretical commands to induce higher vibration level in terms of % overshoot and final angle as compared to the optimized command that keep the different values within the same range for all steps (for result details see Table B-5).

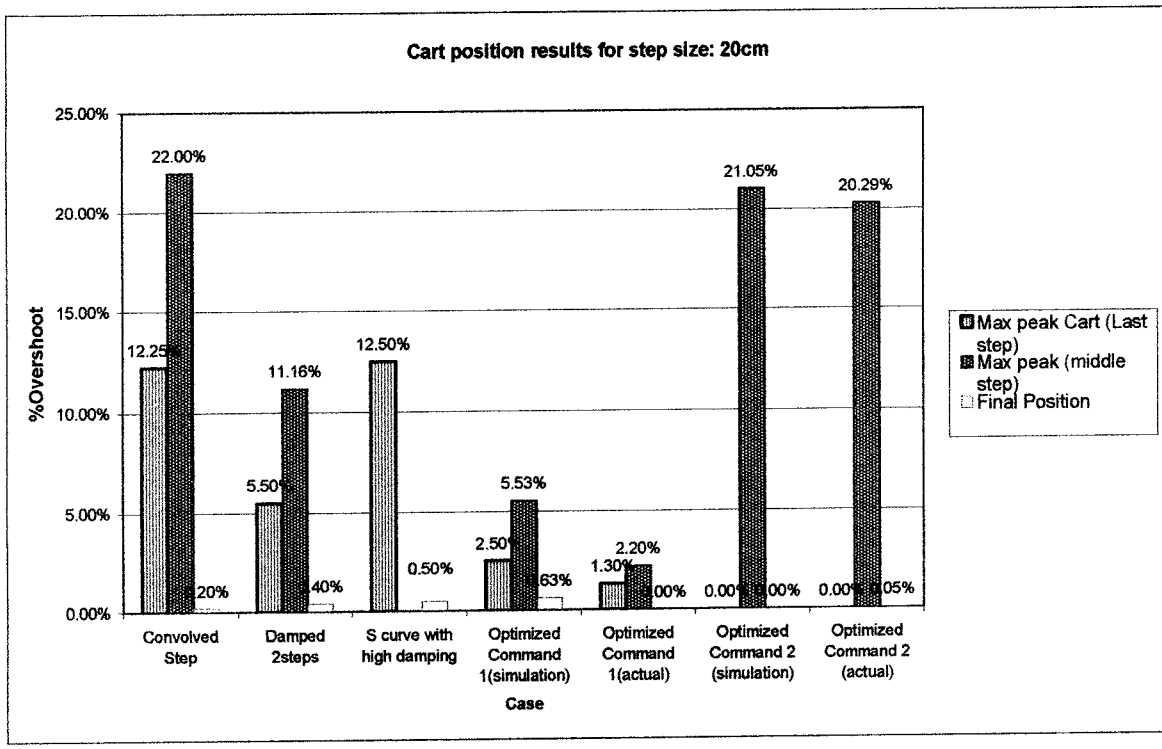

Fig. 5-23: Cart position results for step size 20cm

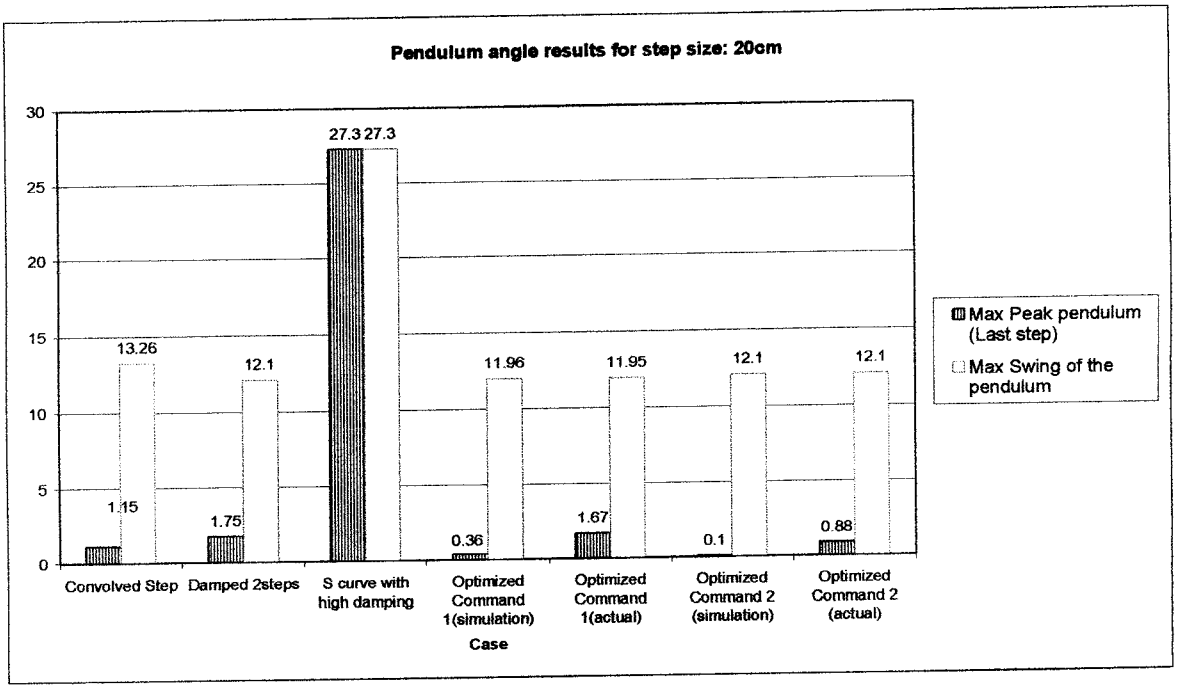

Fig. 5-24: Pendulum angle results for step size 20cm

Step Size: 30cm

The same pattern as the previous step size can be depicted in the results for this step size. Two optimized command where developed. The first one has an advantage in its low cart overshoot which are 0.67% after the last step, and no overshoot after the middle step. Moreover, this command positions the cart exactly at 30cm and causes 0.04° oscillation for the pendulum after the final step. As for the second optimized command, although its parameters are higher than the first one; however, in the practical application, it gave better performance in terms of damping the oscillations of the pendulum with high accuracy in positioning the cart. The results of these commands on the actual system are shown in Fig. 5-25 and Fig. 5-26. The two theoretical commands have a very high overshoots after the final step with considerably longer settling time (1.3 seconds). Moreover, they still produce high overshoots for the middles steps. It can be seen that the optimized commands are able to

one produces a 3.7% overshoot. These values for the worst case (2nd optimized command) represent 50-60% decrease in the overshoot as compared with the theoretical commands. This is also applicable to the results of the angle where the maximum angle of the theoretical steps varies around 16.5° and the maximum angle after the last step varies around 4°. For the optimized cases, the maximum angles don't exceed 14.9°, and the settling angle is 2° for the first command and 0.18° for the second command. As for the positioning of the cart, it can be seen that due to the high value of the step size, all commands position the cart more or less accurately (for result details see Table B-6).

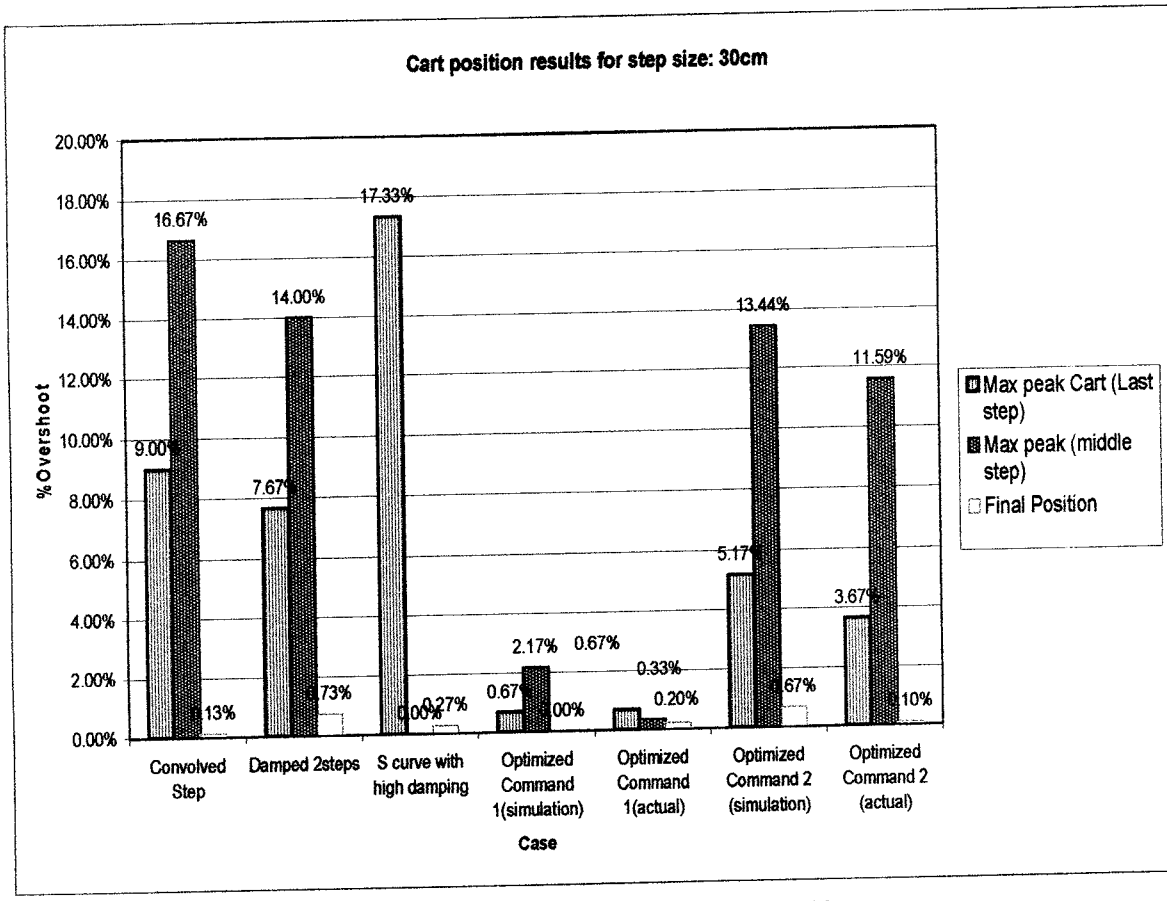

Fig. 5-25: Cart position results for step size 30cm

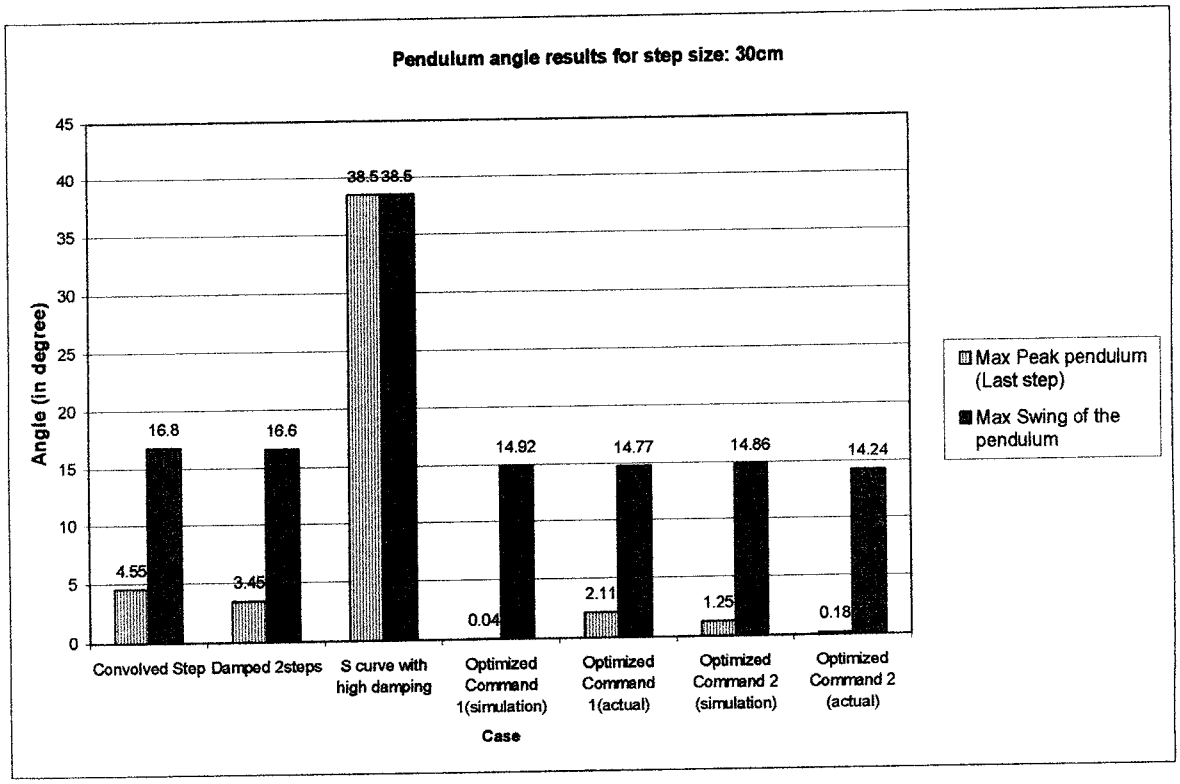

Fig. 5-26: Pendulum angle results for step size 30cm

SUMMARY OF RESULTS

From the above results, general trends of the different types of command could be determined. These trends are depicted by plotting the variation in the percent overshoot of the cart after the last step, the final angle of the pendulum and the final position of the cart versus different step sizes. For the final position of the cart, the convolved steps yield very high % deviation in position for the small step sizes, while it decreases as the step size increases, which is a normal trend showing that this type of command is unable to position accurately the cart. For the damped response, it shows the best positioning ability for small steps, yet, as the steps increases, it fails to position accurately the cart. For the optimized commands, the final position is always better than the previous commands, which can still be improved by

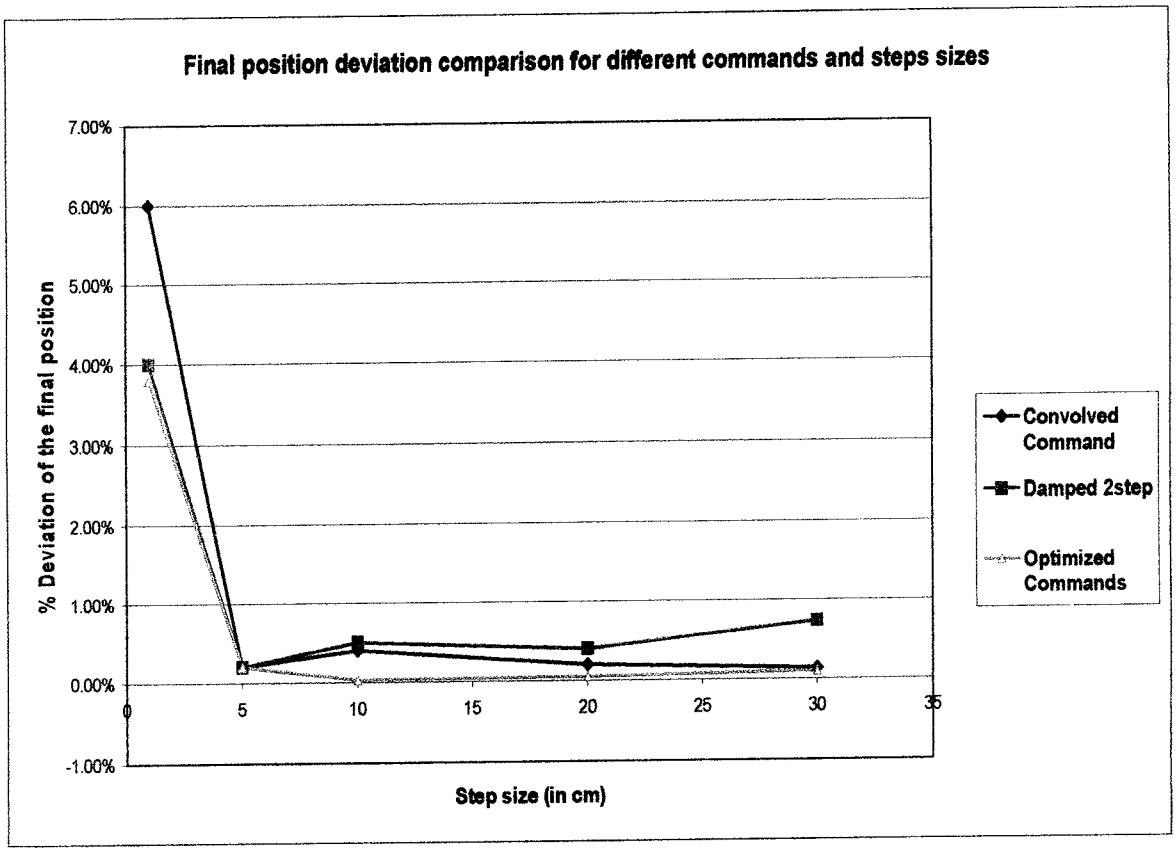

Fig. 5-27: Percent deviation of the final position of the cart for different step sizes and commands

For the final angle of the pendulum, the convolved step command offer acceptable oscillations for small step sizes, while these oscillations increase considerably as the step size increases. The damped two step command fails to damp the oscillations of the pendulum, which is related to the high overshoot of the cart and the saturation of the system. For the optimized commands, the angle is minimum and nearly constant all the time, which indicates the ability of such commands to deal efficient with oscillation reduction of the pendulum (see Fig. 5-28).

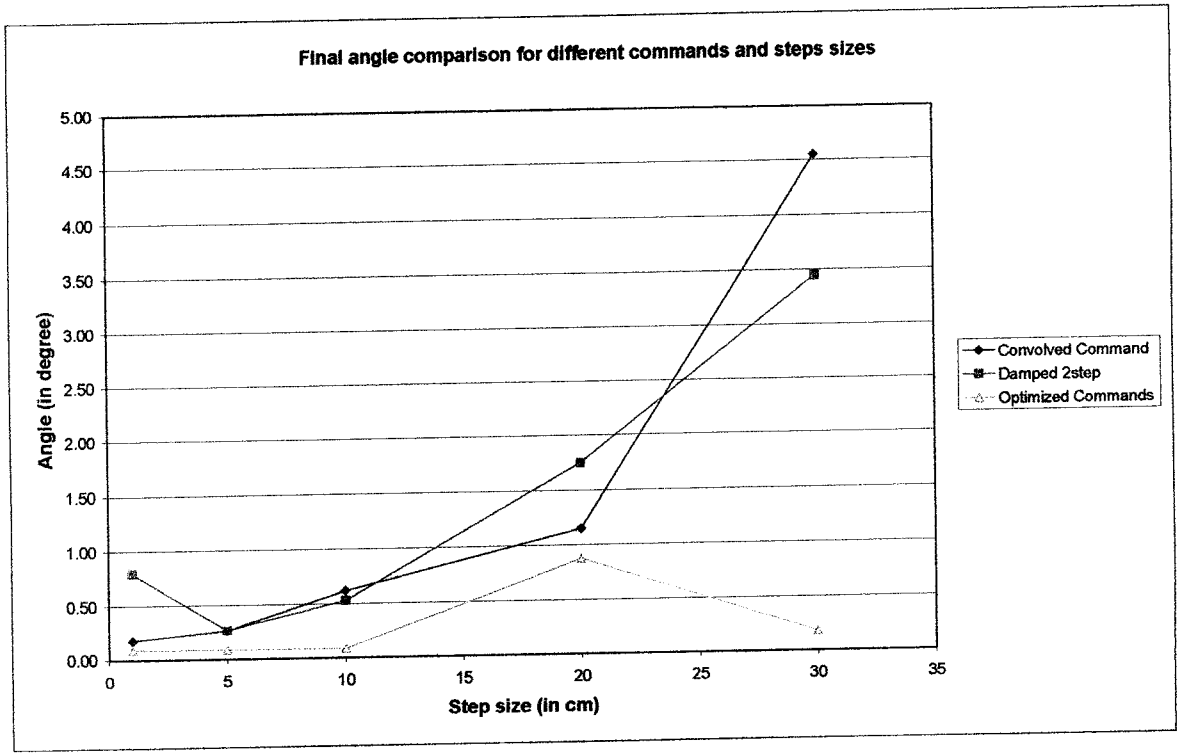

Fig. 5-28:Final angle of the pendulum for different step sizes and commands

For the overshoot of the cart after the final step, the convolved steps command yields low overshoots for small step sizes, which reflect its inability to position accurately the cart at these step sizes. These overshoots increase substantially as the step size increases due to the saturation of the system. For the damped response, the overshoots are always large, which is one of the disadvantages of derivative controllers. The optimized command, although having the same settling time for small steps as the other commands, it has larger overshoot at small step sizes compared with the convolved steps. However, this higher overshoot is required to overcome the effect of friction. As the step size increases, the overshoots follow a constant percentage curve which is very low compared to other commands (see Fig. 5-29).

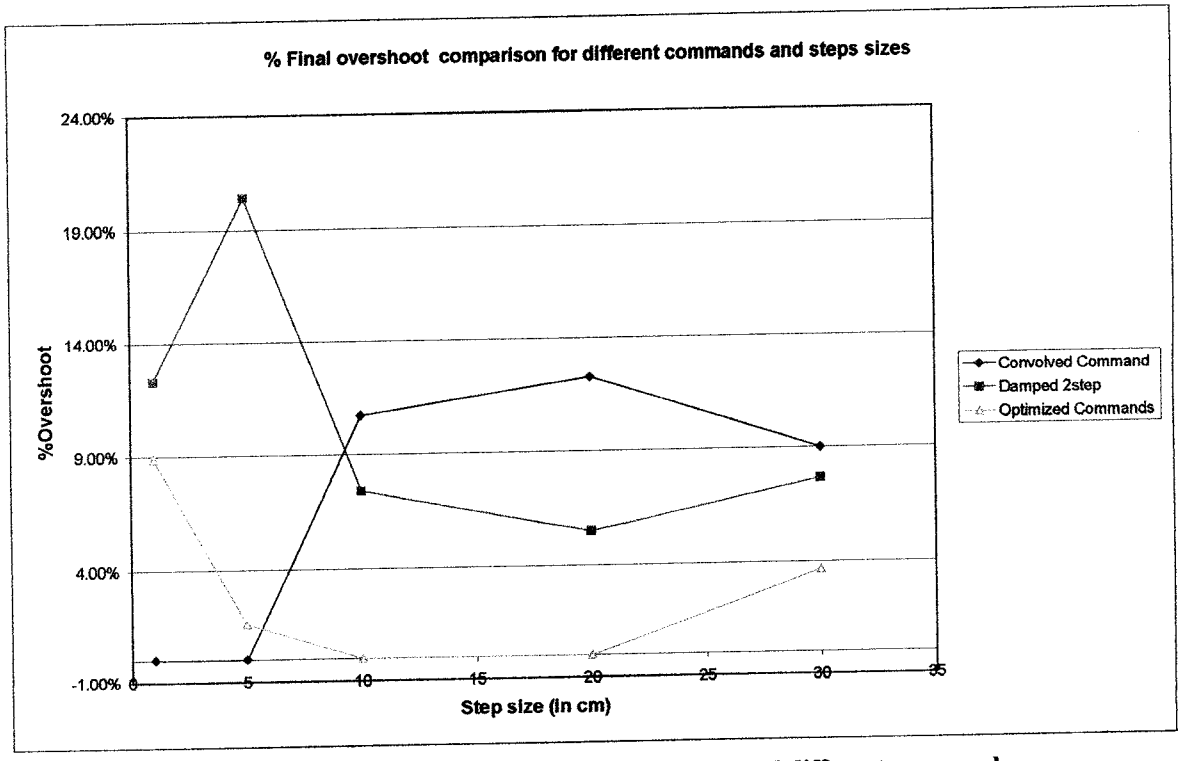

Fig. 5-29: Percent overshoot for different step sizes and different commands.

By comparing these three graphs, it can be seen that the angle of the pendulum is the lowest for the optimized command as compared with the conventional ones. There is a trade off between the overshoot percent and the deviation percent of the cart that the optimization command keep at the minimum as compared with the theoretical commands that offers poor response at the large step size, and variable response at the small step sizes. It can be seen, that the optimized command can deal efficiently with such systems, where the step sizes varies from the very small to the very high ones.

The timing and amplitude of the best optimized command in the computer simulation are analyzed. The timing of the second and fourth input step increases with the displacement step size. This is related to the effect of saturation. Saturation affects mainly the response of the cart. For this reason the timing of the second and the fourth input step increases. For the

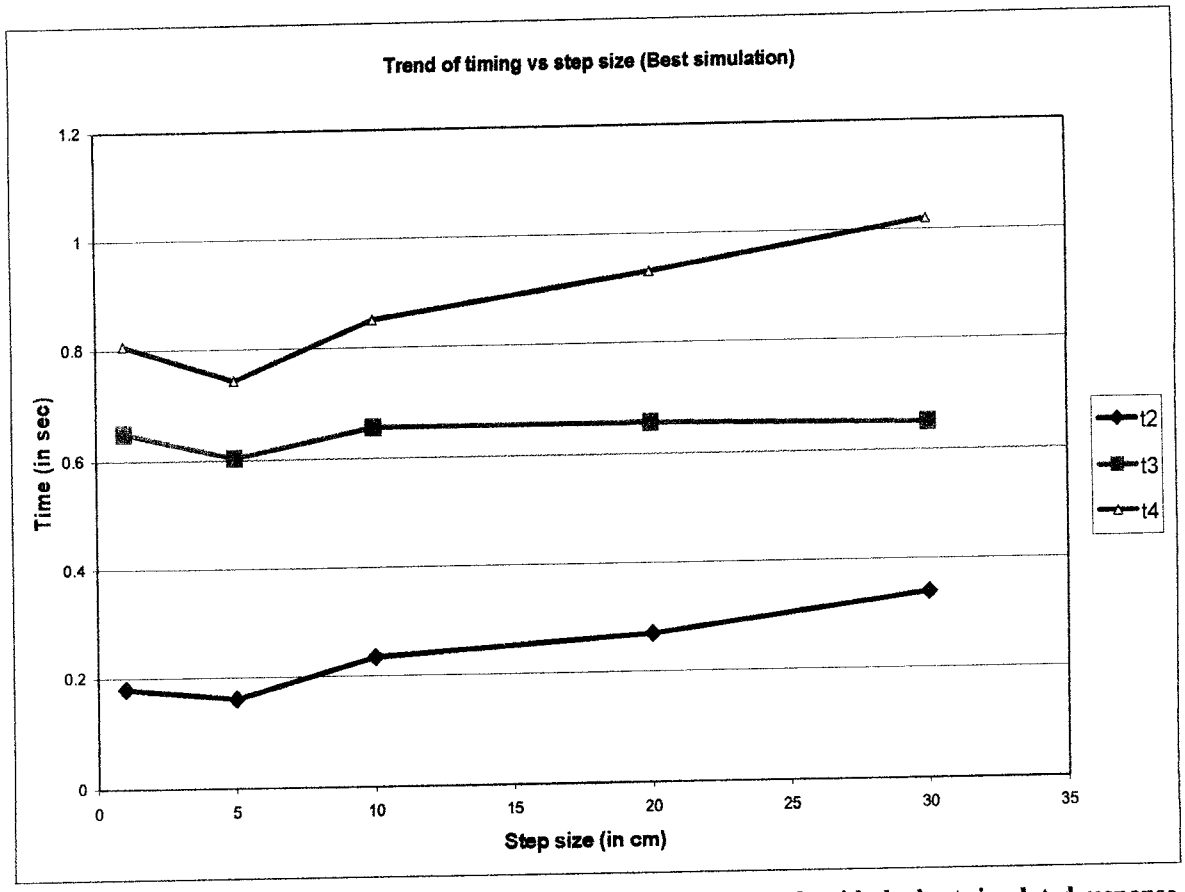

Fig. 5-30: Trend for the input steps timing vs step size for the commands with the best simulated response

As shown in Fig. 5-31, the amplitudes of the first and third step are large for the step size of 1cm, in order to overcome the effect of friction. It can be seen that the amplitude of the second and fourth input step follows the same trend. The summation of the amplitude of the first and the second step represent the first step for the pendulum. It is shown that the value of this step is constant for all step sizes, except for the smallest one where the effect of friction is pronounced.

CHAPTER 6

CONCLUSION

The objective of this thesis was to provide a new methodology for the development of input command sets that cancel the vibration out of flexible structures, while including the nonlinearity effect. Two systems were used to develop such methodology. These systems have no closed form solution in the literature. This methodology consists of using a numerical approach to obtain the system response, then applying a global optimization method to find a near optimum solution for the input shaping problem. This method allowed for the incorporation of nonlinearities in the system, and finding solutions for problems that are tedious to solve.

The first system was a one degree of freedom model which had a PI controller to eliminate the steady state error. Using the optimized input shaping commands, it was shown that the response exhibits less vibration level as compared with the conventional input shaping commands. It was shown that at different step sizes, the optimized commands performed similarly, while for the conventional commands, the increase or decrease in the step size greatly affected the response of the system. A new set of commands were developed for such system.

The second system was a two degree of freedom model. The system consisted of a mass and pendulum setup was a PD controller connected to the mass. Optimized input commands were used to eliminate the oscillations of both the cart and the pendulum, and accurately position the cart at the desired position. It was shown that on the simulation, the optimized

that the optimized command produced much better responses than the conventional commands for large steps. Moreover, it was noticed that the error level for the optimized commands has a constant trend for all types of nonlinearity, contrary to the conventional types of command, which usually produces varying results. Such a feature indicates that the optimized commands are more robust compared to the conventional ones.

Genetic algorithm codes proved to be successful in finding near global optimum for the different problems. Some modifications to the genetic algorithm code were incorporated in order to insure a near global optimum solution. A hybridization of genetic algorithm and local search method was implement and yielded very good results in the input shaping problem.

FUTURE RESEARCH WORK

As this method proved to be effective by the use of numerical integration and global optimization, many nonlinear problems could be solved using it. One challenging problem is the use of input shaping for the vibration elimination of a two degree of freedom model where friction acts on both masses of the system. Also, the combination of input shaping in other controllers such as lead and lag controllers could be investigated. Moreover, other types of nonlinearities could be included in the model such as the variation of the natural frequency of the model during the response.

REFERENCES

- Banerjee, A. K. and Singhose, W.E., (1998). "Command Shaping in Tracking Control of a Two-Link Flexible Robot," Journal of Guidance, Control, and Dynamics, v 21, n 6, Nov-Dec, 1998, pp.1012-1015.
- Franklin, Gene F., Powell, J. D. and Emami-Naeini, Gene, (1994). "Feedback Control of Dynamic Systems," Addison-Wesley Publishing Company, Inc., pp.168-223.
- Lawerence, J., Hekman, K. and Singhose, William, (2002). " An analytical solution for a zero vibration input shaper for systems with Coulomb friction," Proceedings of the American Control Conference, v 5, pp. 4068-4073
- Herrera, F., Lozano, M. and Verdegay, J.L., (1998). "Tackling real-coded genetic algorithms: operators and tools for behavioural analysis," Artificial Intelligence Review, v12, pp. 265-319.
- Kension, M. and Singhose, W., (2000). "Concurrent Design of Input Shaping and Feedback Control for Insensitivity Parameter Variations," International Workshop on Advanced Motion Control, AMC, pp.372-377.
- Kuo, C. F. and Kuo, C.Y., (1992). "Efficient Control of A Flexible Robot Arm by Shaped Inputs," American Society of Mechanical Engineers, Dynamic Systems and Control Division, v 38, Active Control of Noise and Vibration, pp.261-270.
- Michalewicz, Z., and Fogel, D.B., (2002). "How to Solve It: Modern Heuristics, " Springer-Verlag Berlin Heidlberg New York.
- Mohamed, Z. and Tokhi, M.O., (2002). "Vibration Control of a Single-Link Flexible Manipulator Using Command Shaping Techniques," Proceedings of the Institution of

Mechanical Engineers, v216, Part I, Journal of Systems and Control Engineering, pp.191-210.

- Mohamed, Z. and Tokhi, M.O., (2003). "Hybrid Control Schemes for Input Tracking and Vibration Suppression of a flexible Manipulator," Proceedings of the Institution of Mechanical Engineers, v217, Part I, Journal Systems and Control Engineering, pp.23-34.
- Porter, Lisa J., Singer, Neil C. and Singhose, William E., (1995). "Vibration Reduction Using Multi-Hump Extra-Insensitive Input Shapers," Proceedings of the American Control Conference, v15, pp.3830-3834.
- Rao, S.S., (1996). "Engineering Optimization," John Willey and Sons, Inc :New York.
- Romano, M. A., Brij N. and Bernelli-Zazzera, F., (2002). Experiments on Command Shaping Control of a Manipulator with Flexible Links," Journal of Guidance, Control, and Dynamics, v 25, pp.232-239.
- Sahinkaya, M.N., (2001). "Input Shaping for Vibration-Free Positioning of Flexible Systems," Proceedings of the Institution of Mechanical Engineers. Part I, Journal of Systems and Control Engineering, v 215, n 5, pp.467-481.
- Singer, N.C. and Seering, W.P., (1990). " Preshaping Command Inputs to Reduce System Vibration," Journal of Dynamic Systems, Measurement, and Control, v112, pp. 76-82.
- Singh, T. and Sinhose, W., (2002). " Tutorial on input sharping/time delay control of maneuvering flexible structures," Proceedings of the American Control Conference, v3, pp.1717-1731.
- Singhose, William E., Porter, Lisa J. and Seering, Warren P., (1997). " Input Shaped Control of a Planar Gantry Crane with Hoisting," Proceeding of the American Control

- Singhose, W. and Pao, L., (1997). "Comparison of Input Shaping and Time-Optimal Flexible-Body Control," Control Engineering Practice, v 5, pp.459-467
- Smith, O.J.M., (1958). "Feedback Control Systems, New York: McGraw-Hill Book Co, Inc., pp.331-345.
- Wilson, David G. and Starr, Gregory P., (1996). "Vibration Suppression of a Single Flexible Link," Proceedings of SPIE-The International Society for Optical Engineering, v 2717, pp.608-618.
- www.quanser.com/english/downloads/toolbox/labs/May,2002/Linear%20-%20Self%20Erecting%20Inverted%20Pendulum%20(IP02).pdf

APPENDICES

APPENDIX A: ONE DEGREE OF FREEDOM RESULTS

VALUES USED IN THE MODEL

Table A-1: Values used in the one degree of freedom model

Mass of Block: m_b (Kg)	0.522
Half the Length of Pendulum: l (m)	0.305
Derivative controller gain: K_d(underdamped cases) (Volt.sec/cm)	0
Derivative controller gain: K_d(overdamped cases) (Volt.sec/cm)	1
Proportional controller gain:K_p (Volt/cm)	3
Integral controller gain:K_I (Volt/sec/cm)	12
Damping of the motor:c (cm/sec)	0.05
Correction factors for the cart	1.32
Dynamic friction voltage:μ_k (Volts)	0.4

The amplitudes of the steps are incremental A_3=*Step_Size-*A_1-A_2

Table A-2: Results for One degree of freedom system-1cm step size

Step Size: 1cm

Case	Overshoot	Rise Time	Settling Time	Deviation :2sec	Overshoot 15% variation	Deviation 15% variation	Settling time 15% variation	Input Commar [A_1 t_2] [/ A_2 t_2 t_3]
ZV Theoretical	7.55%	0.3	0.7	0.27%	.....			[0.5476 0.165]
Damped Step	11.87%	0.1	0.6	0.04%	.....			
ZV:(Trad.Obj.)	1.15%	0.1	0.1	0.04%	12.90%	0.65%	0.2	[0.6476 0.1577]
ZV:(FFt)	6.86%	0.1	0.7	0.87%				[0.6502 0.1578]
ZVD Theoretical	22.30%	0.3	0.5	0.87%	20.64%	0.74%	0.5	[0.2999 0.4955 0.1663 0.3325]
ZVD Obifun(1)	2.50%	0.4	0.4	0.42%	2.51%	0.40%	0.5	[0.5672 0.2887 0.1217 0.3667]
								[0.6509

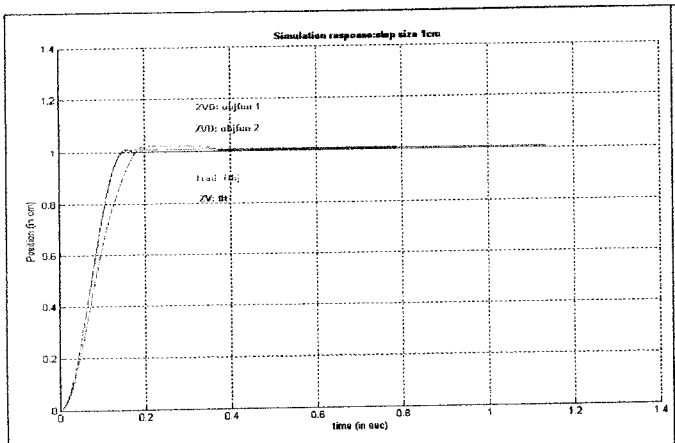

Fig. A-1: Simulation response for optimized commands (step size 1cm)

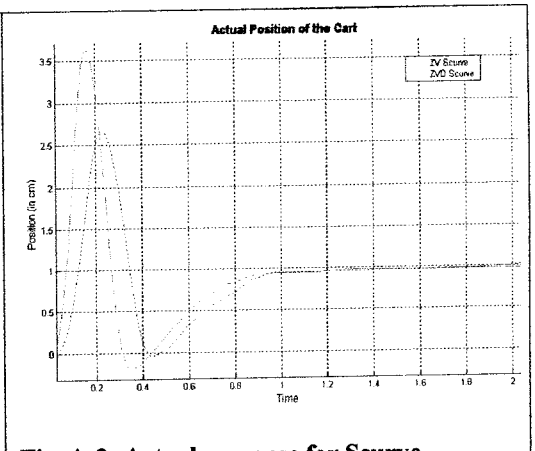

Fig. A-2: Actual response for Scurve commands (step size 1cm)

Table A-3:Results for One degree of freedom system-5cm step size

Step Size: 5cm								
Case	% Overshoot	Rise Time	Settling Time	Deviation %:2sec	% Overshoot-15%	% Deviation-15%	Settling time-15%	Input Comma [A_1 t_2] [A_2 t_2 t_3]
ZV Theoretical	16.19%	0.2	0.4	0.4%				[2.738 0.165]
Damped Step	33.12%	0.1	0.6	0.2%				
ZV:(Trad.Obj.)	6.08%	0.2	0.5	0.2%				[2.870 0.181]
ZV:(FFt)	7.05%	0.2	0.5	0.2%	7.36%	0.15%	0.5	[2.997 0.189]
ZVD Theoretical	10.00%	0.3	0.5	0.1%	10.43%	0.33%	0.4	[1.4995 2.4775 0.1663 0.3325]
ZVD:Objfun (1)	4.96%	0.2	0.3	0.1%	6.31%	0.67%	0.4	[1.9305 1.0893 0.0483 0.1816]
ZVD:Objfun (2):	7.91%	0.2	0.4	0.1%	8.45%	0.00%	0.4	[2.9305 0.0668 0.0237 0.1852]

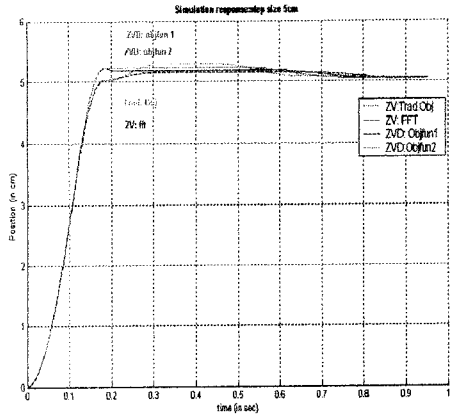

Fig. A-3: Simulation responses for optimized commands (step size 5cm)

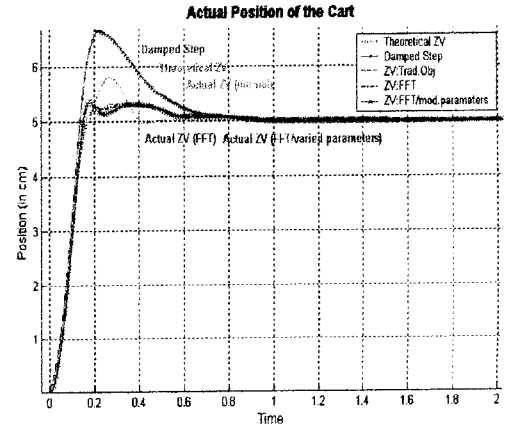

Fig. A-4: Actual responses for different ZV commands (step size 5cm)

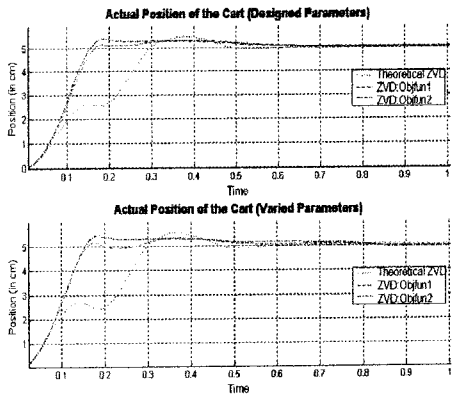

Fig. A-5: Actual responses for different ZVD commands (step size 5cm)

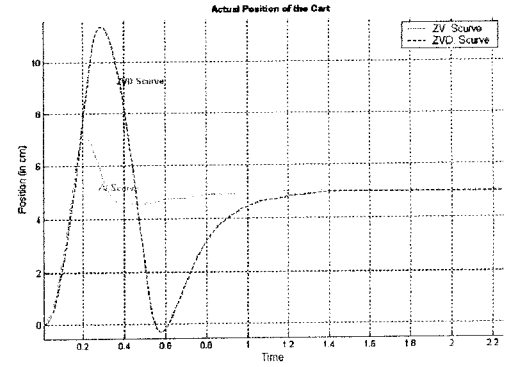

Fig. A-6:Actual response for Scurve commands (step size 5cm)

Table A-4:Results for One degree of freedom system-10cm step size

Step Size: 10cm								
Case	% Overshoot	Rise Time	Settling Time	Deviation %:2sec	% Overshoot-15%	% Deviation-15%	Settling time-15%	Input Commar [A_1 t_2] [A_2 t_2 t_3]
ZV Theoretical	51.11%	0.2	1.2	0.25%				[5.476 0.165]
Damped Step	49.00%	0.2	0.8	0.06%				
ZV:(Trad.Obj.)	13.37%	0.2	0.6	0.25%				[5.738 0.259]
ZV:(FFt)	16.44%	0.2	0.6	0.03%	16.76%	0.3%	0.6	[6.575 0.288]
ZVD Theoretical	11.31%	0.3	0.5	0.24%	10.51%	0.10%	0.5	[2.999 4.955 0.1663 0.3325]
ZVD:Objfun (1)	8.30%	0.2	0.5	0.19%	8.04%	0.45%	0.5	[4.296 2.599 0.1412 0.2792]
ZVD:Objfun (2):	8.73%	0.2	0.3	0.08%	9.37%	0.11%	0.3	[2.615 4.368 0.0897 0.2780]

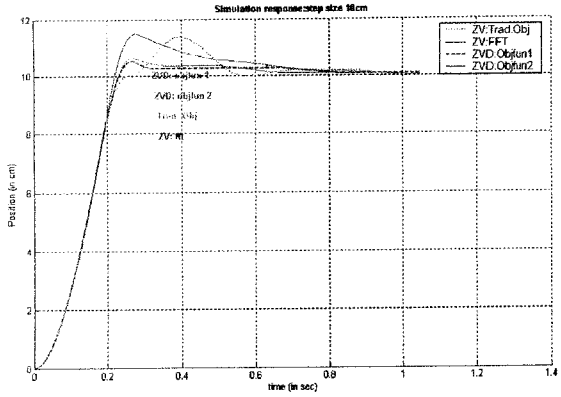

Fig. A-7:Simulation responses for optimized commands (step size 10cm)

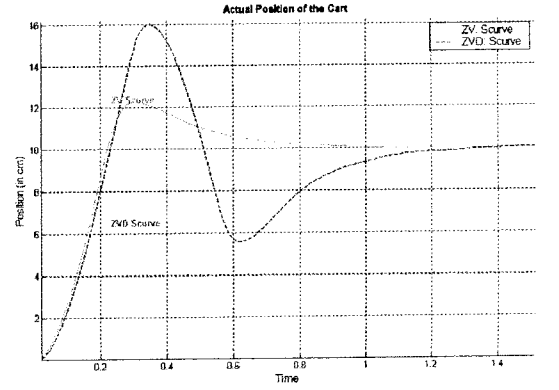

Fig. A-8:Actual response for Scurve commands (step size 10cm)

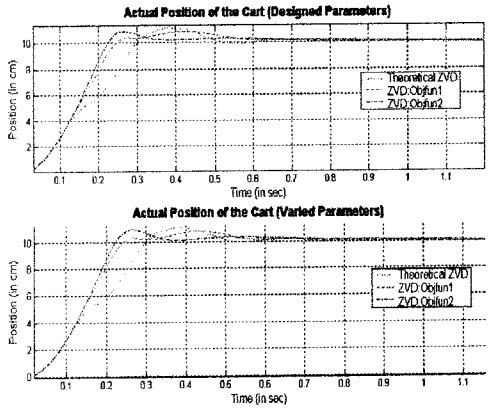

Fig. A-9:Actual responses for different ZVD commands (step size 10cm)

Table A-5:Results for One degree of freedom system-20cm step size

Step Size: 20cm								
Case	% Overshoot	Rise Time	Settling Time	Deviation %:4sec	% Overshoot-15%	% Deviation-15%	Settling time-15%	Inp Co [A A_2
ZV Theoretical	62.37%	0.4	1.5	0.34%				[10 0.1
Damped Step	66.97%	0.3	0.9	0.01%				
ZV:(Trad.Obj.)	21.53%	0.4	1.0	0.23%				[11 0.3
ZV:(FFt)	19.58%	0.4	0.7	0.18%	19.00%	0.06%	0.7	[13 0.4
ZVD Theoretical	38.18%	0.3	1.3	0.05%	38.0%	0.15%	1.3	[5. 9.9 0.1 0.3
ZVD:Objfun (1)	8.08%	0.4	0.7	0.2%	6.6%	0.13%	0.7	[5. 9.7 0.1 0.4
ZVD:Objfun (2):	10.00%	0.4	0.5	0.08%	10.1%	0.02%	0.5	[7. 8.0 0.2 0.4

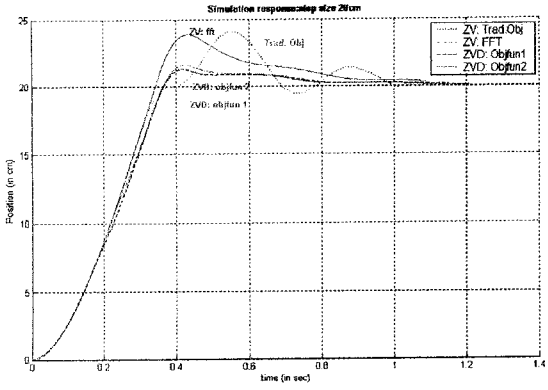

Fig. A-10:Simulation responses for optimized commands (step size 20cm)

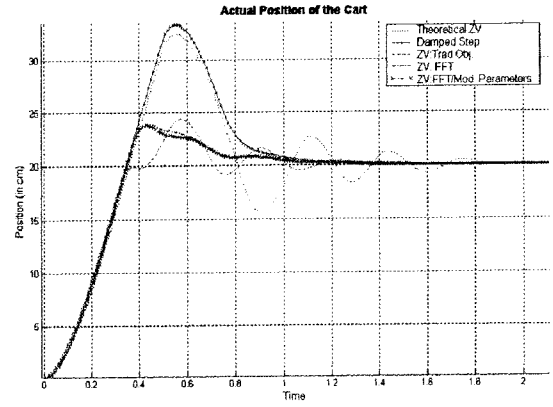

Fig. A-11: Actual responses for different ZV commands (step size 20cm)

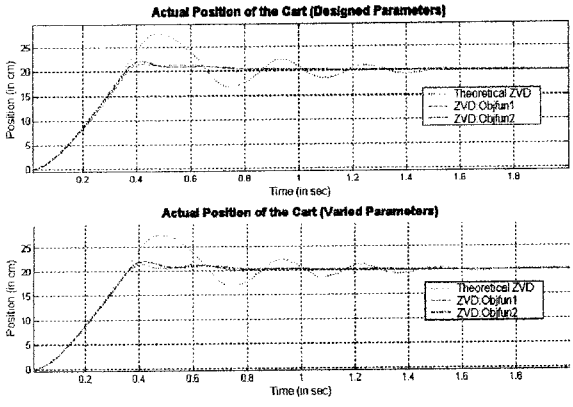

Fig. A-12: Actual responses for different ZVD commands (step size 20cm)

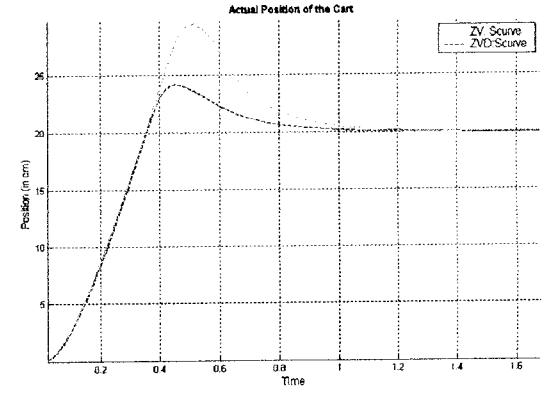

Fig. A-13: Actual response for Scurve commands (step size 20cm)

Table A-6:Results for One degree of freedom system-30cm step size

Step Size: 30cm								
Case	% Overshoot	Rise Time	Settling Time	Deviation %:4sec	% Overshoot-15%	% Deviation-15%	Settling time-15%	Inp Co [A1 A2
ZV Theoretical	68.81%	0.5	1.9	0.13%				[16 0.1
Damped Step	75.49%	0.5	1.5	0.15%				
ZV:(Trad.Obj.)	23.43%	0.5	1.2	0.04%				[16 0.3
ZV:(FFt)	18.15%	0.5	0.9	0.00%	18.15%	0.07%	0.9	[19 0.6
ZVD Theoretical	49.84%	0.5	1.6	0.15%	50.30%	0.16%	1.6	[8.9 14. 0.1 0.3
ZVD:Objfun (1)	11.02%	0.5	0.9	0.12%	10.84%	0.09%	0.9	[13 10. 0.3 0.6
ZVD:Objfun (2):	9.49%	0.5	0.8	0.10%	9.66%	0.12%	0.8	[12 10. 0.3 0.5

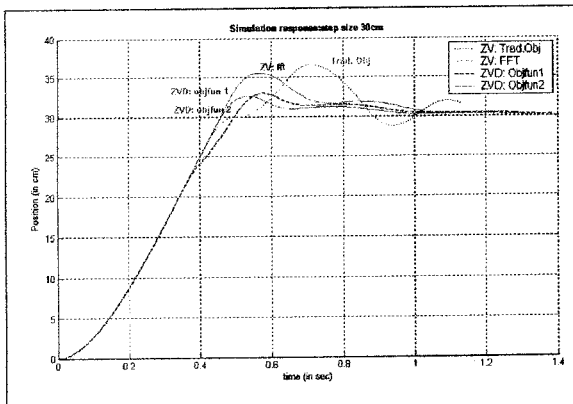

Fig. A-14:Simulation responses for optimized commands (step size 30cm)

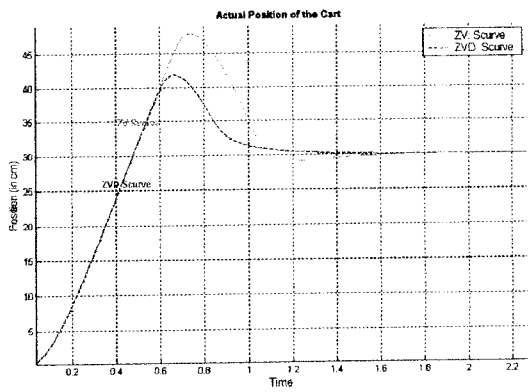

Fig. A-15:Actual response for Scurve commands (step size 30cm)

APPENDIX B: TWO DEGREE OF FREEDOM RESULTS

Table B-1: Values used in the two degree of freedom model

Mass of Block: m_b (Kg)	0.522
Mass of Pendulum: m_r (Kg)	0.21
Half the Length of Pendulum: l (m)	0.305
Derivative controller gain: K_d(underdamped cases) (Volt.sec/cm)	0
Derivative controller gain: K_d(overdamped cases) (Volt.sec/cm)	1
Proportional controller gain:K_p (Volt/cm)	5
Damping of the motor:c (cm/sec)	0.05
Correction factors for the cart	1.568
Dynamic friction voltage:μ_k (Volts)	0.6

The amplitudes of the step size are incremental. A_4=*Step_Size-* $A_1+A_2+A_3$

Table B-2: Results for two degree of freedom system-1cm step size

Step Size: 1cm								
Case	Position Settling Time	Angle Settling time	Max peak Cart (Last step)	Max peak (middle step)	Final Position error %	Max Peak pendulum (Last step)	Max Swing of the pendulum	Input Command [A_1 A_2 t_2 t_3] or [A_1 A_2 A_3 t_2 t_3 t_4]
Convolved Step	0.9	0.9	0.00%	0.00%	6.00%	0.18	0.44	[0.30 0.20 0.30 0.131 0.642 0.773]
Damped 2steps	0.9	0.9	12.30 %	18.33 %	4.00%	0.09	0.80	[0.5 0.6424]
S curve with high damping	0.6	none	0.00%	NA	0.04%	1.05	1.05	NA
Optimized Command 1(simulation)	0.8	0.8	0.00%	0.00%	0.50%	0.02	0.81	[0.48 0.125 0.353 0.18 0.65 0.807]
Optimized Command 1(actual)	0.9	0.8	8.90%	23.08 %	3.80%	0.09	0.80	
Optimized Command 2(simulation)	0.8	0.8	0.00%	0.00%	5.00%	0.02	0.79	[0.475 0.115 0.31 0.132 0.66 0.75]
Optimized Command 2(actual)	0.8	0.8	0.00%	6.35%	2.50%	0.26	0.79	
Optimized Command 3	0.7	0.9	0.00%	0.00%	0.00%	0.02	0.77	[0.4 0.23 0.34 0.11 0.62 0.84]

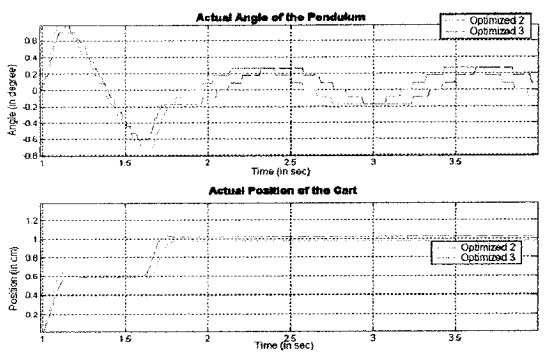

Fig. B-1: Actual response for the optimized command 2 and 3

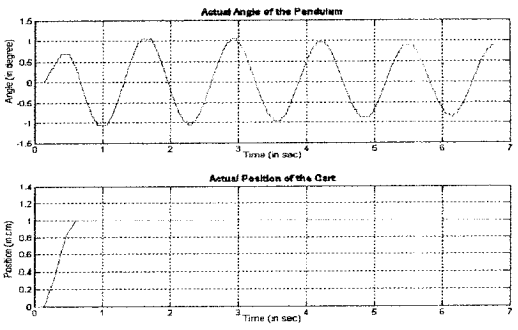

Fig. B-2: Actual response of an Scurve command (step size 1cm)

Table B-3:Results for two degree of freedom system-5cm step size

Step Size: 5cm

Case	Position Settling Time	Angle Settling time	Max peak Cart (Last step)	Max peak (middle step)	Final Position	Max Peak pendulum (Last step)	Max Swing of the pendulum	Input Command $[A_1\ A_2\ t_2\ t_3]$ or $[A_1\ A_2\ A_3\ t_2\ t_3\ t_4]$
Convolved Step	0.9	0.9	**0.00%**	0.00%	**0.20%**	**0.26**	2.90	[1.48 1.02 1. 0.131 0.642 0.
Damped 2steps	1	1	20.40%	38.00%	0.20%	0.27	4.30	[2.5 0.642
S curve with high damping	0.85	noe	9.20%	NA	0.80%	6.40	6.40	NA
Optimized Command 1(simulation)	0.745	0.8	0.00%	5.71%	0.20%	0.00	3.40	[1.7 0.9 1.4 0.161 0.604 0.
Optimized Command 1(actual)	0.8	0.8	0.00%	4.26%	0.20%	0.74	3.30	
Optimized Command 3 (simulation)	0.8	0.8	4.00%	26.92%	2.00%	0.00	4.30	[2.31 0.24 1. 0.246 0.643 0
Optimized Command 3(actual)	0.8	0.8	1.60%	30.95%	0.20%	0.09	4.20	

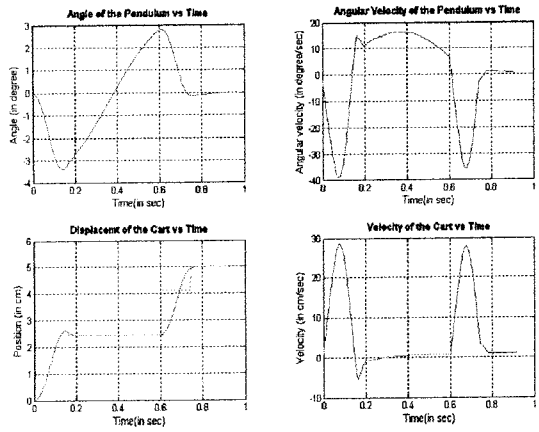

Fig. B-3: Simulation response of the optimized command 1 (step size 5cm)

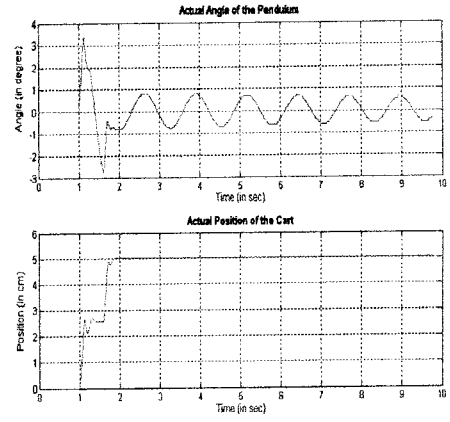

Fig. B-4: Actual response of the optimized command 1 (step size 5cm)

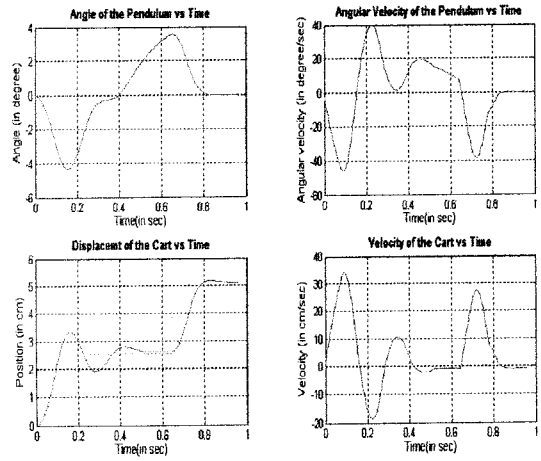

Fig. B-5: Simulation response of the optimized command 3 (step size 5cm)

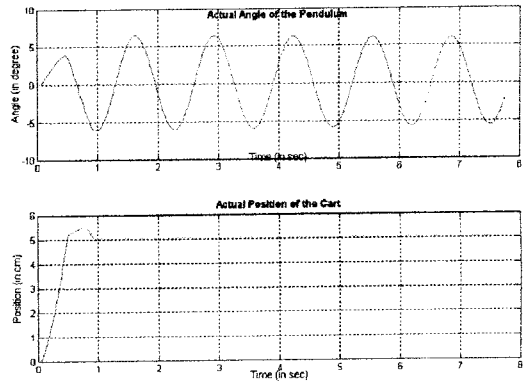

Fig. B-6: Actual response of an Scurve command (step size 5cm)

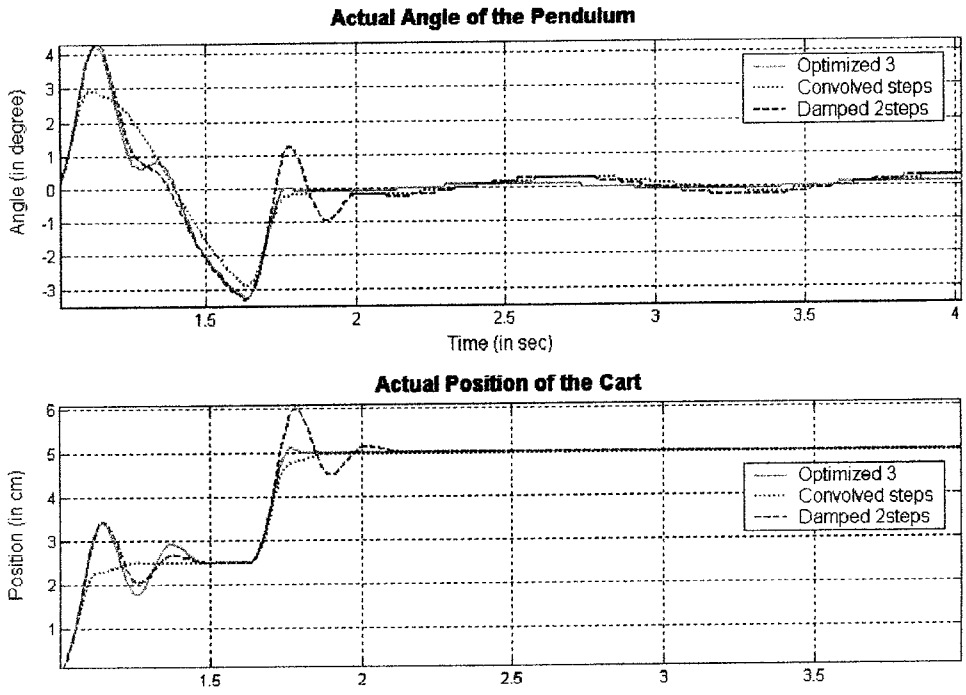

Fig. B-7: Actual results for the following commands: Optimized 3, Convolved steps and Damped 2steps

Table B-4: Results for two degree of freedom system-10cm step size

Step Size: 10cm

Case	Position Settling Time	Angle Settling time	Max peak Cart (Last step)	Max peak (middle step)	Final Position	Max Peak pendulum (Last step)	Max Swing of the pendulum	Input Command $[A_1\ A_2\ t_2\ t_3]$ or $[A_3\ t_2\ t_3\ t_4]$
Convolved Steps	1.1	1.1	**10.70%**	24.49%	**0.40%**	**0.62**	7.2	[2.97 2.03 2. 0.131 0.642 0.
Damped 2steps	0.95	0.95	**7.40%**	18.67%	**0.50%**	**0.53**	6.9	[5 0.6424
S curve with high damping	0.8	10	11.00%	NA	0.10%	13.9	13.9	NA
Optimized Command 1(simulation)	0.8	0.8	0.00%	3.80%	1.00%	0.02	6.8	[3.99 1.27 3. 0.234 0.656 0
Optimized Command 1(actual)	0.8	0.8	0.87%	8.12%	0.30%	0.44	6.6	
Optimized Command 2 (simulation)	0.8	0.8	0.00%	13.73%	1.30%	0.1	6.6	[2.98 2.11 3. 0.154 0.656 0.
Optimized Command 2 (actual)	0.8	0.8	0.00%	9.96%	0.03%	0.088	6.05	

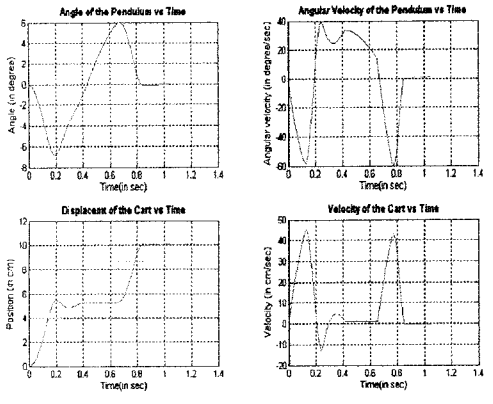

Fig. B-8: Simulation response of optimized command 1(step size 10cm)

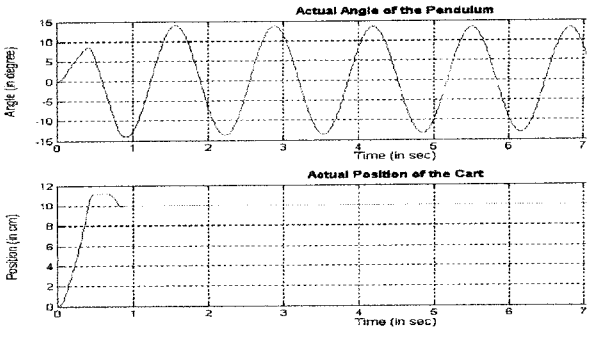

Fig. B-9: Actual response of an Scurve command (step size 10cm)

Table B-5:Results for two degree of freedom system-20cm step size

Step Size: 20cm

Case	Position Settling Time	Angle Settling time	Max peak Cart (Last step)	Max peak (middle step)	Final Position	Max Peak pendulum (Last step)	Max Swing of the pendulum	Input Command $[A_1\ A_2\ t_2\ t_3]$ or $[A_3\ t_2\ t_3\ t_4]$
Convolved Step	1.3	1.3	**12.25%**	22.00%	**0.20%**	**1.15**	13.26	[5.93 4.07 5 0.131 0.642 0.7
Damped 2steps	0.95	0.95	**5.50%**	11.16%	**0.40%**	**1.75**	12.1	[10 0.642
S curve with high damping	0.85	none	12.50%	NA	0.50%	27.3	27.3	NA
Optimized Command 1(simulation)	0.93	0.93	2.50%	5.53%	0.63%	0.36	11.96	[8.58 1.96 7 0.269 0.657 0.
Optimized Command 1(actual)	0.9	0.9	1.30%	2.20%	0.00%	1.67	11.95	
Optimized Command 2 (simulation)	0.9	0.9	0.00%	21.05%	0.00%	0.1	12.1	[3.42 6.14 8. 0.14 0.63 0.
Optimized Command 2 (actual)	0.9	0.9	0.00%	20.29%	0.05%	0.88	12.1	

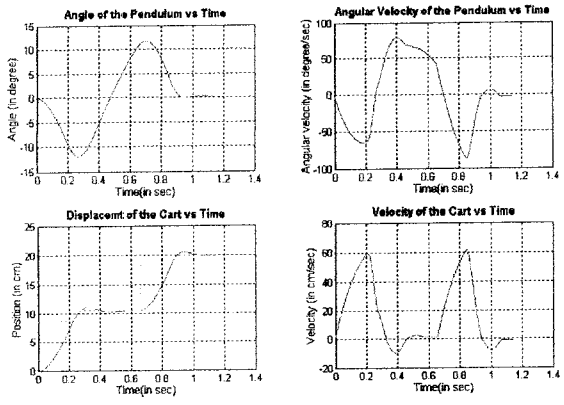

Fig. B-10: Simulated response of the optimized command 1(step size 20cm)

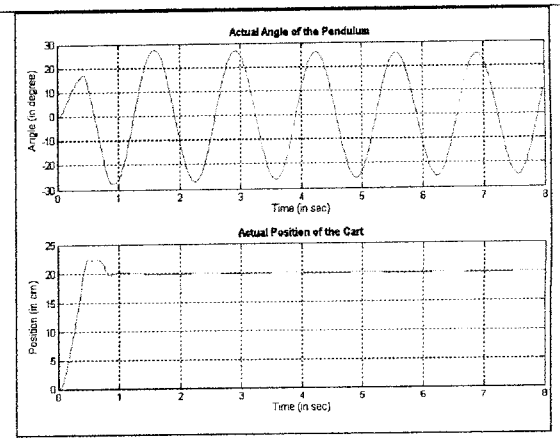

Fig. B-11: Actual response for an Scurve (step size 20cm)

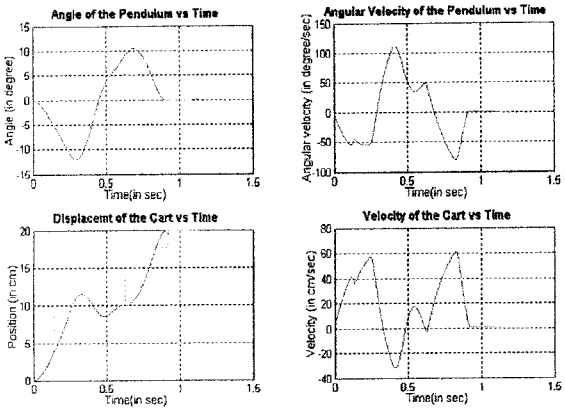

Fig. B-12: Simulated response of the optimized command 2(step size 20cm)

Table B-6: Results for two degree of freedom system-30cm step size

Step Size: 30cm

Case	Position Settling Time	Angle Settling time	Max peak Cart (Last step)	Max peak (middle step)	Final Position	Max Peak pendulum (Last step)	Max Swing of the pendulum	Input Command $[A_1\ A_2\ t_2\ t_3]$ or $[A_1\ A_2\ t_2\ t_3\ t_4]$
Convolved Step	1.3	1.3	**9.00%**	16.67%	**0.13%**	**4.55**	16.8	[8.9 15 8.9 0.131 0.642 0.
Damped 2steps	1.2	1.2	**7.67%**	14.00%	**0.73%**	**3.45**	16.6	[15 0.642
S curve with high damping	0.9	none	17.33%	NA	0.27%	38.5	38.5	NA
Optimized Command 1(simulation)	1	1	0.67%	2.17%	0.00%	0.04	14.92	[12.23 2.97 1 0.34 0.65 1.
Optimized Command 1(actual)	1	1.1	0.67%	0.33%	0.20%	2.11	14.77	
Optimized Command 2 (simulation)	1.2	1.2	5.17%	13.44%	0.67%	1.25	14.86	[8.17 6.92 13 0.24 0.68 1.
Optimized Command 2 (actual)	1.2	1.2	3.67%	11.59%	0.10%	0.18	14.24	

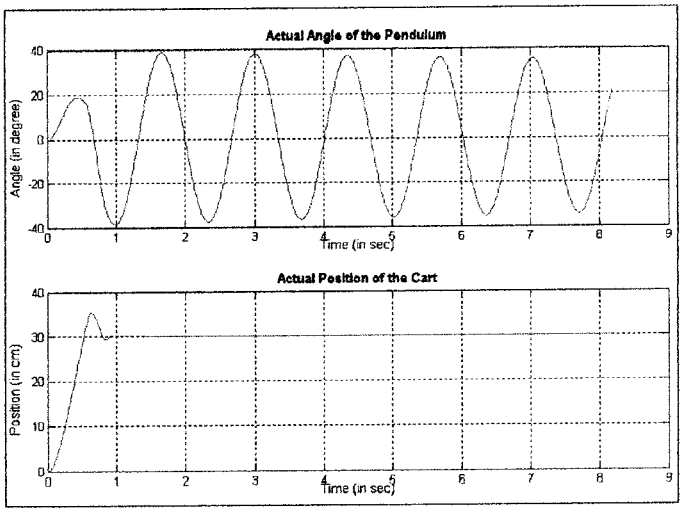

Fig. B-13: : Actual response for an Scurve (step size 30cm)

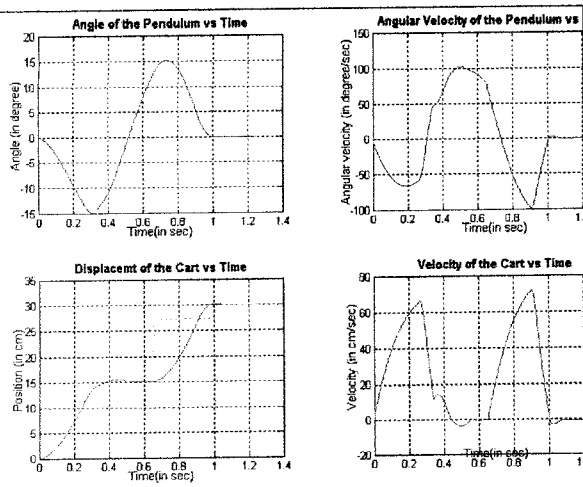

Fig. B-14: Simulated response of the optimized command 1 (step size 30cm)

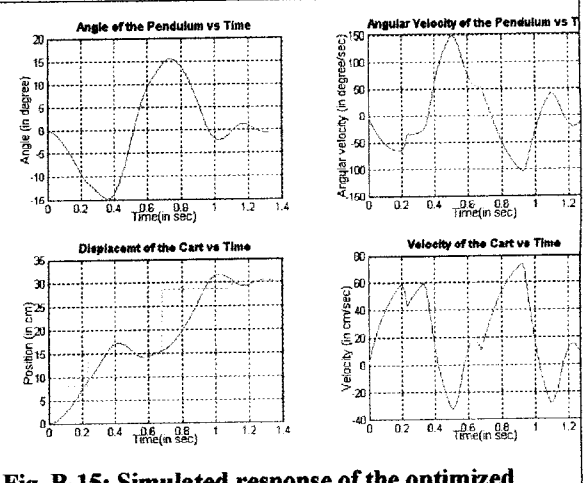

Fig. B-15: Simulated response of the optimized command 2 (step size 30cm)

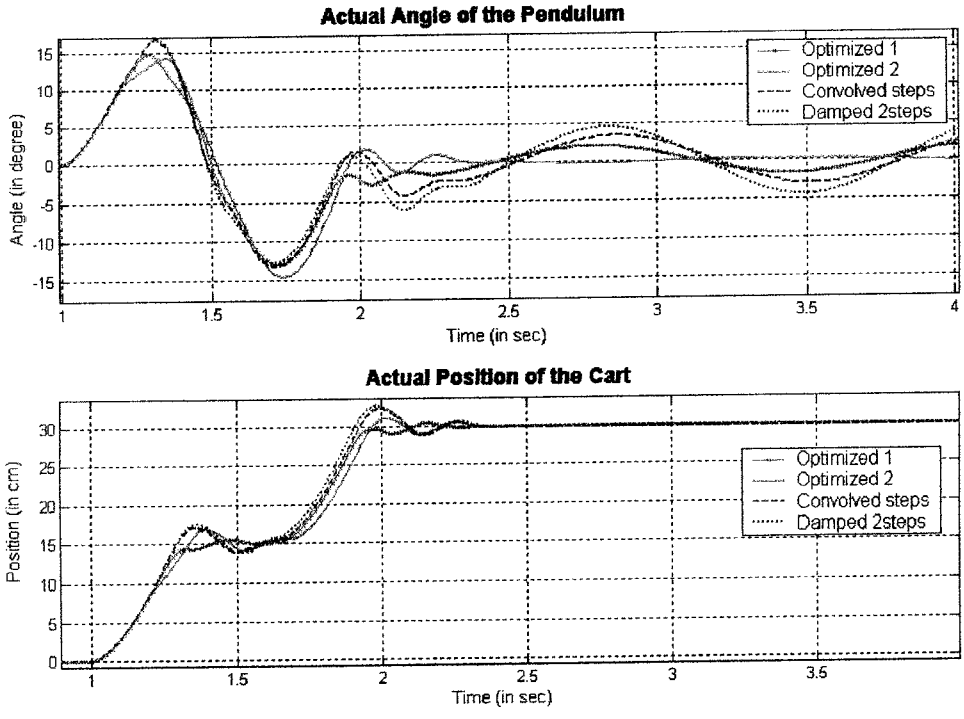

Fig. B-16: Actual response for the following commands: Optimized 1, Optimized 2, Convolved Steps and Damped 2steps